universität wien

MASTERARBEIT | MASTER'S THESIS

Titel | Title

The development of PM10 and PM2.5 concentrations in four industrial regions in Austria between 2002 and 2022

verfasst von | submitted by

Nikolaus Gamperl BSc

angestrebter akademischer Grad | in partial fulfilment of the requirements for the degree of

Master of Science (MSc)

Wien | Vienna, 2025

Studienkennzahl lt. Studienblatt | Degree programme code as it appears on the student record sheet:	UA 066 876
Studienrichtung lt. Studienblatt | Degree programme as it appears on the student record sheet:	Masterstudium Physics
Betreut von | Supervisor:	Univ.-Prof. Dr. Paul Winkler Privatdoz.

Acknowledgments

I would like to express my honest gratitude to Professor Dr. Paul Winkler for his guidance and support throughout this master thesis in the field of atmospheric aerosol physics. Especially the freedom he provided allowed me to focus on my individual strengths and skills, explore the fascinating field of aerosol physics, and dive deeper into the field of air pollution and particulate matter concentration in Austria's industrial regions and its impact on climate, the environment and human health.

I also sincerely thank the University of Vienna and especially the Faculty of Physics for giving me the opportunity to pursue my dream and academic education in the field of physics, enabling me to deepen my understanding and knowledge in various fields of natural sciences.

In addition, I am deeply grateful to my family and friends, whose unwavering support has been a constant source of strength throughout my entire physics studies and working life. Their encouragement and understanding in many moments have been invaluable, not only in completing this thesis but throughout my entire academic journey of the past years.

Abstract

This master thesis examines the development of particulate matter concentrations (PM10 and PM2.5) in Austria's four most significant industrial regions - Greater Vienna, Greater Linz, Greater Graz, and the Greater Mur-Mürz-Furche - over the period from 2002 to 2022. The focus is on changes in particulate matter levels and their comparison with measurements from rural background monitoring stations to highlight temporal trends and regional differences in Austria.

The results reveal a significant reduction in PM10 and PM2.5 concentrations across all four industrial regions. On average, the PM10 concentration in the four industrial regions decreased by -38.4 % from the beginning of their respective monitoring periods to 2022, while PM2.5 concentrations dropped by -36.3 %. In contrast, at the rural background monitoring stations, PM10 concentrations fell by an average of -49.5 %, and PM2.5 concentrations by -39.0 %. Among the industrial regions, the Graz region recorded the highest average PM10 concentration at the "Graz-Süd Tiergartenweg" monitoring station, with 28.9 $\frac{\mu g}{m^3}$ (2005–2022). This was followed by the Linz region at the "Linz Römerberg" station with 27.0 $\frac{\mu g}{m^3}$ (2005–2022), the greater Linz area with multiple combined monitoring stations with 23.7 $\frac{\mu g}{m^3}$ (2005–2022), the Mur-Mürz-Furche with 20.7 $\frac{\mu g}{m^3}$ (2003–2022), the Vienna region at inner-city stations with 20.4 $\frac{\mu g}{m^3}$ (2002–2022), the Vienna region near Schwechat with 20.3 $\frac{\mu g}{m^3}$ (2013–2022), and the Linz region at "Linz Neue Welt" with 20.1 $\frac{\mu g}{m^3}$ (2013–2022). In comparison, the average PM10 concentration at the rural background stations was significantly lower, at 14.5 $\frac{\mu g}{m^3}$ (2002–2022). For PM2.5, the Graz region again recorded the highest average concentration at the "Graz-Süd Tiergartenweg" monitoring station, with 20.3 $\frac{\mu g}{m^3}$ (2007–2022). This was followed by the Vienna region at inner-city stations with 16.3 $\frac{\mu g}{m^3}$ (2005–2022), the Graz region at "Graz Nord" with 15.2 $\frac{\mu g}{m^3}$ (2009–2022), the Linz region at "Linz Römerberg" with 15.2 $\frac{\mu g}{m^3}$ (2013–2022), the Linz region at "Linz Stadtpark" with 14.7 $\frac{\mu g}{m^3}$ (2009–2022), the Linz region at "Linz Neue Welt" with 14.0 $\frac{\mu g}{m^3}$ (2013–2022), and the background stations with 11.3 $\frac{\mu g}{m^3}$ (2013–2022).

At the beginning of the study period, specifically the PM10 concentrations in industrial regions were significantly higher on average than those at rural background stations. Over time, these concentrations converged, illustrating the effectiveness of regulatory measures such as the European Air Quality Directive and Austria's Immission Control Act-Air and targeted regional air quality management strategies.

This thesis also explains four key particulate matter measurement techniques that are particularly relevant in Austria: the gravimetric method, Tapered Element Oscillating Microbalance (TEOM), beta-ray absorption, and light scattering. This analysis of different measurement methods provides a fundamental understanding of the physical principles underlying the devices. Additionally, the study describes the key physical processes of aerosol particle interactions, dynamics, and behavior in the atmosphere, as well as their impact on climate and air quality, including formation, transformation, and deposition processes. In addition, the thesis addresses the health impacts of increased particulate matter concentrations on humans as well as the regulatory framework regarding air pollution legislation.

Zusammenfassung

Diese Masterarbeit untersucht die Entwicklung der Feinstaubkonzentrationen von PM10 und PM2.5 in den vier bedeutendsten Industrieregionen Österreichs – Großraum Wien, Großraum Linz, Großraum Graz und dem Großraum Mur-Mürz-Furche – im Zeitraum von 2002 bis 2022. Der Schwerpunkt liegt auf den Veränderungen der Feinstaubbelastung und deren Vergleich mit den Messergebnissen ländlicher Hintergrundmessstationen, um zeitliche Entwicklungen und regionale Unterschiede in Österreich herauszuarbeiten.

Die Ergebnisse zeigen einen deutlichen Rückgang der Feinstaubkonzentrationen von PM10 und PM2.5 in allen vier österreichischen Industrieregionen. Im Durchschnitt betrug der Rückgang der PM10-Konzentration in den vier Industrieregionen von Beginn der jeweiligen Messreihen bis 2022 -38,4 %, während die Konzentration von PM2.5 um -36,3 % zurückging. An den ländlichen Hintergrundmessstationen sanken die Feinstaubkonzentrationen im Durchschnitt um -49,5 % für PM10 und um -39,0 % für PM2.5. Im Durchschnitt wies die Industrieregion Graz an der Messstelle „Graz-Süd Tiergartenweg“ die höchsten PM10-Konzentrationswerte auf, mit 28,9 $\frac{\mu g}{m^3}$ (2005–2022). Es folgte die Industrieregion Linz an der Messstelle „Linz Römerberg“ mit 27,0 $\frac{\mu g}{m^3}$ (2005–2022), der Großraum Linz an mehreren zusammengefassten Messstellen mit 23,7 $\frac{\mu g}{m^3}$ (2005–2022), die Mur-Mürz-Furche mit 20,7 $\frac{\mu g}{m^3}$ (2003–2022), die Industrieregion Wien an den innerstädtischen Messstellen mit 20,4 $\frac{\mu g}{m^3}$ (2002–2022), die Industrieregion Wien an der Messstelle nahe Schwechat mit 20,3 $\frac{\mu g}{m^3}$ (2013–2022) und die Industrieregion Linz an der Messstelle „Linz Neue Welt“ mit 20,1 $\frac{\mu g}{m^3}$ (2013–2022). Die durchschnittliche PM10-Konzentration an den ländlichen Hintergrundmessstationen betrug lediglich 14,5 $\frac{\mu g}{m^3}$ (2002–2022). Im Falle von PM2.5 verzeichnete erneut die Industrieregion Graz die höchste durchschnittliche Konzentration, mit 20,3 $\frac{\mu g}{m^3}$ (2007–2022) an der Messstation „Graz-Süd Tiergartenweg“. Es folgte die Industrieregion Wien an den innerstädtischen Messstellen mit 16,3 $\frac{\mu g}{m^3}$ (2005–2022), die Industrieregion Graz am Messstandort „Graz Nord“ mit 15,2 $\frac{\mu g}{m^3}$ (2009–2022), die Industrieregion Linz am Messstandort „Linz Römerberg“ ebenfalls mit 15,2 $\frac{\mu g}{m^3}$ (2013–2022), die Industrieregion Linz am Standort „Linz Stadtpark“ mit 14,7 $\frac{\mu g}{m^3}$ (2009–2022), die Industrieregion Linz am Messstandort „Linz Neue Welt“ mit 14,0 $\frac{\mu g}{m^3}$ (2013–2022) und zuletzt die ländlichen Hintergrundmessstellen mit 11,3 $\frac{\mu g}{m^3}$ (2013–2022).

Zu Beginn des Untersuchungszeitraums lagen die Feinstaubkonzentrationen speziell von PM10 in den Industrieregionen im Durchschnitt deutlich über denen der Hintergrundmessstationen. Im Verlauf der Jahre näherten sich die Konzentrationen jedoch einander an. Diese Entwicklung verdeutlicht die Wirksamkeit gesetzlicher Maßnahmen, wie der europäischen Luftqualitätsrichtlinie und dem österreichischen Immissionsschutzgesetz-Luft sowie gezielte regionale Luftreinhaltungsstrategien.

Weiters werden auch die vier zentralen Messtechniken für Feinstaub erläutert, die in Österreich von besonderer Relevanz sind: die gravimetrische Methode, die Tapered Element Oscillating Microbalance (TEOM), die Beta-Strahlungs-Absorption und die Streulichtmessung. Diese Analyse der verschiedenen Messmethoden ermöglicht ein grundlegendes Verständnis der physikalischen Prinzipien, die den Geräten zugrunde liegen. Zudem wurden die wesentlichen physikalischen Prozesse erläutert, einschließlich der Wechselwirkungen, Dynamik und des

Verhaltens von Aerosolpartikeln in der Atmosphäre, ihres Einflusses auf Klima und Luftqualität sowie ihrer Entstehungs-, Transformations- und Depositionsprozesse. Darüber hinaus befasst sich die Arbeit mit den gesundheitlichen Auswirkungen erhöhter Feinstaubkonzentrationen auf den Menschen sowie mit dem rechtlichen Rahmen für die Luftverschmutzungs-Gesetzgebung.

Contents

Particulate matter (PM10 and PM2.5) and important physical properties

Aerosol particles differ in their origin, size, shape, chemical composition, and physical properties. In aerosol physics, a distinction is typically made between PM10 and PM2.5, based on the aerodynamic diameter of the particles. PM10 includes particulate matter with an aerodynamic diameter of 10 micrometers (10 µm) or less. Similarly, PM2.5 refers to particulate matter with an aerodynamic diameter of 2.5 micrometers (2.5 µm) or less. These classifications are used to group particles into size fractions that influence their behavior in the atmosphere and their impact on health, the environment and climate. While PM10 includes coarser particles, PM2.5 consists of finer particles, which are considered particularly harmful to health, as they can penetrate deep into the lungs and even enter the bloodstream, which is described specifically in the chapter “Health effects of particulate matter and air pollutants on human health”. Another important factor is the source of the particles. They can come from natural sources, such as volcanic activity or desert dust, or from human activities, like combustion processes in industry and traffic as well as agriculture activities. Particulate matter from human-made sources is especially concerning because it can contain multiple harmful substances like heavy metals, soot and chemicals, further increasing health risks. There is also a distinction made between primary and secondary particles. Particles that can be directly traced to a specific emission source are referred to as primary particles. These are generated for example by combustion and mechanical processes in industrial activities. They are typically larger and can reach sizes of up to many micrometers. In contrast, secondary particles are formed through chemical transformation processes in the atmosphere, where gaseous precursors like sulfur dioxide (SO_2), nitrogen oxides (NOx), or ammonia (NH_3) are converted into solid or liquid particles. These particles are usually smaller and in the nanometer range and can grow into larger aggregates through condensation or collisions with other particles. [1] [2]

The history of aerosol physics in Austria and in Vienna

The development of aerosol physics in Austria is closely tied to Othmar Preining, a pioneering figure in the field. Despite the challenges posed by the 20th century, such as World War II and limited research funding, Preining succeeded in establishing a renowned research group in Vienna. Born in 1927, Preining faced significant health issues during his youth, which disrupted his education. Nevertheless, he developed a passion for mathematics and astronomy, leading him to pursue studies in these subjects at the University of Vienna in 1946. He was particularly influenced by physicist Felix Ehrenhaft, whose work on the electrical charge of particles greatly shaped Preining's scientific direction.
Preining quickly focused on the study of nanoscale aerosol particles, earning his doctorate in 1951 with a dissertation on the photophoretic movement of steel particles. After completing his Ph.D., he began his academic career in Vienna, while also expanding his research in the U.S., notably at the California Institute of Technology (CALTEC). There, Preining worked on submicroscopic aerosol particles and developed an aerosol spectrometer. Despite receiving a job offer in the U.S., he chose to return to Vienna in 1960, where he continued his research.
He established a research group dedicated to ultrafine particles and mentored several prominent scientists. In 1968, Preining became a professor of experimental physics at the

University of Vienna, holding this position until 1995. During this time, he was heavily involved in the development of aerosol analysis instruments and became a supporter for environmental protection, particularly concerning air quality improvements in Austria. He chaired various environmental commissions, including the CO_2-Commission, and contributed to the formulation of national air quality standards. His international engagements, including guest professorships in the U.S. and Japan, earned him global recognition and solidified his influence in the field of aerosol research.
Even after his official retirement, Preining remained active in scientific circles. He chaired the Austrian Commission for Clean Air and spearheaded the AUPHEP project, which focused on the health impacts of aerosols. He also organized international symposiums on the history of aerosol science and contributed to the development of key instruments, such as the Size Analyzing Nucleus Counter. Despite significant health challenges, Preining continued his scientific pursuits until his death in 2007, leaving a lasting impact on the field.
Preining's most notable contributions to aerosol physics include the development of advanced measurement instruments and his research into the health and climate impacts of aerosol particles. His work on nanoparticle formation and aerosols' role in climate change brought worldwide attention. Under his guidance, his students and colleagues developed numerous innovative tools widely used in international aerosol research, including the Berner Impactor, the Telephotometer, and the Vienna Differential Mobility Analyzer (DMA). These instruments were deployed in projects like the Southern California Air Quality Study and EUROTRAC.
The Vienna aerosol research group that Preining founded became a player in international aerosol research. Under his leadership, the group participated in numerous international collaborations and hosted significant scientific events. He was awarded with the Erwin-Schrödinger-Preis in 1982 and was full member of the Austrian Academy of Sciences from 1992 onwards. [3] [4]

Aerosol particle production processes

Homogeneous and heterogeneous nucleation processes

Through two fundamental processes, nucleation and dispersion, new aerosol particles can enter the atmosphere in addition to the direct release of primary particles. One key mechanism is homogeneous nucleation (also referred to as homogeneous condensation of supersaturated vapors), where supersaturated vapor molecules condense directly from the gas phase to form new particles, typically smaller than 1 µm. This process occurs when a gas becomes supersaturated due to chemical reactions or rapid temperature changes, leading to the formation of new molecules that aggregate and condense into stable particles. A notable example of this is the formation of sulfuric acid vapor from sulfur dioxide (SO_2), which reacts chemically in the atmosphere to produce sulfuric acid (H_2SO_4). This sulfur dioxide is a relevant precursor to fine particulate matter through various chemical and physical processes.
Homogeneous nucleation occurs in the absence of any pre-existing solid or liquid surfaces, requiring very high vapor supersaturation to initiate the process. Specifically, this reaction from sulfur dioxide to sulfur acid plays an important role regarding the particulate matter emission from the industry sector and the anthropogenic sources in general, which will be discussed later.

The formation of sulfuric acid in the atmosphere plays a critical role in the creation of new condensation nuclei, primarily through the oxidation of sulfur dioxide. Due to its extremely low vapor pressure, sulfuric acid tends to condense in the presence of water vapor and ammonia, making it a key component for homogeneous nucleation. Anthropogenic ammonia (NH_3) is released into the atmosphere in large quantities, primarily from agricultural activities, which account for approximately 80 % of global ammonia emissions. [5] Typical SO_2 concentrations in central Europe range from 2 to 10 $\frac{\mu g}{m^3}$ in urban areas, especially in winter the values can be higher. This seasonal increase is due to greater emissions during heating periods and weather conditions that inhibit air exchange. While sulfur dioxide emissions have decreased significantly in Europe, North America, and Japan over the past decades, countries like China saw increased concentrations (up to 400 $\frac{\mu g}{m^3}$) due to extensive coal usage for energy and industry production. In urban and industrial areas with high levels of SO_2 emissions and other pollutants, this process significantly increases the concentration of fine particulate matter in the air. The increased presence of fine particles exacerbates air quality problems and increases health risks, as exposure to such particles is linked to respiratory diseases, cardiovascular problems, and other adverse health effects. Since around 2007, China has also been experiencing a decline in SO_2 emissions. Sulfur dioxide has an average atmospheric lifetime of 1 to 4 days, during which about half is oxidized into sulfuric acid or sulfate. The remaining SO_2 is either removed by precipitation or absorbed at the Earth's surface. Slightly more than half of the sulfur dioxide remaining in the atmosphere is involved in heterogeneous processes, the other portion contributing to homogeneous nucleation. [6] Once released into the atmosphere, SO_2 undergoes chemical reactions, primarily photochemical oxidation by adding hydroxyl radicals (highly reactive molecules consisting of one oxygen atom bonded to one hydrogen atom (OH)) to sulfur dioxide, to form sulfuric acid (H_2SO_4). These reactions are especially efficient in the presence of sunlight and water vapor, making them more prominent in the summer when photochemical reactions are faster. [6] [7]

It is worth mentioning that in the free troposphere, homomolecular homogeneous condensation or nucleation of a single type of molecule hardly ever occurs. Due to the absence of other molecular species, the necessary supersaturation is not given. If the system consists of two or more molecular species, nucleation is possible, which then takes place in a hetereomolecular system if the mixture of the components is exothermic. This is because the so-called saturation vapour pressure, which marks the equilibrium where evaporation and condensation rates are equal, can be significantly lower than that of a single molecule species. A higher free energy barrier ΔG, which represents the energy needed to form a new stable nucleus, usually leads to a lower nucleation rate J, meaning fewer nuclei are formed in a given time and volume.
An example of this hetereomolecular system is the addition of water to sulphuric acid, which already has a very low saturation vapour pressure ($3.3 \cdot 10^{-5}$ hPa at 23 °C for sulphuric acid [8]), can be reduced by two orders of magnitude if only 20 % water is added. However, this combination of those two does not occur very frequently in the natural troposphere, as there is significantly more water vapour in the atmosphere than sulphuric acid. [6] [8] [9]

In the presence of existing aerosol particles, sulphuric acid molecules and water vapour can also form new particles by heterogeneous nucleation, i.e. condensation on existing aerosol particles. In contrast, heterogeneous nucleation (heterogeneous condensation) occurs when condensation takes place on pre-existing solid or liquid particles, known as condensation nuclei. Particles like mineral dust or sea salt can serve as these nuclei. If the radii of the existing particles, the condensation nuclei, are large enough, then the supersaturation does not have to

be as high as in the case of homogeneous nucleation in order to form new particles. For seed particles smaller than 5 nm, heterogeneous nucleation is enhanced by electrical charges and also influenced by surface wettability, typically described by the contact angle. Furthermore, if the contact angle is less than 180 °, any size of the condensation nuclei would essentially lower the necessary supersaturation. In contrast to homogeneous nucleation, where the nucleation rate changes monotonically with temperature, in heterogeneous nucleation it can either increase or decrease depending on temperature variations. Overall, it can be said, that heterogeneous nucleation has a thermodynamic and energetic advantage over homogeneous nucleation. It is important to emphasize that homogeneous nucleation still plays a prominent role in the formation of new particles, as heterogeneous condensation not only depends on the energy for condensation on existing particles but is also restricted by the limited diffusion speed of the molecules to these particles. This means that not all molecules can diffuse quickly enough to the surfaces of the existing aerosol particles and adhere. If many new condensable molecules are created at the same time, they can therefore accumulate in sufficient concentration to form new particles on their own through homogeneous nucleation. This was already proven at the end of the 1970s by Middleton and Kiang that under real atmospheric conditions, homogeneous nucleation is still a relevant process even if a certain amount of nuclei are already present for condensation, but with lower nucleation rates than in a completely vaporized system. [10] [11] [12]

Dispersion processes

In addition to nucleation, dispersion and resuspension from surfaces plays a crucial role in particle formation, most of them in the range between 1 µm to 10 µm, but up to 100 µm. In this process, particles that are already in condensed form, such as mineral dust on the ground or sea salt nuclei through bursting of water bubbles on sea’s surface, are lifted from the Earth's surface and transported into the atmosphere. Dispersion particles are produced through complex processes at the Earth's surface, influenced by various mechanisms. Two important ones are the resuspension of dust by wind or human activities, and the production of sea salt particles from ocean surfaces. Dust resuspension begins when particles are moved across the surface by wind or mechanical activities. As the particles roll or slide, the contact between them and the surface weakens, reducing the adhesion forces that hold them to the ground.
This allows aerodynamic forces to lift the particles into the air. For very small particles, typically those under a few tenths of a micrometer, adhesion forces dominate, which explains why such small particles are less commonly found in large quantities in natural dispersions.
A consequence of the movement is that particles can collide with surface irregularities, gaining vertical momentum. This "bouncing" mechanism causes particles to jump off the ground, potentially setting more particles in motion, creating a sort of "avalanche effect." This increases the number of particles being lifted into the air. Studies indicate that this natural process only begins at a certain wind speed, but once initiated, the amount of particles resuspended grows rapidly with increasing wind velocity. The wind speed required to lift particles depends on their size: smaller particles stick more firmly to the ground due to stronger adhesion forces, while larger particles need significantly stronger winds to be lifted. The optimal size for resuspension is around 10 µm in diameter, as these particles are neither too strongly bound to the surface, nor do they require excessive wind force to be mobilized. [6] [13]

In urban and industrial areas, human activities such as mining and landfills significantly contribute to the generation and resuspension of particulate matter, beyond what is produced by natural processes. On the other hand, a considerable portion of atmospheric dispersal aerosols originates from organic material such as plant fragments, bacteria, fungal spores (typically ranging from 1 µm to 10 µm), and pollen (which range from 10 µm to 100 µm in size). [14] These organic components are constantly present in the air and contribute to the overall aerosol particle exposure, especially during specific seasonal and biological events.
Most particles up to a maximum size range of 10 µm to 20 µm remain in the atmosphere for a relatively long time; if they are heavier and larger, gravitational sedimentation predominates and they are lowered to the ground relatively quickly.

Another key process in the formation of aerosol particles is the creation of sea salt particles. Alongside common mineral dust, these sea salt particles play an essential role as natural aerosol particles. They can act as cloud condensation nuclei, which are critical in the formation of cloud droplets and can influence the climate and global radiation balance. The liquid particles are formed when bubbles at the ocean's surface burst, particularly when wind speeds exceed approximately $3\,\frac{\mathrm{m}}{\mathrm{s}}$ or when dry sea salt particles evaporate from the sea spray. [6]

Impact of aerosol particles on earth's atmosphere and solar radiation

In addition to the fundamental chemical composition of our atmosphere, which consists of approximately 78.09 % nitrogen (N_2), 20.95 % oxygen (O_2), 0.93 % argon (Ar), and trace amounts of neon (Ne), helium (He), krypton (Kr), and xenon (Xe), aerosol particles and other variable trace gases play a significant role in atmospheric processes. The most crucial trace gases include water vapor (H_2O), carbon dioxide (CO_2), methane (CH_4), ozone (O_3), nitrous oxide (N_2O), nitrogen oxides (NOx), carbon monoxide (CO), sulfur compounds, and ammonia (NH_3), among many others. Aerosol particles in the atmosphere ranging in size from approximately 10 nm to 100 µm, mostly around 10 µm, typically have a concentration near the Earth's surface of about 10^4 particles per cm^3 over land. In cleaner air environments, this concentration drops to about 10^3 particles per cm^3, while in densely populated urban regions, the concentration can significantly exceed 10^5 particles per cm^3. In maritime clean air, the concentration regularly falls to about 10^2 particles per cm^3. At altitudes greater than 5 km above the ground, the particle concentration further decreases, sometimes reaching only a few hundred particles per cm^3. [6]

When it comes to the Earth's radiation balance and climate, only a select few of these trace gases, mostly carbon dioxide, water vapor, ozone, methane, and nitrous oxide, along with aerosol particles, are particularly significant. These components greatly impact the radiation and energy balance of the atmosphere due to their ability to absorb and scatter radiation. They influence the properties of the atmosphere and have profound effects on the global climate. The global CO_2 concentration in the year 2023 was recorded at 419.55 ppm (parts per million). This marks a 5 % increase compared to the year 2015, when a concentration of approximately 400 ppm was observed in Central Europe. In the pre-industrial era, during the first half of the 19th century, the CO_2 concentration was significantly lower, at just 280 ppm.
In contrast to carbon dioxide, the concentration of water vapor and ozone is not as globally uniform. Water vapor levels are mainly regulated by local evaporation and condensation processes, which determine their lifespan and concentration, while ozone concentrations are mostly influenced by atmospheric chemical reactions. [6] The current globally consistent

concentration of atmospheric carbon dioxide varies locally by about 10 ppm, depending on the season. For example, in colder months in Austria, there is a greater need for heating, often using fossil fuels or biomass power plants, which leads to higher fine particulate matter pollution during the winter months compared to warmer seasons. A study by Li et al. [15] from the year 2021 investigated the seasonal concentration and characterization of particulate matter in an industrial region in Southeast Asia. The results showed that there was an increased concentration of particulate matter larger than 1.8 micrometers during spring and summer and an increased concentration of fine particulate matter between 1.8 and 0.1 micrometers during autumn and winter. In addition, water-soluble ions, metallic elements, mostly Na, Fe, Ca, Al, and Mg as well as dioxins were analyzed. The results showed that the number of metals sampled from the ambient air correlates with the activity of the local steel and iron industry, especially the activity of burning fossil fuels and the high-tech industry. [6] [16]

Tropospheric aerosol particles in the deepest layer of the atmospheric structure affect the Earth's radiation and energy balance by influencing both direct and indirect processes.
Directly, tropospheric aerosol particles can alter the radiation budget and energy budget of the Earth's atmosphere through the direct backscattering of solar radiation, the absorption of solar radiation and the absorption and thermal emission of terrestrial radiation, changing the planet's overall reflectivity, known as the planetary albedo. According to Yu et al. [17], the direct influence on terrestrial radiation is not particularly large and only for larger particles, the first two mentioned direct effects have a larger impact on the radiation budget.
Indirectly, tropospheric aerosol particles contribute to cloud formation and development by acting as cloud condensation nuclei. This process changes the reflectivity of clouds, or albedo, as well as their lifetime and thickness, which further affects climate dynamics. These indirect effects of tropospheric aerosol particles are specifically relevant regarding the influence on the radiation budget of short- and long-wave radiation by changing the mentioned cloud properties. Aerosol particles, by enhancing this reflective capacity through altering cloud properties, can lead to cooling effects on the climate. Tropospheric aerosols particles, particularly those resulting from anthropogenic sulfur dioxide emissions, have a cooling effect and thus act as a kind of "correction" to the climate-relevant trace gas emissions like CO_2 from human activities, which have a significant warming effect. This interaction between aerosols and radiation is a critical factor in understanding global climate patterns and variability. [6]
The mentioned albedo is a measure of how much solar radiation is reflected by a surface.
It ranges from 0, indicating total absorption, to 1, indicating total reflection. Earth’s surface and atmosphere reflect sunlight differently, with the surface (ground albedo) reflecting a variable amount depending on the material. For example, fresh asphalt reflects about 4 %, grasslands reflect around 25 %, and freshly fallen snow can reflect as much as 80 %. The planetary albedo, which measures the Earth's total reflective capacity, averages around 29.4 %. [6] [18]

A larger number of small aerosol particles in the range of a few tenths of a micrometer and larger increases this reflectivity of clouds. This is because the existing amount of water meets a larger number of small aerosol particles, the condensation nuclei, so that more small cloud droplets are formed, and these together have a larger total scattering cross-section.
This phenomenon is also known as the Twomey-effect and was discovered in 1977 by Sean Twomey. This increases the reflectivity of clouds, but also their lifespan. The small cloud droplets also have a longer residence time in the ambient air than larger particles because they fall to the ground less quickly and exhibit fewer coalescence processes. The amount of suitable aerosol particles that act as condensation nuclei is especially important when evaluating the relevance of indirect aerosol effects of aerosol-cloud interactions. The chemical composition

and age of aerosol particles is considered less critical and important when it comes to their effectiveness as cloud condensation nuclei, while the size distribution of these particles plays a much more significant role. [19] [20]

Coming back to the direct effects on the radiation budget, i.e. the scattering and absorption of radiation from the sun, attracts a great amount of attention from the public. Well-known examples of this nowadays are the smog layers from various air pollutants nowadays in many large Indian and Chinese cities (Figure 1). The poor air quality in these areas with heavy traffic and industrial activities, where necessary measures and filtration systems are lacking, has a massive impact by significantly weakening solar radiation (by almost an order of magnitude) and severely harming human health by far exceeding the established limit values. The problem has been known for a long time, for example the smog of London in 1952 or the smog events in Los Angeles in the 1940s. [6]

Figure 1: Smog in a city in India [21]

However, this very strong regional phenomenon, where sometimes one can't even see the blue sky on a cloudless day, caused by the massive presence of smog, does not have such a large influence on global cimate. On the other hand, sulphuric acid or sulphate have a considerable global influence on the climate. These absorb almost no solar radiation, as they have a very large specific scattering cross-section and reflect solar radiation very well. This in turn increases the Earth's albedo and leads to a loss of energy and a cooling effect for the climate. Sulfuric acid and sulfate particles are particularly effective in increasing the Earth's planetary albedo, contributing significantly to the cooling effect. These particles form, as mentioned before, through the oxidation of sulfur-containing precursor gases, which originate from both natural sources, such as oceans and volcanic activity, and anthropogenic emissions, like industrial processes. Per year approximately 30 Mt sulfuric acid and 60 Mt sulfur dioxide are emitted from natural sources according to Charlson et al. [22]. Since the late 19th century, human emissions of sulfur dioxide, primarily from combustion processes, have steadily increased. It was only in the last two decades that Europe and North America saw a decline in these emissions, largely due to more efficient flue gas cleaning systems in the industry and reduced reliance on furnance heating. In contrast, emissions in East Asia, especially China, have raised at this time significantly. Currently the anthropogenic emissions reach approximately 50 Mt to 60 Mt of

sulfur annually, which is equivalent to about 100 Mt to 120 Mt of sulfur dioxide. Since the 1940s, anthropogenic-caused production rates have surpassed natural sources. As previously mentioned, a fraction of sulfur dioxide is transformed into sulfuric acid, with approximately 25 % of the available amount being oxidized in the gas phase. This leads to an annual production of around 80 Mt of sulfuric acid, with roughly 70 % originating from human activities and 30 % from natural sources. The sulfuric acid then condenses into droplets, forming either sulfuric acid-water mixtures or sulfate particles in the presence of substances like ammonium. These particles coagulate within hours, with their radius typically measuring a few tenths of a micrometer. [6]

On a global scale, approximately 0.25 % of incoming radiation, or about 1 $\frac{W}{m^2}$, is scattered back into space by aerosol particles. Of this, around 0.3-0.4 $\frac{W}{m^2}$ is attributed to natural sources, and 0.6-0.7 $\frac{W}{m^2}$ results from human activities. While these values are smaller compared to the effect of anthropogenic greenhouse gases on the Earth's radiation balance (about 3 $\frac{W}{m^2}$), they are of a similar magnitude but with an opposite sign, as aerosol particles generally have a cooling effect. To put this in perspective, the best current estimate for the annual average energy flux of solar radiation hitting the Earth vertically, averaged over one year an, known as the solar constant, is about 1360 $\frac{W}{m^2}$ ± 3.4 %. This highlights the significance of aerosol particles in influencing the Earth's climate, albeit smaller compared to greenhouse gases. To be mentioned is, that localized anomalies can occur because concentrations can differ in specific regions, particularly in industrial areas, where the backscattering of radiation from these particles can reach levels between 2 $\frac{W}{m^2}$ and 5 $\frac{W}{m^2}$. This uneven distribution leads to regional effects on the radiation balance and local air pollution and thus residents' health conditions. [6] [22]

Cleaning the atmosphere from particles and substances through wet deposition

The process of removing particles and substances from the atmosphere through wet deposition/precipitation involves two main aspects: the cleaning of the air from various particles, such as PM2.5 and PM10, and the chemical composition of rainwater. While precipitation effectively removes aerosol particles and air pollutants from the atmosphere, its influence on the concentration of trace gases is generally minimal. When examining the washout processes of aerosols, two main mechanisms are identified: "rain-out" and "wash-out." The "rain-out" occurs within the cloud before raindrops form, while "wash-out" refers to the removal of aerosol particles by falling raindrops. In recent literature, "wash-out" is often used as a general term for both processes. The "rain-out" mechanisms can be categorized into three primary groups before the actual forming of precipitation within the cloud

1. Condensation nuclei consumption: The tiny particles in the atmosphere serve as condensation nuclei, on which water vapor condenses, and cloud droplets are forming.
2. Diffusion: Tiny particles diffuse toward already-formed cloud droplets due to their random motion.

3. Phoretic effects, such as the Stefan-Flow: As water vapor condenses on the surface of droplets, it generates a flow toward the droplet. This flow, known as Stefan-Flow, carries nearby particles toward the droplet.

When a new cloud forms, it typically contains about 100 to 300 cloud droplets per cubic centimeter. In general, one finds also this amount of aerosol particles with a diameter larger than 0.1 μm per cubic centimeter. This could be interpreted as that these particles mostly serve as condensation nuclei. Looking at the size distribution of aerosol, one finds that most of the aerosol's mass in an average atmospheric aerosol is brought into cloud droplets due to condensation. [6]

Smaller particles, those less than 0.1 μm in size, attach to the droplets primarily through diffusion. It's important to note that diffusion and phoretic effects contribute only minimally to the concentration of substances and particles in rainwater, which occur in the "rain-out" processes. The main factor in this process is the role of condensation nuclei, which allows most aerosol particles to become part of cloud droplets. Thus, while smaller particles do join cloud droplets via diffusion, the presence of condensation nuclei remains the critical mechanism driving cloud formation and the subsequent removal of aerosol particles. The mechanism of phoretic effects has an even smaller contribution to the concentration of substances in rainwater than diffusion, in some cases an order of magnitude smaller than the contribution of diffusion. [6]

One can find the partial concentration of substances $c_{rain,condensation}$ in precipitation water through the process of condensation nuclei, with the following approximation in Formula 1

$$c_{rain,condensation} = \frac{c_{air}}{L} \cdot \varepsilon_c$$

Formula 1: Substance concentration in rainwater through condensation nuclei processes

with c_{air} as the concentration of the substance in the air, L the liquid water content of the cloud and ε_c as the partial washout efficiency, which is between 0.5 and 1 for particles larger than 0.1 μm. [6] One can find the equivalent assumption in Formula 2 for the partial concentration of substances through the process of attachment by diffusion of particles on cloud droplets for smaller particles

$$c_{rain,diffusion} = \frac{c_{air}}{L} \cdot \varepsilon_d \cdot (1 - \varepsilon_c)$$

Formula 2: Substance concentration in rainwater through diffusion processes

ε_d as the partial washout efficiency of the diffusion process and the last term ensures, that the part of particles, which were used in the condensation nuclei processes, are not included more than once. ε_d is around the value of 0.1 for small particles around 0.01 μm. [6]

This "rain-out" process was originally based on the models developed by Christian E. Junge in 1963 and 1975 and Rudolf J. Engelmann in 1970. This model was extended by Pao K. Wang in 1978 with his paper "On the Effect of Electric Charges on the Scavenging of Aerosol Particles by

Clouds and Small Raindrops" to include electrostatic forces. This extension showed a clear increase in the accumulation rate and probability of small particles in the size range of 0.01 µm and 0.1 µm on cloud droplets through electric effects. In this size range, the effects of diffusion and further attachment of particles as well as their effect as condensation nuclei are very ineffective. [6] [23] [24]

If the concentration of a substance in the atmosphere does not vary significantly with altitude, the proportion of material of the total amount washed out by falling rain below the clouds is generally small. However, if the concentration of the substance is significantly higher under the cloud layer, such as in areas near industrial emission sources, the proportion of the effectiveness of the “wash-out” increases significantly. This effect is especially effective for larger particles with diameters exceeding 10 µm. Due to their size, these particles are removed from the atmosphere more efficiently by precipitation. This process plays an important role in regions with high concentrations of particulate matter, especially PM10, as rainfall can significantly reduce the amount of airborne pollutants in such areas.

Various mechanisms contribute to the "wash-out" of particles by rain, depending on particle size. Larger particles can be directly captured by falling raindrops in a process similar to coalescence, where droplets merge together. For smaller particles with radii below 0.1 µm, aerodynamic effects prevent direct capture, and thermal diffusion is effective only for the smallest particles, although even then it is not highly efficient. Particles around 0.1 µm are in a size range where neither direct capture nor diffusion plays a significant role due to the low efficiency of these mechanisms. In such cases, the mentioned electrostatic forces may increase the likelihood of capture. Another phenomenon occurs below the clouds with undersaturation of the water vapor, where raindrops partially evaporate. As the drops cool due to a partial evaporation of the water, thermal forces create an air flow that transports aerosol particles from the warmer surroundings toward the cooler droplets.

To complement the partial concentration $c_{rain,wash-out}$ of substances in rainwater, we find for the wash-out process in Formula 3, with the assumption, that the concentration of the substances in the rainwater is proportional to the one in air and height of fall *H*, that

$$dc_{rain,wash-out} = -\sigma * \ c_{air} * \ dz$$

$$c_{rain,wash-out} = \int_0^H dc_{rain,wash-out} = -\sigma \cdot \int_0^H c_{air} \cdot dz = \sigma \cdot \bar{c}_{air} \cdot H$$

Formula 3: Substance concentration in rainwater through wash-out

with the proportionality factor σ (cross section of an air column), *z* as the vertical coordinate and $\bar{c}_{air}$ as its concentration in the air, over the distance *H* averaged. [6]

On average, for typical rainfall amounts, the quantity of substances from aerosols contained in one liter of rainwater is approximately equivalent to the amount found in 300 to 1000 cubic meters of air. Therefore, one can assume that the aerosol particles inside in rain and cloud water significantly impact the chemical composition of the water. However, due to the considerable variability in aerosols and the composition of rainwater, it is challenging to make generalized statements. A rough estimate suggests that approximately 10 mg to 100 mg of aerosol particle mass per liter of rainwater is present, with the most common components

being soot, silicates, sulfates, nitrates, chlorides, calcium, sodium, iron, aluminum, and ammonium. When cloud droplets hold particles, they incorporate them as solid or dissolved components. As rain falls, these particles are typically removed from the atmosphere. About 90% of the falling droplets evaporate before reaching the Earth's surface, especially in drier air layers. During this evaporation process, the dissolved or solid aerosol components remain, resulting in modified particles. This cycle of absorption and evaporation can repeat multiple times, further altering the composition of the aerosol particles in the atmosphere. [6] [25] [26] [27]

The average lifespan of aerosol particles due to wet deposition is estimated to be around 4 to 6 days, and as the majority of aerosol mass falls within this intermediate size range, this is a good indicator for the average lifetime of aerosol mass in the atmosphere. Ruprecht Jaenicke developed an approximate Formula 4 to calculate the mean lifetime of aerosol particles in the atmosphere as a function of their particle radius as follows

$$\frac{1}{\tau} = \frac{1}{\tau_{wet}} + \frac{1}{\tau_0} \cdot \left(\frac{r}{r_0}\right)^{-2} + \frac{1}{\tau_0} \cdot \left(\frac{r}{r_0}\right)^{2}$$

Formula 4: Mean lifetime of aerosol particles dependent on their radii

where τ_{wet} is the partial life span of a particle for wet deposition, r the radius of the particle, while τ_0 and r_0 are constants. Thus, the primary factor determining the lifetime of aerosol particles is their size. Very small particles (< 0.001 µm) typically remain in the atmosphere for only a few minutes due to rapid removal by diffusion and coagulation. Similarly, larger particles (> 100 µm) settle quickly mainly due to gravitational sedimentation. Particles in the size range between 1 µm till 10 µm have the longest lifetime and travel as well the longest distances. [28] [29]

Dry deposition of aerosol particles

The dry deposition of aerosol particles refers to the process in which particles reach the earth's surface directly without the influence of precipitation. This occurs through various mechanisms, depending on the particle size. For very small particles, under 0.1 μm, diffusion plays a dominant role, where this random movement deposit particles. When it comes to larger particles with few micrometers, like PM2.5 and PM10, diffusion becomes more ineffective, and processes such as inertial deposition and gravitational sedimentation take dominance, which we will discuss now. In the case of inertial deposition, particles cannot follow the air stream due to their mass and are carried towards surfaces. For very large particles, over 10 μm, gravity becomes the dominant force, causing them to settle more rapidly toward the ground. PM2.5 and PM10 are particularly significant in these processes as they can be effectively removed from the air by both inertia and gravity.

The gravitational deposition, also known as sedimentation, is a relative movement of aerosol particles in a carrier gas which is determined by the driving gravitational force F_G and braking viscous frictional force $F_{frictional}$. In the size and velocity range that is important for gravitational separation, the resistance that a particle experiences during its movement relative to the carrier

gas is described by the Stokes law [1] [6], describing the frictional force $F_{frictional}$ acting on spherical particles in Formula 5

$$F_{frictional} = -6 * \pi * \eta * r * v$$

Formula 5: Friction force $F_{frictional}$

The dynamic viscosity η of the gas, the particle radius r, and the relative velocity v between the carrier gas and the particle are central parameters in Stokes' law. At the same time, the particle is acted upon by the gravitational force F_G, seen in Formula 6

$$F_G = \frac{4\pi}{3} \cdot r^3 \cdot \rho \cdot g$$

Formula 6: Gravitational force F_G

determined by its particle density ρ, particle radius r, and gravitational acceleration g. The sedimentation velocity v, which describes the rate at which particles settle due to gravity, is derived from the equilibrium between the friction force and the gravitational force acting on the particle, seen in Formula 7 as

$$v = \frac{2 \cdot r^2 \cdot \rho \cdot g}{9 \cdot \eta}$$

Formula 7: Sedimentation velocity v

For instance, using the formula above for particles with a density of approximately 1 $\frac{\mathrm{g}}{\mathrm{cm}^3}$ and with a radius of 1 µm, they have a sedimentation velocity of around 0.013 $\frac{\mathrm{cm}}{s}$, while a particle with a radius of 10 µm falls at a rate of about 1.3 $\frac{\mathrm{cm}}{s}$. For particles smaller than 1 µm, especially under 100 nm, the slip-correction needs to be considered, as the interaction between particles and gas molecules becomes relevant. These differences in sedimentation velocity are crucial for understanding how long particles remain in the atmosphere and how effectively gravity removes them from the air. Specifically, PM2.5 tends to stay suspended longer, increasing its dispersion and the associated health risks, whereas PM10 particles settle more quickly and are thus removed from the air more efficiently. [1] [6]

Inertial deposition describes the process where particles, due to their inertia, are unable to follow the air stream, particularly when it curves near surfaces or in turbulent regions. Two crucial parameters here are the brake relaxation time τ and the stopping distance Λ. The brake relaxation time τ refers to the time it takes for a particle to slow down due to viscous frictional force and adjust its velocity relative to the carrier gas (e.g., air). The stopping distance Λ is the distance the particle travels before coming to a stop. Assuming an aerosol particle is moving relative to a carrier gas, viscous friction tries to slow the particle. Provided, that this relative velocity v between aerosol particle and carrier gas is not too high, proportionality can be assumed between the frictional force $F_{frictional}$ and the change in velocity over time $\frac{dv}{dt}$ to v. The

brake relaxation time τ [1] [6], i.e. the time it takes for a particle to adapt to the surrounding fluid velocity and slow down, can be expressed as

$$\tau = -\frac{v}{\frac{dv}{dt}} = -\frac{v}{\frac{F_{frictional}}{m}} = -\frac{v * m}{F_{frictional}}$$

Formula 8: Brake relaxation time τ

The mass *m* is the particle mass in this Formula 8. For particles in air under ideal atmospheric conditions, the brake relaxation time primarily depends on the particle's properties, such as size and density, and the characteristics of the gas. For instance, a spherical particle with a radius of 1 µm and a density of 1 $\frac{g}{cm^3}$ has a brake relaxation time of approximately 1.3×10^{-5} seconds. In contrast, a particle with a radius of 10 µm requires about 1.4×10^{-3} seconds to decelerate. This difference in brake relaxation times highlights how larger particles tend to maintain their momentum for a longer duration, which is important for understanding processes like inertial or gravitational deposition, where heavier particles are more likely to be deposited onto surfaces due to their inability to follow the air stream as easily as smaller particles.

The distance travelled during brake relaxation time τ in a constant moving or at rest carrier gas, is the stopping distance Λ. It is the length, which a particle with initial velocity v_0 and no other forces acting travels till its relative velocity to the gas is zero, as seen in the following Formula 9

$$\Lambda = v_0 * \int_0^\infty e^{-\frac{t}{\tau}}\, dt = v_0 * \tau$$

Formula 9: Stopping distance Λ

Another concept is the mobility *B*, which is a measure of how easily a particle moves under the influence of an external force *F*. When a particle is subjected to an external force, it can accelerate, but as its velocity increases, the frictional force $F_{frictional}$ between the particle and the surrounding gas also increases. This frictional force is proportional to the particle's velocity. Once the frictional force becomes equal to the applied external force, the particle reaches a constant velocity.
This constant velocity is directly proportional to the applied force, which leads to the relationship in Formula 10 [1] [6]

$$v = B * F = -B * F_{frictional}$$

Formula 10: Mobility relation

The mobility can be rewritten in Formula 11 with the particle's mass and brake relaxation time as

$$B = \frac{\tau}{m}$$

Formula 11: Mobility *B*

To come back to inertial separation, it is based on the fact that larger particles are no longer able to follow the microturbulent movement due to their inertia as soon as their stopping distance reaches approximately the dimensions of the turbulence elements. In this case, a particle that no longer follows the curvature of the turbulent flow near a surface may fly towards the surface due to its inertia and be separated there. [1] [6]

Life cycle of aerosol particles and distribution in the troposphere

After having discussed the production processes of particles, their effects on the climate and their possible depositions, the following Figure 2 illustrates and summarizes the entire transformation cycle of aerosol particles in the troposphere.

It shows the possible processes of aerosol particles, starting with the formation of new particles through nucleation of very small particles or direct emissions of particles, and continuing with their transformation via processes such as coagulation, dispersion, condensation, cloud formation, chemical reactions and accumulation. These processes change the original properties of the particles, like their chemical composition, size and concentration. These aged mixed aerosol particles after their transformation processes are then removed from the atmosphere either by wet or by dry deposition after time.

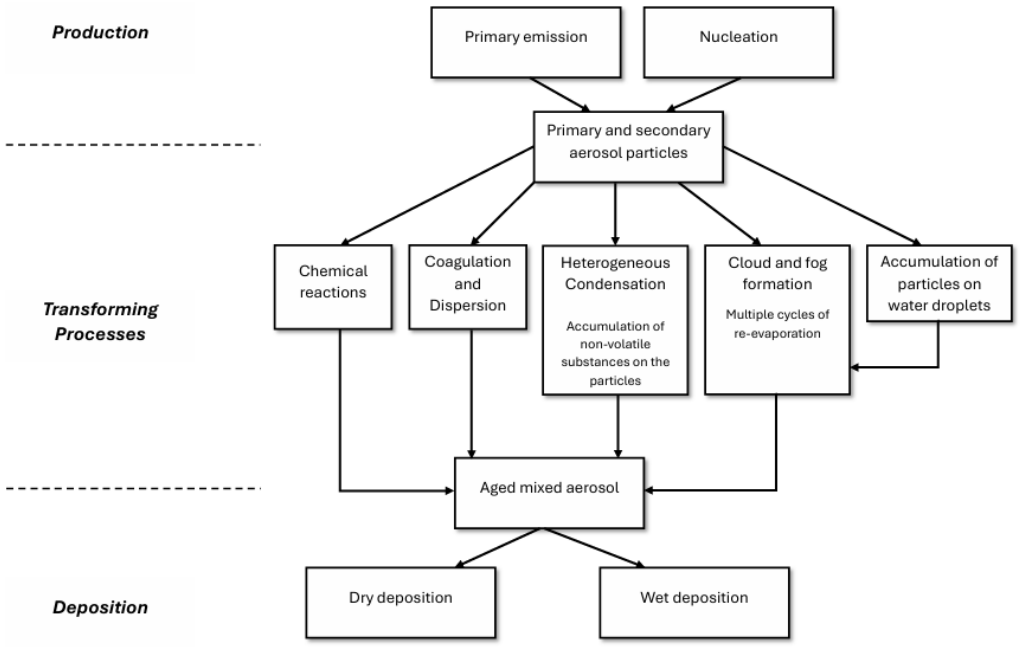

Figure 2: Transformation processes of aerosol particles in the Troposphere (inspired by [6])

These aged mixed aerosols often contain soluble or hygroscopic (water attracting) substances that absorb moisture from the surrounding air. Even particles that were initially hydrophobic (water repellent), such as carbonaceous aerosol particles or soot, can be transformed into hydrophilic particles over a period of hours or days. This transformation occurs through photochemical reactions or the condensation of water-soluble compounds like sulfuric acid on the outer layers of particles. Once converted to hydrophilic particles, they begin to attract moisture from the air, causing changes in both their size and their physical properties, especially how they scatter or absorb light. [6] [25]

The following Figure 3 roughly outlines the vertical distribution of the number density of tropospheric aerosol particles, distinguishing between continental and maritime aerosol particles. The vertical distribution of aerosols in the troposphere depends on the region and the type of particle. Over continental areas, the number density of aerosol particles decreases by about two orders of magnitude up to an altitude of approximately 5 km and remains relatively constant up to the tropopause at around 13 km. In contrast, the density of sea salt particles drops sharply above a few hundred meters and is almost non-existent above 3 km. This is due to the high solubility of sea salt particles, making them effective condensation nuclei.

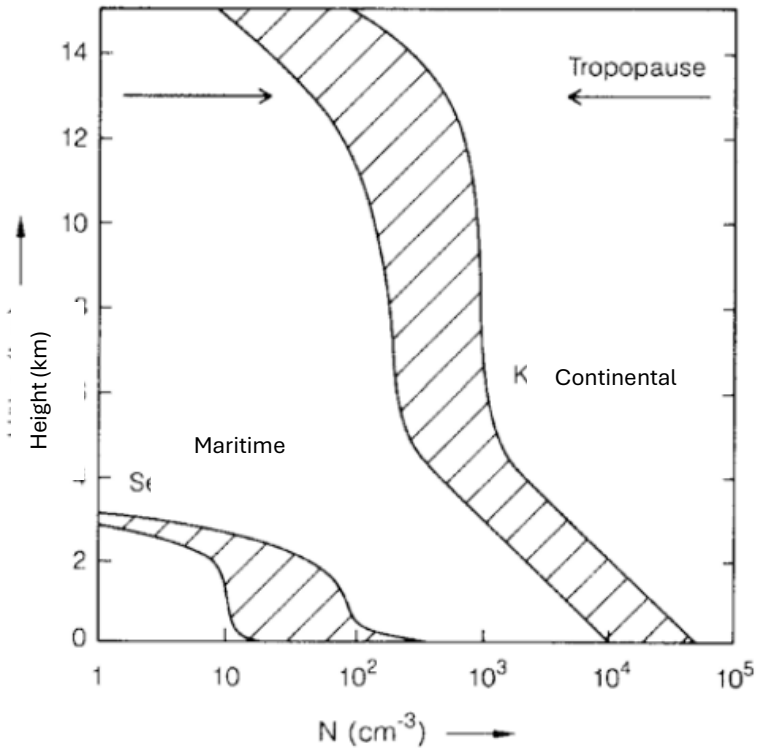

Figure 3: Vertical distribution and number concentration of tropospheric aerosol particles - continental and maritime [6]

Building on the model of Christian E. Junge of altitude distributions of aerosols, most particles formed (through nucleation or dispersion) over continents are removed from the atmosphere through the discussed processes like precipitation, sedimentation, and inertial deposition to the surface. However, a small portion of these particles reach the upper troposphere, above 5 km in altitude, where they experience much lower rates of precipitation and therefore have a longer lifespan. These particles can become globally dispersed. An example of this long-range transport is the spread of Saharan dust across Austria, Germany, and Switzerland during Easter

2024, where concentrations reached up to 1.2 $\frac{g}{m^3}$ of air of Saharan dust, which is immensely high in comparison to normal particulate matter concentrations. At these higher altitudes, the aerosol particle concentration is around 300 particles per cubic centimeter. Over time, these particles diffuse back down into the lower troposphere, where they contribute to the background aerosol particle concentration, often referred to as tropospheric background aerosol particles. [6] [30]

Measuring methods and techniques

The measurement of air quality and particulate matter in Austria is subject to strict requirements to ensure accuracy and comparability. The Measuring Concept Regulation of the IG-L regulates the requirements for measuring stations, including their location, number and technological equipment. Section 6 of the Regulation [31] specifies the minimum requirements of the measuring stations for SO_2, PM_{10}, NO_2, CO, B(a)P, Cd, As and Ni. Another example is the flow rate of continuous particulate matter meters and high-volume samplers (e.g. Digitel High Volume Sampler), which are often used for sampling PM10 and PM2.5, which must be checked at least once a year with the current legal situation in Austria. Cleaning of the measurement technology elements such as the particulate matter sampling heads is carried also out regularly as part of station maintenance. The sampling filters for PM10 and PM2.5 must be prepared and weighed in accordance with the EN 12341:2014 standard. A standardized approach must be followed to ensure consistent results. In addition, routine functional checks of the measuring devices are carried out. [32] [33] [34]

The following four measurement methods represent the most commonly used and well-established devices worldwide, with particular relevance to Austria. Based on the information from public reports on air pollution and particulate matter measurements from the Environmental Agency of Austria, the focus was placed on the specific types of devices most frequently used in Austrian regions. To provide a better understanding of the evolution of these methods and devices from 2001 to 2020 in Austria, each chapter on a different measurement method will briefly outline the number of devices employing that technique in 2001, 2010, and 2020 according to the Immission Control Act-Air (IG-L).

Gravimetric measuring method

Many measuring points for PM10 and PM2.5 in Austria are equipped with gravimetric measuring methods. A particularly frequently used gravimetric measuring device in Austria is the Digitel DHA-80 High Volume Aerosol Sampler (e.g. 98 % of all gravimetric PM10 measuring stations were equipped with this in 2010 and 86 % in 2020). Due to this high presence, this device and its gravimetric measuring method will be explained in more detail. In 2001, 12 of the 52 PM10 monitoring stations were operated with gravimetric measurement methods in accordance with IG-L, none for PM2.5. In 2010, a total of 49 of the 145 PM10 measuring points and 11 of the 13 PM2.5 measuring points used gravimetric measuring methods in accordance with IG-L. In 2020, 37 of the 125 PM10 measuring stations and 21 of the 58 PM2.5 measuring stations were operated using gravimetric methods in accordance with IG-L. [32] [35] [36]

The Digitel DHA-80 High Volume Aerosol Sampler in Figure 4 is a complete device for sampling and subsequent later analysis (gravimetric and analytical determination) of aerosol particles and dust.

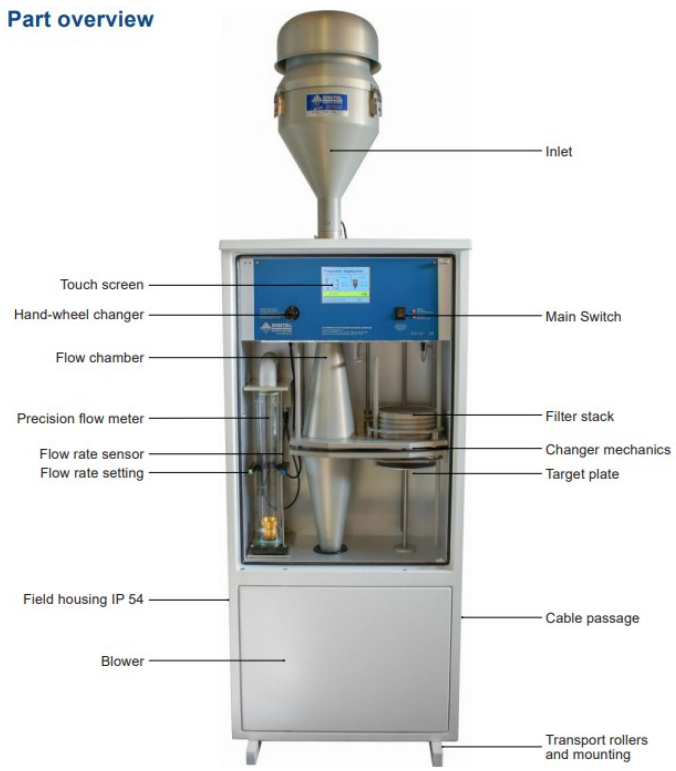

Figure 4: Digitel DHA-80 HVAS part overview [37]

The flow range of this device is between 100-1500 $\frac{\mathrm{l}}{\mathrm{min}}$. The device has 15 different filters with a diameter of 150 mm. A built-in microprocessor controls and collects all relevant measurement data. A constant and precise air flow through the device and filter is also provided, which leads to more accurate evaluation and analysis. The air inlets of this device are available for the measurements of total TSP (total suspended particles), PM10, PM2.5 and PM1. The PM10 and PM2.5 measurements that take place in compliance with EU standard EN12341:2014. The European standard EN 12341:2014 specifies the requirements and procedures for the gravimetric measurement of particulate matter fractions such as PM10 and PM2.5 in ambient air to ensure reliable and comparable results in air quality monitoring within the EU. [38]
This device can also be integrated into various automatic real time monitoring systems through different interfaces. Due to its robust construction, it is well suited for outdoor use and operates at a very low noise level and the blower unit has a service life of over 36,000 hours without maintenance. [37]

The following Figure 5 shows the schematic design of the Digitel DHA-80 High Volume Aerosol Sampler.

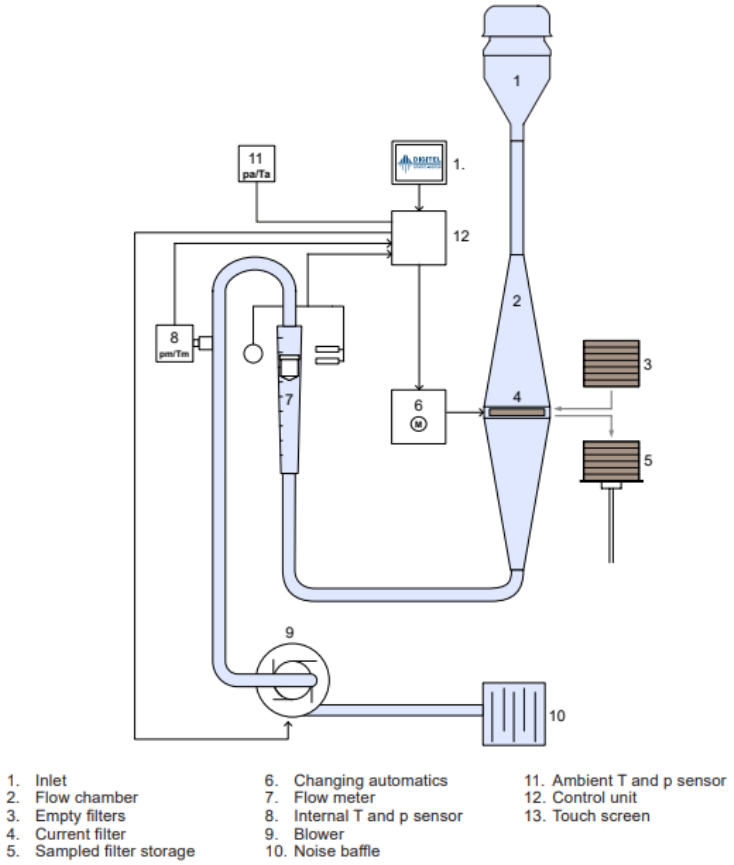

Figure 5: Digitel DHA-80 High Volume Aerosol Sampler schematic design [37]

The collected air sample is first passed through a suitable PM10, PM2.5 or similar sampling tube at the inlet, which separates the particles according to size. This separation is based on the principle of inertia: larger particles have a higher inertia and are deposited on a collection surface, while smaller particles, which one wants to measure in this specific case, follow the air flow. In more detail, the previously introduced brake relaxation time τ and stopping distance Λ are helpful. Depending on its size and properties, a particle requires a certain time τ_{flow} to adapt to new flow conditions. This adaptation process is described in by the dimensionless Stokes number Stk in Formula 12, which represents the ratio of a particle's relaxation time τ to the time τ_{flow}it takes to change from its initial trajectory. If τ_{flow} is shorter than the τ, the particle cannot adjust quickly enough to the changing conditions and will impact on the surface. Conversely, if the τ is shorter, the particle adapts rapidly and continues following the airflow. Similarly, the stopping distance Λ and a characteristic dimension of the obstacle l_0 can be used to describe the Stokes number. If Λ is larger than l_0, the particle will not adjust quickly enough and will be deposited.

Thus, the Stokes number provides useful information for determining particle behavior: if $Stk \gg 1$, the particle is likely to be removed by impaction, thus if $Stk \ll 1$, it will likely follow the airflow. [1] [2] [37]

$$Stk = \frac{\tau}{\tau_{flow}} = \frac{\Lambda}{l_0}$$

Formula 12: Stokes number

While following the airflow, then the air sample passes vertically, from top to bottom, through the flow chamber. In the center of this flow chamber is an active filter to filter the particulate matter, which is automatically replaced at a preset time by another of the unused filters after measurement. The active filter position is marked with the number 4 in the figure above. Used filters that have filtered particles from the ambient air are moved to a separate and protected filter storage position with constant conditions (strictly in accordance with the EU standard) for later analysis, when changing to a new filter to determine their mass later on. [37]

The difference in mass before and after filtering and thus the mass increase is used to calculate the concentration of particles in the air. The upper part of the flow chamber functions like a diffuser, which is responsible for distributing the air evenly over the filter surface. This prevents turbulence and ensures that particles are deposited evenly on the filter, and due to the relatively large 150 mm filter diameters, the air flow velocity passing through the filter is only around 0.5 $\frac{\mathrm{m}}{\mathrm{s}}$. This air flow velocity is achieved when the flow rate is around 500 $\frac{\mathrm{l}}{\mathrm{min}}$. In order to protect the filters from tearing or similar, the pressure drop is limited to 130 mbar at the filter. Behind the filter is a flow meter with a float that monitors the air flow. An optical dual photo sensor detects the position of the float and passes this information on to the control electronics. This adjusts the output of the blower to ensure that the air volume remains constant at the specified setpoint, even if the ambient conditions change. Air pressure and temperature are continuously measured and averaged to guarantee precise data in the device. The extracted air is channeled through a silencer to quieten the operation. All measured values, such as air volume, pressure, temperature, operating status and possible errors, are recorded in a sampling protocol. [37]

To obtain the filtered particle mass, the difference between the mass of the filters before and after use is given in the following form

$$c = \frac{M_2 - M_1}{V} = \frac{\Delta M}{V}$$

Formula 13: Gravimetric concentration *c*

In the above Formula 13, *c* is the particle gravimetric concentration in $\left[\frac{\mu\mathrm{g}}{\mathrm{m}^3}\right]$, which is determined by the difference in mass of the filter, where M_2 is the mass of the filter after use and M_1 before use. *V* is the volume $[\mathrm{m}^3]$ of air sucked through in the range 100-1500 $\frac{\mathrm{l}}{\mathrm{min}}$. [37]

Tapered element oscillating microbalance (TEOM) method

In addition to the gravimetric and non-continuous measurement option, which has just been presented in chapter above, there are other widely used measurement methods like Tapered Element Oscillating Microbalance (TEOM) that were and are still in use in Austria.
In the year 2001, in accordance with the IG-L, 46 of 53 PM10 sampling points used a continuous measurement, like TEOM or beta absorption/ beta attenuation method, which will be discussed in the next chapter in more detail. In 2010, the concentration of PM10 was measured at 52 of the 96 continuous monitoring stations in Austria using a TEOM method and also at two of 13 monitoring stations for the measurement of PM2.5 in accordance with the IG-L. In 2020, 12 of the 125 PM10 measuring stations operated in accordance with the IG-L were operated using the TEOM method. For PM2.5 measurements, one measuring station was operated with TEOM in 2020 in accordance with IG-L, compared to two in 2010. [32] [35] [36]

The TEOM is an instrument for continuous measurement of the particle concentration in ambient air. The functionality is based on a conically shaped element that oscillates at its natural frequency. As soon as particles are collected on the filter, the oscillation frequency of the element changes in proportion to the mass of the deposited particles. This frequency change is recorded in real time, allowing the system to precisely determine the particle mass concentration (5 $\frac{\mu g}{m^3}$ to several $\frac{g}{m^3}$). In the following Figure 6 one can see the schematic structure of this measuring method.

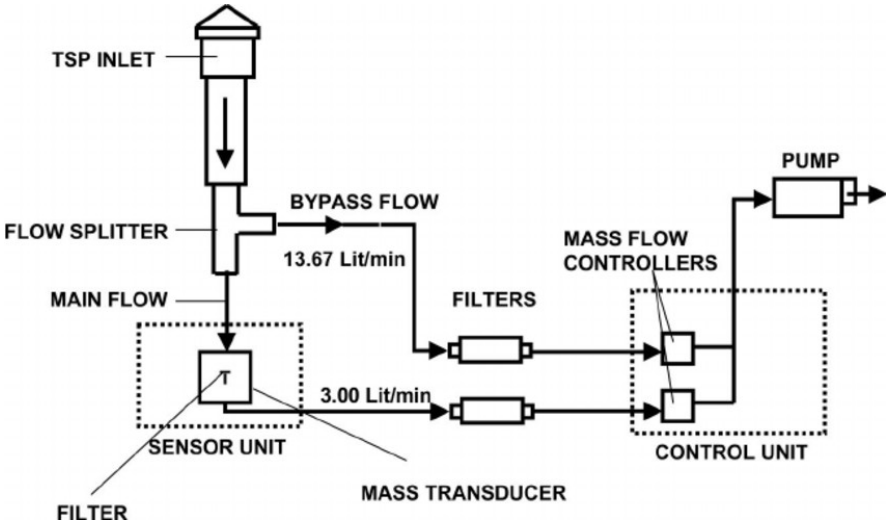

Figure 6: TEOM schematic design [39]

The ambient air is passed through the device at a constant flow rate of 16.67 $\frac{l}{min}$. At the inlet of the device there is an inlet that only allows particles depending on their inertia of a certain size (PM10 or PM2.5). The air flow is then split into two streams in the flow splitter: the main flow of 3.00 $\frac{l}{min}$ is directed to the sensor unit, while the remaining air flow of 13.67 $\frac{l}{min}$ is discharged via the bypass.

In the sensor unit, the particles are collected on a filter that is directly connected to the conical element. This element vibrates in a similar way to the teeth's of a tuning fork and its vibration

frequency is continuously monitored. If particles are deposited on the filter, the mass changes and so does the frequency decreases, which the system registers in real time. Thus, when measuring the change of the frequency, it is possible to conclude the particle mass deposited on the filter. To ensure that no moisture influences the measurement results, the entire system is heated to 50 °C, as moisture could put additional load on the filter. [40]

The following Figure 7 illustrates in more detail the design of the TEOM method, developed by Patashnick and Rupprecht in 1983. [41] In this setup, an LED emits light and is positioned opposite a phototransistor, perpendicular to the oscillation plane, to detect frequency changes. The oscillating element in the middle blocks the light from the LED to the phototransistor, which controls the frequency change and outgoing signal. This signal is then amplified and sent to a conductive coating on the tapered element. With an electric field between two plates, the signal is strong enough to maintain the oscillation. Finally, the signal from the phototransistor, and thus the oscillation frequency, is recorded. [42]

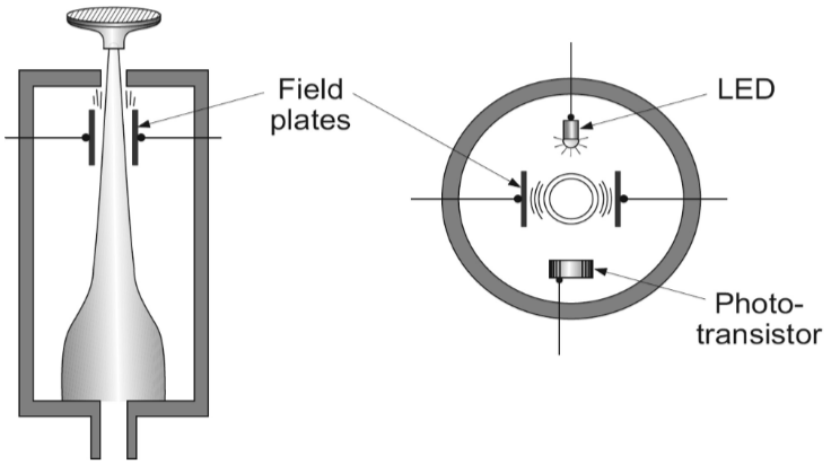

Figure 7: TEOM method from Patashnick and Rupprecht in 1983 [42]

The oscillating element can be seen as a harmonic oscillator, which can be described in Formula 14 as follows

$$\omega = 2\pi f = \left(\frac{k}{m}\right)^{0.5}$$

Formula 14: Harmonic oscillator

with the mass of the oscillating element m, the restoring force constant k and the natural frequency f. [41] The relationship between the change in mass Δm and different frequencies f_1 and f_0 in such a system can be described by the following relationship in Formula 15

$$\Delta m = k_0 \frac{1}{f_1^2} - \frac{1}{f_0^2}$$

Formula 15: Relation between mass change and frequencies

Where k_0 is the spring constant, f is the final frequency and f_0 is the original frequency.

The system is equipped with mass flow regulators in the control unit that monitor and adjust the air flow. These regulators take pressure and temperature fluctuations into account and ensure that the main flow of $3\,\frac{\mathrm{l}}{\mathrm{min}}$ remains constant. The pump generates the necessary vacuum to draw the airflow through the unit, while the control unit monitors and controls all measurements.

Overall, the TEOM system provides precise, real-time data on particle mass by continuously recording the mass changes on the filter. Due to the automated control and adjustment of the airflow, no manual intervention is required, and the system can be operated over long periods of time to collect reliable air quality data. This technology is particularly useful in urban or industrial environments where rapid and continuous responses to changes in particle concentrations are required. [40] [41]

Beta absorption/ Beta attenuation method

In addition to gravimetric, TEOM-based, beta-radiation absorbing measurement methods have been and are also used in Austria to detect PM10 and PM2.5. In the year 2001, 46 of 53 PM10 sampling points used a continuous measurement, like TEOM or beta absorption/ beta attenuation method in accordance with the IG-L. In 2010, 40 of the 145 monitoring stations in Austria used beta-absorption technology to measure PM10, but none for PM2.5 concentrations in accordance with the IG-L. In 2020, 50 of the total of 125 measuring stations for PM10 in Austria operated in accordance with the IG-L using the beta absorption method. Six of the 58 monitoring stations for PM2.5 operated in accordance with the IG-L were also operated using the beta absorption method.
A common measuring device that was used for the measurement of PM10 and PM2.5 in 2020 is the MetOne Beta attenuation mass (BAM)1020 monitor device, which is used to explain the measurement method in more detail and is the most widely used device worldwide for measuring PM10 and PM2.5. The BAM 1020 by Met One Instruments Inc. was the pioneering device to receive the U.S. EPA Federal Equivalent Method (FEM) certification also for continuous PM2.5 monitoring. This recognition complemented its long-standing approval for PM10 monitoring, which the device had been awarded earlier. [32] [35] [36] [43]

This measuring device can automatically measure the fine dust particle mass concentration in ambient air by beta ray attenuation of a filter and thus determine the particle concentration in ambient air. For this purpose, carbon isotopes (^{14}C) is used as a constant source of beta radiation. The radiation intensity is 60 µCi ±15 µCi (microcuries). This emitted radiation passes through a glass fibre filter tape inside the device and is then measured by a scintillation detector. Initially, the beta particle number I_0, which passes through a clean and unloaded filter, is measured. Subsequently, a known volume of ambient air containing fine dust particles is sucked in with a pump and passed through the filter. The beta radiation emitted by the ^{14}C isotopes which has passed through the loaded filter is then detected again in the detector. This beta particle number I_1 differs from the original I_0. The ratio of these two different radiations intensities indicates the mass density of the fine dust particles on the filter. [44]

The schematic structure of this device is shown in the following Figure 8.

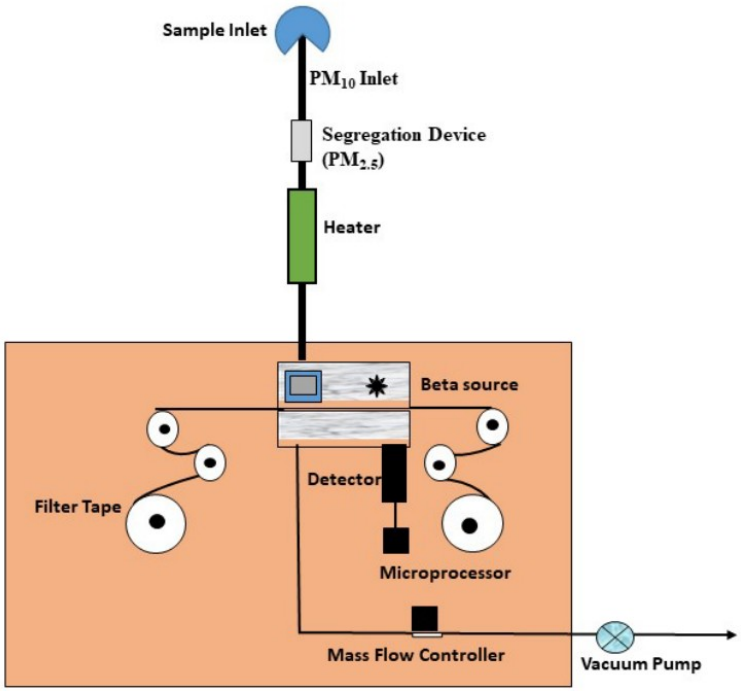

Figure 8: Schematic design of the beta absorption method [45]

As shown in the figure above, particles (PM10 or PM2.5) are let into the device through a suitable sample inlet using a vacuum pump. A heater keeps the relative humidity at or below 35 %. The basic measuring cycle for this device takes about 1 hour. A typical cycle for e.g. PM2.5 measurements starts with automatically moving the filter band to a clean, uncontaminated location on it between the beta source and the detector. The beta radiation is now sent through the filter for eight minutes and the beta particle count I_0 arriving in the detector is measured. After eight minutes, the measurement of the radiation in the detector stops. The filter belt is then automatically moved further under the air inlet and the vacuum pump is turned on so that particle-laden air is constantly drawn in at 16.7 $\frac{\text{l}}{\text{min}}$ for 42 minutes and the particles are deposited on the filter band. The mass flow control meter keeps the flow constant at 16.7 $\frac{\text{l}}{\text{min}}$. After these 42 minutes, the vacuum pump is automatically stopped, and the filter belt is moved back so that this particle loaded filter piece is between the beta source and the detector. The beta radiation is now sent through the loaded filter section and the new beta particle count I_1 arriving in the detector is measured. After another eight minutes, the measurement of the incoming radiation in the detector stops again. The mass of the deposited PM2.5 particles is now determined using the number of I_1 and I_0. Using the total volume of air sampled, it is now possible to calculate the concentration of PM2.5 per cubic meter of air.

The use of ^{14}C is advantageous in this case, as it is converted to ^{14}N by beta decay, releasing beta particles (electrons/positrons) that can be detected. This beta radiation averages 49,000 eV in a ^{14}C decay. These particles can normally travel about 22 cm in ambient air before they are completely absorbed. Another advantage is the particular half-life of ^{14}C, namely 5730 years. The device can therefore be operated without changing the beta particle source. [44]

The beta particles emitted from the source follow a continuous energy distribution with a characteristic maximum energy E_{max} depending on the chosen isotopic source, where most electrons are found around 40 % of E_{max}, seen in the following Figure 9, representing an idealized beta spectrum.

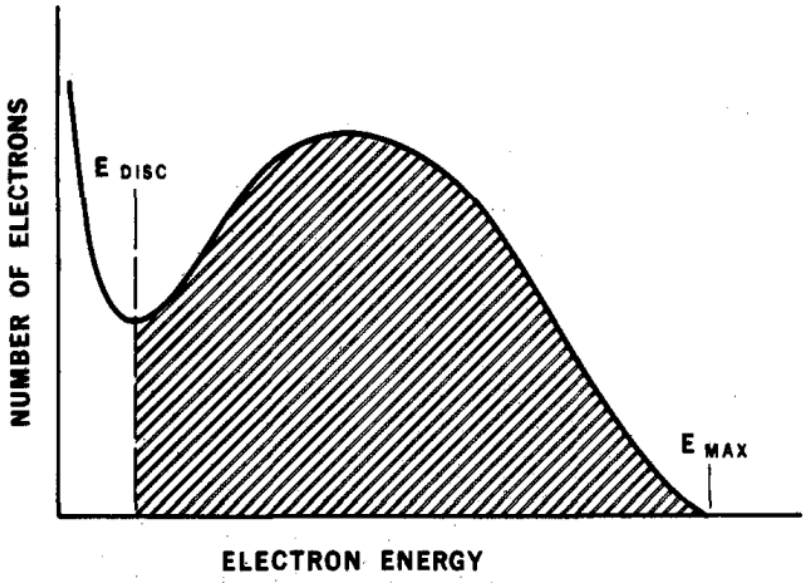

Figure 9: Beta particle spectrum from an isotopic source [[46]

A threshold energy E_{disc} defines the detection limit, so only the number of beta particles with energies above this limit are part of the counting and measurement. As beta particles pass through a sample, they lose energy gradually through electron collisions, altering their direction. Thicker samples lead to a shift toward lower energies, with lower-energy particles being fully absorbed. The exponential relation in Formula 16 arises from the interplay between the energy loss characteristics of the low energy electrons and the shape of the beta particle spectrum. [42] [46]

The underlying formula describing the beta radiation absorption process and the relation of the transmitted flux and mass of the sample [47] is as follows

$$I_1 = I_0 * e^{-\frac{\mu * M}{S}}$$

Formula 16: Beta ray absorption process

In this Formula 16, as already mentioned above, I_1 is the beta particle count or beta ray flux for the particle-loaded filter piece. I_1 is the beta particle count of the uncontaminated and clean filter band piece. M stands for the mass [mg] that is deposited on the filter piece, which has the size S [cm^2].

μ is the beta ray absorption cross section $\left[\frac{\mathrm{cm}^2}{\mathrm{mg}}\right]$ and is related to the atomic number of the sample material, because the mentioned loss of energy of the beta particles arises more from

the scattering process with electrons of the atom and less with the nuclei itself. Klein et. al [48] has shown this relationship as

$$\mu = 16 \left(\frac{Z}{m}\right)^{\frac{4}{3}} * {E_{max}}^{-1.37}$$

Formula 17: Relation between beta ray absorption cross section and atomic number and weight

with Z as the specific atomic number and m as the related atomic weight in Formula 17. It should be emphasized that the beta ray absorption cross section μ depends mainly on the mass of the deposited particles and less on their chemical composition. This means that μ is approximately the same for the most common particulate matter species such as salt, iron oxide, soot or silica. This has the advantage that it is not necessary to know the exact particulate matter species to be measured in order to carry out an accurate mass measurement. [42] [44] [46]

Light scattering method

Finally, the fourth and frequently used scattered light measurement method in Austria is explained. Particular focus is placed on the Grimm EDM 180 device type, as this is the only one used at measuring stations in accordance with IG-L in Austria. In the year 2001 no light scattering method was used for PM10 or PM2.5 measurements. In 2010, one of 145 IG-L monitoring stations was operated using this method, none for PM2.5. In 2020, 23 of the 125 measuring stations operated in accordance with the IG-L were already using the scattered light measurement method and the Grimm EDM 180 device type for PM10 measurements, while 30 of the 58 IG-L measuring stations were used for PM2.5. [32] [35] [36]

Particles in 31 size ranges (31-multi-channel size classifier ranges: 0,25 µm, 0,28 µm, 0,30 µm, 0,35 µm, 0,40 µm, 0,45 µm, 0,50 µm, 0,58 µm, 0,65 µm, 0,70 µm, 0,80 µm, 1,0 µm, 1,3 µm, 1,6 µm, 2,0 µm, 2,5 µm, 3,0 µm, 3,5 µm, 4,0 µm, 5,0 µm, 6,5 µm, 7,5 µm, 8,0 µm, 10,0 µm, 12,5 µm, 15,0 µm, 17,5 µm, 20,0 µm, 25,0 µm, 30,0 µm und 32,0 µm) and in the mass range of 1 $\frac{\mu g}{m^3}$ to 500 $\frac{\mu g}{m^3}$ can be continuously detected with this device. The device uses light-scattering technology for single particle counting, with a semicondutor laser as the light source. This device can also derive the size distribution of the particles by measuring the scattering intensity. In general, the optical size parameter α in Formula 18 gives the ratio of the wavelength of the incident radiation λ to the size of the spherical particle D_p, so

$$\alpha = \pi * D_p * \frac{1}{\lambda}$$

Formula 18: Optical size parameter α

When the particle is much smaller than the incoming wavelength of the light, so when $\alpha \ll 1$, the Rayleigh scattering theory is applicable. When $\alpha \sim 1$, Mie scattering occurs. In this range the interplay between the particle and the light is especially significant. [42]

The following Figure 10 shows the functional principle of this measuring method.

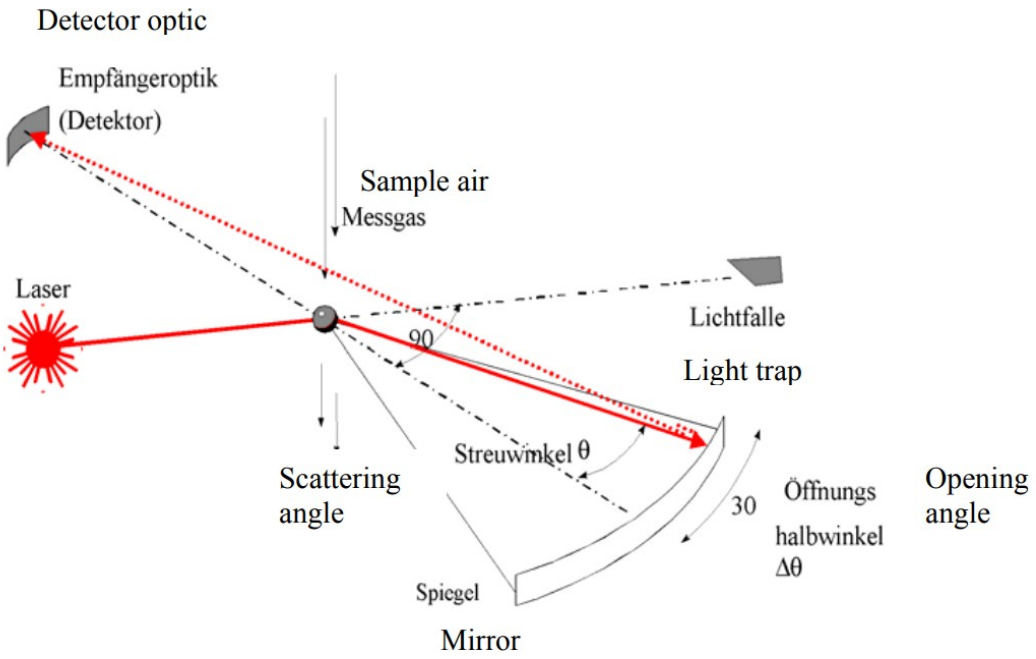

Figure 10: GRIMM EDM 180 principle [49]

Particles sucked in by a pump come through a suitable sampling inlet (PM10 or PM2.5) and pass vertically through the laser beam (λ = 655) of a semiconductor, scattering the light from the laser in the so-called optical measuring cell. The pump used to draw in the ambient air pumps constantly at a rate of 1.2 $\frac{l}{min}$. The pump is also responsible for ensuring that the clean sheath air is filtered and returns to the system in the optical chamber and does not contain dust and interfere with the light measurement. The light is scattered by the particle at around 90 degrees at a small scattering angle θ in the direction of a mirror with an aperture angle of around 30 degrees, which is then transferred to a recipient diode/detector. This geometry of the GRIMM EDM 180 is specially designed to reduce the impact of the refractive index on the scattering intensity and resolve the uncertainties associated with Mie-scattering. The unscattered light is collected in a light trap, which is opposite the laser. The incoming signal in the detector is now counted and amplified and passes through the 31 multi-channel size classifier. A pulse height analyzer is then responsible for classifying the signals intensity in each channel. These scattering pulses in the respective channels are finally stored in a data storage and are available for further analysis. Thus, the GRIMMM EDM 180 gives the particle number concentration of the 31 different sizes. This number-size distribution can then be converted into the desired PM10 and PM2.5 concentration. It is important to note that the refractive index of aerosol particles affect the measurements and if it is unknown or varies, it can lead to incorrect size distributions. [42] [49] [50]

Health effects of particulate matter and air pollutants on human health

Different air pollutants have varying impacts on the environment and human and animal health. Particulate matter, for example, has direct effects when inhaled, causing damage to the lungs and respiratory system. This can significantly reduce life expectancy by triggering cardiovascular diseases, lung inflammation, and other body disfunctions. The health effects of inhaling air pollutants vary depending on the type of particles and the duration of exposure with soot particles being more harmful than mineral components. According to the World Health Organization (WHO), short-term exposure can lead to pneumonia, respiratory symptoms, cardiovascular problems, increased medication use, and more hospitalizations. Long-term exposure is associated with chronic respiratory diseases, reduced lung function, lung cancer, cardiovascular diseases, and a decrease in life expectancy. [32] [51]

According to the WHO and the Global Burden of Disease project, the excessive inhalation of fine particulate matter (PM2.5) is responsible for approximately 4.3 million deaths annually. The majority of these deaths, particularly over half, are attributed to cardiovascular diseases triggered by the heightened presence of PM2.5 particles in the air. Recent studies by the Global Exposure Mortality Model (GEMM), which offers a more comprehensive analysis of the health effects linked to PM2.5, suggest the death rate from PM2.5 exposure is significantly higher. These studies estimate that close to 9 million deaths globally, including 800,000 in Europe, are now attributed to extensive PM2.5 exposure. This level of pollution has resulted in a reduction of global life expectancy by nearly three years, which is greater than the estimated 2.2 years mean life expectancy loss due to smoking cigarettes. Some particles are capable of traveling long distances under certain circumstances, spanning hundreds of kilometers in the atmosphere. In a study by Lelieveld et al. [52], it was found that natural sources of particulate matter, such as deserts, have also significant impact on human mortality, contributing to up to 750,000 deaths annually. The contribution of desert dust to mortality rates in central Europe is minimal. The primary factors influencing variations in average air pollution concentrations over time are not so much fluctuations in the emission intensity from sources like industry, but rather weather conditions. Factors such as precipitation, wind speed, wind direction, and large-scale weather patterns play a major role in determining the concentration and movement of air pollutants. [53]

Primary particles, for example soot particles with a carbon core can enter the atmosphere directly from combustion processes and then being inhaled by humans if preventative measures are not in place. Industrial combustion processes that contribute to PM2.5 and PM10 emissions consist of a variety of harmful components, including carbon cores, heavy metals, endotoxins, sulfates, nitrates, and ammonium. Secondary particles, which are often smaller particles, are usually formed through chemical reactions in the Earth's atmosphere. [53] [54] [55]

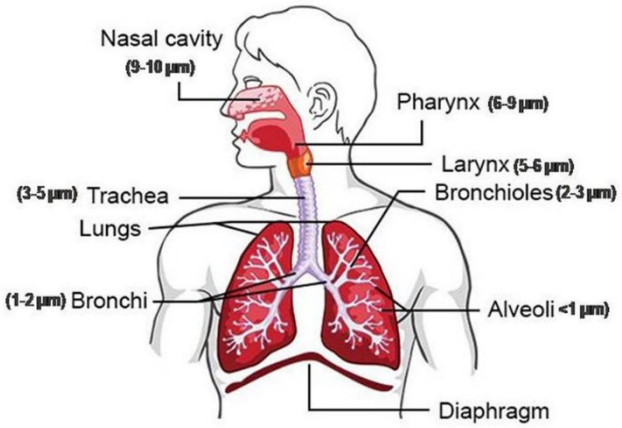

Figure 11: Human respiratory tract and penetration depth of particles [56]

In Figure 11 one can see that different particle sizes (1-10 µm) are filtered at different positions in the respiratory tract of a human body. An adult human typically inhales around half to one liter of air with every breath. In clean air conditions, this means inhaling approximately 10^7 particles with each breath, which leads to a significant amount of particles entering the respiratory tract and lungs. The health impact of these particles largely depends on their size, chemical composition and where they settle within the respiratory system in the human body. As air travels from the nose (9-10 µm) and mouth (6-9 µm) through the throat into the trachea (3-5 µm), it splits into the main bronchi (1-2 µm), which carry air into both lungs. From there, it is further directed into increasingly smaller airways, the bronchioles (2-3 µm), and finally reaches the alveoli (<1 µm). These tiny air sacs are responsible for the essential exchange of oxygen and carbon dioxide between the lungs and bloodstream. Protecting the surfaces of these alveoli from harmful particles is crucial, as pollutants can damage this part of the respiratory system and lead to serious health issues, making the avoidance of inhaling particulate matter, particularly PM2.5 and smaller, important.

The respiratory system performs multiple essential functions beyond gas exchange; it also helps to warm, humidify, and filter the air we breathe. Larger particles tend to be removed in the upper airways through impaction. This occurs when particles, due to their inertia, cannot follow the air stream and thus collide with airway walls. In contrast, very fine particles penetrate deeper into the lungs and are deposited there through diffusion, sticking to the airway walls. Particles in the range of around 200 nm (lowest filtering efficiency) pose a particular risk as they can reach the deepest parts of the lungs, including the critical alveoli, where they may cause serious harm. The speed of airflow also plays a critical role, as faster airflows emphasize inertial impaction. Most airways are coated with mucus, which traps inhaled particles and moves them toward the throat for expulsion. The alveoli, where gas exchange occurs, lacks this protective layer, and particles that reach these air sacs can remain for long periods, potentially causing harm. Fibrous, insoluble particles such as asbestos are especially concerning as they resist removal by the body's macrophages (human immune cells), leading to the potential accumulation in the lungs and, over time, to diseases like fibrosis or even lung cancer. [2]

Effects of particulate matter on the cardiovascular system

As previously mentioned, smaller particulate matter significantly impacts human health due to their ability to penetrate deeply into the respiratory system. PM2.5 particles can pass through the lung epithelium (a cell wall protecting the lung) and the alveoli, entering the bloodstream and adhering to the vascular walls. These deposits of fine particles on the vascular walls stimulate the production of reactive oxygen species (ROS), which are pro-oxidative compounds, along with pro-inflammatory mediators, proteins, and hormones. [57] These reactive processes contribute to the accelerated formation of atherosclerotic changes, meaning the buildup of fat, cholesterol, and other substances in the arterial walls. This leads to the narrowing and hardening of the arteries. Research indicates that these atherosclerotic processes occur more rapidly with smaller particulate matter, as larger particles are much more likely to be filtered out in the mouth and throat. This process is also associated with an increased activation of blood clotting mechanisms, which can lead to conditions such as thrombosis and embolism. Thrombosis occurs when blood clots form in vessels, hindering blood flow. Embolism, on the other hand, refers to blood clots that break loose and travel to other parts of the body, potentially causing blockages in different blood vessels. Furthermore, prolonged inhalation of PM2.5 can contribute to arterial hypertension, which is characterized by persistently elevated pressure in the arteries, commonly known as high blood pressure. [53] [57] [58]

The paper by Münzel [53] states that a short-term increase of PM2.5 by 10 $\frac{\mu g}{m^3}$ is linked to a rise in overall mortality by 1.04 %, mainly due to cardiovascular and respiratory diseases, but differs strongly between different regions. Another study focusing on data from Europe and North America revealed a similar trend, showing that a short-term increase in PM10 levels by 10 $\frac{\mu g}{m^3}$ led to a rise in overall mortality by 0.2 % to 0.6 %. Furthermore, a large-scale study highlights the significant impact of long-term exposure to particulate matter. According to this research, a persistent increase in PM2.5 concentration of 10 $\frac{\mu g}{m^3}$ is associated with a 6 % increase in overall mortality and an 11 % rise in cardiovascular-related deaths. [59] [60] [61]

Cardiovascular mortality

Cardiovascular diseases encompass a range of conditions affecting the heart and blood vessels, including heart attacks, where blood flow to the heart muscle is blocked, strokes, caused by an interrupted blood supply to the brain, hypertension, or chronically elevated blood pressure in the arteries and heart failure, where the heart is unable to pump blood effectively. According to recent studies, short-term exposure to PM2.5 at concentrations of just 10 $\frac{\mu g}{m^3}$ increases the relative risk of heart attacks by approximately 2.5 %. Globally, this type of exposure is estimated to contribute up to around 5 % of all heart attacks, given the large number of people continuously exposed to particulate matter exposure. Lifelong exposure to particulate matter could lead to a high risk of cardiovascular diseases. [53] [62] [63] [64]

According to a Canadian study [65], even low levels of PM2.5 (below 10 $\frac{\mu g}{m^3}$) can increase the risk of cardiovascular diseases. These findings are supported by long-term studies [66] conducted by the American National Institutes of Health, which found a 10 % increase in cardiovascular mortality per 10 $\frac{\mu g}{m^3}$ PM2.5 exposure. Additionally, a recent study in China revealed that increased morbidity (illness) and mortality (death) risks correlate with significantly higher levels

of air pollution, with average PM2.5 concentrations at around 44 $\frac{\mu g}{m^3}$. This study demonstrated a 9 % increase in relative cardiovascular mortality risk for every 10 $\frac{\mu g}{m^3}$ rise of PM2.5. It is also important to note that individuals already suffering from cardiovascular illnesses face a substantially higher risk of further complications when exposed to elevated levels of particulate matter. [67] [68]

Cerebrovascular diseases

Cerebrovascular diseases are conditions caused by disruptions in blood flow to the brain. These include strokes, which can result from sudden blockages in brain vessels, and transient ischemic attacks, which are temporary episodes of reduced blood flow to the brain. An analysis of around 100 studies found that a 10 $\frac{\mu g}{m^3}$ increase in PM2.5 levels is associated with a heightened risk of stroke, as well as a 1.1 % rise in stroke-related mortality. [53] [69]

Cardiac insufficiency

Heart failure, also known as cardiac insufficiency, is a clinical condition where the heart is unable to pump enough blood to meet the body's needs. This insufficiency results in poor circulation and a lack of oxygen to organs and tissues. A review of 35 studies demonstrated that increased exposure to particulate matter raises the risk of heart failure. Specifically, a rise in PM2.5 concentration by 10 $\frac{\mu g}{m^3}$ is linked to a 2.1 % increase in the relative risk of death due to heart failure. Additionally, a Chinese study across 26 cities found that elevated PM2.5 exposure led to a relative 1.2 % increase in hospitalization for heart failure or cardiac insufficiency. [53] [70] [71]

Cardiovascular risk factors

Cardiovascular risk factors are conditions that increase the likelihood of heart diseases, such as hypertension (high blood pressure), and metabolic disorders, such as diabetes. Studies increasingly find that air pollution influences these risk factors. There is a demonstrated correlation between PM2.5 exposure and conditions like high blood pressure and insulin resistance. [72] [73]
Specifically, an increase in diastolic blood pressure (the lower number in a blood pressure reading) by 1-3 mm Hg was observed with a 10 $\frac{\mu g}{m^3}$ rise in PM2.5 concentration. Furthermore, long-term exposure to PM2.5 has been associated with higher average blood pressure and an increased risk of hypertension. Structural changes in blood vessels due to high levels of particulate pollution were also noted. [64] Overall, multiple studies have confirmed a clear link between particulate matter, especially PM2.5, exposure and a corresponding rise in diabetes risk. [53] [74] [75]

Regulatory development of environmental and air protection legislation at European and National Level

The European Commission proposed limit values for particulate matter (PM10) to minimize health risks from particulate matter pollution. The EU Directive 1999/30/EC came into force in 1999 and had to be transposed into the national law of the EU member states by 2001. It set binding limit values for PM10, which had to be fulfilled by 2005 (50 $\frac{\mu g}{m^3}$ as the daily average limit value, whereby 25 exceedances are permitted by the IG-L and 35 exceedances by the EU Directive), and stricter, values by 2010 (40 $\frac{\mu g}{m^3}$ as the maximum yearly average). In addition, it was planned to set limit values for PM2.5 and carry out corresponding measurements as part of a review of this EU Directive. In Austria, this EU Directive was implemented by the Immission Control Act-Air (IG-L) and corresponding ordinances (BGBl. No. I 62/2002). With the introduction of the Immission Control Act-Air (IG-L) in 2001, PM10 measurements were conducted at several locations throughout Austria. Starting in 2002, it became possible for the first time to carry out representative measurements over the entire year in accordance with the IG-L regulations. The IG-L marked a significant step forward in monitoring particulate matter concentrations, as air pollution from particulate matter had previously been inadequately assessed. It is particularly noteworthy that the measurement of PM2.5 concentrations in 2001 in Austria was extremely limited, with data available from only one single monitoring station. The Immission Control Act-Air (IG-L) is the most legally relevant law for air quality control and air pollution protection in Austria. It focuses primarily on the long-term protection of ecosystems and public health from air pollutants, the preventive minimization of pollutant exposure, and the preservation and improvement of air quality. As a result, a national and standardized monitoring network and concept was introduced to provide a comprehensive overview of potential exceedances of limit values. [35] [76]

In 2010, the European Air Quality Directive from 2008 (Directive 2008/50/EC), part of the European "Clean Air for Europe" program, served as the legal foundation for monitoring outdoor air and measuring pollutants such as SO_2, NO_2, NO_x, PM10, PM2.5, CO, ozone, lead, and benzene. In July 2010, an amendment to the Immission Control Act-Air (IG-L) was enacted to implement the European Air Quality Directive of 2008. This amendment introduced, for the first time, legal regulations for PM2.5, including target and limit values aimed at reducing exposure to fine particulate matter of this size. [32] [51]

Since 2020, Austria had specific emission reduction obligations for anthropogenic emissions of NOx (nitrogen oxides), SO_2 (sulfur dioxide), NMVOC (non-methane volatile organic compounds), NH_3 (ammonia), and particulate matter (PM2.5), which follow the revised Gothenburg Protocol from 2012. These reduction goals are legally anchored in the European National Emission Ceilings Directive (Emissionshöchstmengenrichtlinie/ NEC) from 2016 and the National Emission Act Air (Emissionsgesetz-Luft) from 2018. Due to the NEC-Directive from 2016, all EU member states were required to develop an updated Clean Air Program by 2019 and submit it to the EU Commission, with the obligation to update it every four years. The National Air Pollution Control Program (Luftreinhalteprogramm), first created in 2010 and then revised, is now legally anchored within Austria's National Emission Act Air (Emissionsgesetz-Luft) and serves to meet the emission reduction targets of the European NEC-Directive. On March 20, 2024, an update to Austria's Air Pollution Control Program (Luftreinhalteprogramm) was approved to ensure compliance with air pollutant reduction commitments by 2030 (-46 % from 2005 by 2030 for

PM2.5). As part of the European Green Deal and later with the European Action Plan "Zero Pollution for Air, Water and Soil", the EU implemented more concrete measures to reduce pollutants in May 2021. The overarching goal is to reduce pollutant concentrations in air, water, and soil by 2050 to levels that are no longer classified as harmful to human health or the environment. [51] [77]

According to the European NEC-Directive on the reduction of national emissions of the mentioned air pollutants, all EU member states are obliged by Articles 8 and 10 to identify their current national emissions every two years and project their future development. Under the Austrian Environmental Control Act (Umweltkontrollgesetzes), the Environmental Agency of Austria is required to conduct an annual National Air Pollutant Inventory (Luftschadstoff-Inventur). In addition to greenhouse gases such as CO_2, CH_4, N_2O, and fluorinated gases, the inventory includes emissions of NOx, SO_2, NMVOC, NH_3, particulate matter (TSP = total suspended particles, PM10, and PM2.5), persistent organic pollutants (POP), and heavy metals (HM). These mentioned greenhouse gases are defined by the United Nations Framework Convention on Climate Change (UNFCCC), and the air pollutants are defined by the United Nations Economic Commission for Europe (UNECE) under the Convention on Long Range Transboundary Air Pollution (CLRTAP).

The continuous monitoring of air pollutants provides the Austrian Government and relevant entities with the necessary data foundation for mandatory international reporting (e.g. EU NEC-Directive). Specifically, this includes the annual reporting of Austria's Informative Inventory Report for Air Pollutants (IIR) and Austria's National Inventory for Greenhouse Gases (NIR), as well as the biannual reporting of GHG Projections and Assessment of Policies and Measures in Austria for the EU-Governance Regulation and Austria's National Air Emission Projections for Air Pollutants under the NEC-Directive. In addition to these mandatory international reports, the Environmental Agency of Austria also publishes the Climate Protection Report (Klimaschutzbericht), the Emission Trends Report for Austria (Emissionstrends in Österreich), and the Federal State Pollutant Inventory (Bundesländer-Schadstoff-Inventur) annually. [51] [78] [79]

The current EU limit values for particulate matter (PM10) are set at 40 $\frac{\mu g}{m^3}$ as an annual average. From 2030 onward, this limit will be reduced to 20 $\frac{\mu g}{m^3}$. The World Health Organization (WHO) recommends a much lower annual average of 15 $\frac{\mu g}{m^3}$. For the daily average, the current EU limit for PM10 is 50 $\frac{\mu g}{m^3}$, allowing up to 35 exceedances per year. Starting in 2030, this limit will be lowered to 45 $\frac{\mu g}{m^3}$, with a maximum of 18 exceedances per year. In comparison, the WHO recommends a daily limit of 45 $\frac{\mu g}{m^3}$ but allows no more than 4 exceedances annually.

For PM2.5, the current EU annual average limit is 25 $\frac{\mu g}{m^3}$, which will be reduced to 10 $\frac{\mu g}{m^3}$ by 2030. The WHO, however, recommends a stricter limit of 5 $\frac{\mu g}{m^3}$. For the daily average, the EU limit from 2030 will be 25 $\frac{\mu g}{m^3}$ with up to 18 permitted exceedances. In contrast, the WHO advises a daily limit of 15 $\frac{\mu g}{m^3}$ with a maximum of 4 exceedances per year. [80]

PRTR – Austrian Pollutant Release and Transfer Register

The Austrian PRTR (Pollutant Release and Transfer Register) provides information about air pollutants in Austria to the public. Since 2007, larger industrial plants and wastewater treatment facilities have been required to report pollutant emissions to the relevant authority if certain thresholds are exceeded, so the first PRTR reporting period thus took place in Austria in 2007. The PRTR has established a transparent and publicly accessible electronic database where large Austrian industrial enterprises must report their releases of pollutants into the air, soil, and water. The sectors required to report include energy, metal and steel industries, mineral processing industries, chemical industries, waste and water management, wood, paper, and cardboard industries, intensive livestock farming and aquaculture, production of animal and plant-based goods, as well as the beverage sector and other industries such as tanneries. Companies performing activities under Annex 1 of the "EC PRTR Regulation" (166/2006/EC) are obligated to submit their pollutant emission data annually to the relevant authority. After review by the Environmental Agency of Austria, the data is forwarded to the European Commission.

With the data of this accessible PRTR register, an overview of the major emitters of PM10 and PM2.5 that have exceeded the legal limit for particulate matter emission concentrations since 2007 was created to define and further analyze the industrial regions in Austria. It should be emphasized that no PRTR PM2.5 exceedance limit has been reported from the industrial sector since the year 2007, only for PM10. [81]

Table 1 lists all PM10 emitters in Austria that have been required to report their emissions since 2007 under the PRTR regulation, as their PM10 emissions exceeded the reporting thresholds set by law. [82]

Name of installation	Name of operating company	Address of installation	Region	Notifications
Agrolinz Melamine International Linz	Borealis Agrolinz Melamine GmbH	St.-Peter-Straße 25; 4020 Linz; Österreich	Oberösterreich	PRTR-Meldung 2012 / PRTR-Meldung 2013 / PRTR-Meldung 2014 / PRTR-Meldung 2015 / PRTR-Meldung 2016 / PRTR-Meldung 2020 /
Metallveredelung	Collini GmbH Metallveredelung	Schweizerstrasse 59; 6845 Hohenems; Österreich	Vorarlberg	PRTR-Meldung 2007 / PRTR-Meldung 2008 /
PRTR-Betriebseinrichtung_ENAGES_ENAGES	Energie- und Abfallverwertungs Gesellschaft m.b.H.	Proleberstraße 4; 8712 Niklasdorf; Österreich	Steiermark	PRTR-Meldung 2014
EVN AG Kraftwerk Dürnrohr Zwentendorf	EVN AG	Kraftwerksstraße 1; 3435 Zwentendorf an der Donau; Österreich	Niederösterreich	PRTR-Meldung 2007 / PRTR-Meldung 2008 / PRTR-Meldung 2012 /
FKA Linz	Fresenius Kabi Austria GmbH	Estermannstraße 17; 4020 Linz; Österreich	Oberösterreich	PRTR-Meldung 2013 / PRTR-Meldung 2014 / PRTR-Meldung 2015 / PRTR-Meldung 2016 / PRTR-Meldung 2019 / PRTR-Meldung 2020 / PRTR-Meldung 2021 / PRTR-Meldung 2022 /
Hamburger Frohnleiten GmbH	Hamburger Frohnleiten GmbH	Peugen 1; 8130 Peugen; Österreich	Steiermark	PRTR-Meldung 2007 / PRTR-Meldung 2008 / PRTR-Meldung 2009 /
integrierte Faserproduktion	Lenzing AG	Werkstraße 1; 4860 Alt Lenzing; Österreich	Oberösterreich	PRTR-Meldung 2007 / PRTR-Meldung 2008 / PRTR-Meldung 2009 / PRTR-Meldung 2010 / PRTR-Meldung 2011 / PRTR-Meldung 2012 / PRTR-Meldung 2013 / PRTR-Meldung 2014 / PRTR-Meldung 2015 / PRTR-Meldung 2016 / PRTR-Meldung 2017 / PRTR-Meldung 2018 / PRTR-Meldung 2019 / PRTR-Meldung 2020 / PRTR-Meldung 2021 / PRTR-Meldung 2022

Nettingsdorfer Papierfabrik	Nettingsdorfer Papierfabrik AG & Co KG	Nettingsdorfer Straße 40; 4053 Kremsdorf; Österreich	Oberösterreich	PRTR-Meldung 2014
Raffinerie Schwechat - PRTR EEV	OMV Refining and Marketing GmbH	Mannswörther Strasse 28; 2320 Schwechat; Österreich	Niederösterreich	PRTR-Meldung 2007 / PRTR-Meldung 2011 / PRTR-Meldung 2012 / PRTR-Meldung 2013 / PRTR-Meldung 2014 / PRTR-Meldung 2015 / PRTR-Meldung 2021 /
PRTR Betriebseinrichtung_PUT_Steyr	PORR Umwelttechnik GmbH	Thannstraße 47; 4407 Steyr; Österreich	Oberösterreich	PRTR-Meldung 2019
Zellstoff- u Papierproduktion	Sappi Austria Produktions-GmbH & Co. KG	Brucker Straße 21; 8101 Forstviertel; Österreich	Steiermark	PRTR-Meldung 2007 / PRTR-Meldung 2008 / PRTR-Meldung 2009 / PRTR-Meldung 2010 / PRTR-Meldung 2011 / PRTR-Meldung 2012 / PRTR-Meldung 2013 / PRTR-Meldung 2014 / PRTR-Meldung 2015 / PRTR-Meldung 2016 / PRTR-Meldung 2018 / PRTR-Meldung 2019 / PRTR-Meldung 2020 / PRTR-Meldung 2021 / PRTR-Meldung 2022 /
VA Erzberg GmbH	VA Erzberg GmbH	Erzberg 1; 8790 Eisenerz; Österreich	Steiermark	PRTR-Meldung 2010 / PRTR-Meldung 2011 / PRTR-Meldung 2012 / PRTR-Meldung 2013 / PRTR-Meldung 2014 / PRTR-Meldung 2015 / PRTR-Meldung 2016 / PRTR-Meldung 2017 / PRTR-Meldung 2018 / PRTR-Meldung 2019 / PRTR-Meldung 2020 / PRTR-Meldung 2021 /
Verbund KW Dürnrohr, Zwentendorf	VERBUND-Austrian Thermal Power GmbH & Co KG	Kraftwerksstrasse 1; 3435 Zwentendorf an der Donau; Österreich	Niederösterreich	PRTR-Meldung 2007 / PRTR-Meldung 2008 / PRTR-Meldung 2009 / PRTR-Meldung 2010 / PRTR-Meldung 2011 / PRTR-Meldung 2012 / PRTR-Meldung 2013 / PRTR-Meldung 2014 / PRTR-Meldung 2015 /
PRTR Betriebseinrichtung_BÖHLER_Winkl	voestalpine BÖHLER Edelstahl GmbH & Co KG	Mariazellerstraße 25; 8605 Winkl; Österreich	Steiermark	PRTR-Meldung 2017 / PRTR-Meldung 2018 / PRTR-Meldung 2019 / PRTR-Meldung 2020 / PRTR-Meldung 2021 / PRTR-Meldung 2022 /
EZG Stahlerzeugung	voestalpine Stahl Donawitz GmbH & Co KG	Kerpelystraße 199 199; 8700 Donawitz; Österreich	Steiermark	PRTR-Meldung 2007 / PRTR-Meldung 2008 / PRTR-Meldung 2009 / PRTR-Meldung 2010 / PRTR-Meldung 2011 / PRTR-Meldung 2012 / PRTR-Meldung 2013 / PRTR-Meldung 2014 / PRTR-Meldung 2015 / PRTR-Meldung 2016 / PRTR-Meldung 2017 / PRTR-Meldung 2018 / PRTR-Meldung 2019 / PRTR-Meldung 2020 / PRTR-Meldung 2021 / PRTR-Meldung 2022 /
Standort Linz	voestalpine Stahl GmbH	voestalpine-Straße 3; 4020 Linz; Österreich	Oberösterreich	PRTR-Meldung 2007 / PRTR-Meldung 2008 / PRTR-Meldung 2009 / PRTR-Meldung 2010 / PRTR-Meldung 2011 / PRTR-Meldung 2012 / PRTR-Meldung 2013 / PRTR-Meldung 2014 / PRTR-Meldung 2015 / PRTR-Meldung 2016 / PRTR-Meldung 2018 / PRTR-Meldung 2020 / PRTR-Meldung 2021 /

Table 1: PRTR exceedances in Austria since 2007 [82]

The table above shows that 16 companies from four Austrian federal states, though often in multiple years, have exceeded the allowed maximum emission limits for PM10.
Six of the 16 industrial companies were located in the federal state of Upper Austria. These include the chemical company Borealis Agrolinz Melamine GmbH with a total of six PRTR reports (2012-2016, 2020), the pharmaceutical company Fresenius Kabi Austria GmbH Linz with eight PRTR reports (2013-2016, 2019-2022), the textile and chemical company Lenzing AG with 16 PRTR reports (2007-2022), the paper industry company Nettingsdorfer Papierfabrik AG & Co KG with one PRTR report (2014) (renamed in July 2019 in Smurfit Kappa Nettingsdorf), the environmental technology and waste management company PORR Umwelttechnik GmbH with one PRTR report (2019), and the metal and steel company voestalpine Stahl GmbH with 13 PRTR reports (2007-2016, 2018, 2020-2021). [82]

Additionally, six of the reporting companies are based in Styria, namely the waste management and energy company ENAGES Energie- und Abfallverwertungs Gesellschaft GmbH with one PRTR report (2014), the former paper and packaging company Hamburger Frohnleiten GmbH with three reports (2007-2009), the pulp and paper company Sappi Austria Produktions-GmbH & Co. KG with 15 PRTR reports (2007-2016, 2018-2022), the mining and metal company VA Erzberg GmbH with 12 PRTR reports (2010-2021), the metal and steel company voestalpine BÖHLER Edelstahl GmbH & Co KG with six PRTR reports (2017-2022), the metal and steel company voestalpine Stahl Donawitz GmbH & Co KG with 16 PRTR reports (2007-2022), and the pulp and paper company Zellstoff Pöls AG with eight PRTR reports (2013-2017, 2019, 2021, 2022). [82]

Three of these 16 industrial companies are located in Lower Austria and Vienna's border. These include the oil and gas company OMV with its refinery in Schwechat with seven PRTR reports (2007, 2011-2015, 2021), the energy supplier EVN AG with its power plant Dürnrohr Zwentendorf with three reports (2008-2009, 2012), and the energy supplier Verbund AG with its former power plant in Dürnrohr Zwentendorf with nine reports (2007-2015). [82]

Only one of the companies is from the Austrian federal state of Vorarlberg, the metal finishing and surface technology company Collini GmbH with two PRTR reports (2007-2008), which indicates a clear trend in industry density towards the eastern regions of Austria. [82]

Based on this data, it can be concluded that more than two-thirds of the PRTR-reportable companies for PM10 exceedances in Austria are in the federal states of Upper Austria and Styria.

IPPC-Austria (integrated pollution prevention and control)

The Austrian Ministry for Climate Protection and Environment created a public and central database, the so-called IPPC Austria, to present IPPC facilities in Austria. An IPPC facility in Austria refers to industrial plants and facilities that are subject to the European Industrial Emissions Directive, which are particularly important to monitor and control regarding their emission. These facilities require comprehensive permits for operation, monitoring, and decommissioning, covering all environmental areas such as air, water, waste, and soil. The IPPC Directive aims to minimize the environmental impacts of industrial activities by applying the best available techniques. In Austria, the European Industrial Emissions Directive has been incorporated into national legislation at both the federal and state levels, for example, in the Waste Management Act (Abfallwirtschaftsgesetz) and the Immission Control Act-Air (Immissionsgesetz-Luft).

In April 2022, the European Commission proposed a revision of the European Industrial Emissions Directive, which was adopted in its first reading in March 2024. The revised European Industrial Emissions Directive came into effect in June 2024, with the obligation for member states to implement these updates into national law within 22 months. This revision of the European Industrial Emissions Directive includes, among other things, the establishment of stricter air pollutant exposure limits under best available techniques, the introduction of an environmental management system for IPPC facilities, and the obligation for IPPC facility operators to develop a transformation plan for the years 2030-2050 aimed at a climate-neutral and circular operation of their IPPC facilities. [83] [84] [85]

As of September 2024, 825 IPPC facilities are registered in Austria. Of these, 353 facilities are in the waste treatment sector, 127 in metal manufacturing and processing, 95 in the chemical industry, 48 in the mineral processing industry, 43 in the energy sector, and 159 in other operational activities. Using the IPPC Austria platform, it is possible to determine the location of all 825 IPPC facilities in Austria as of September 2024. This allowed for the geographical clustering of relevant IPPC facilities in industrial areas in Austria. In total, four industrial clusters or regions with the highest concentration of relevant IPPC facilities were identified in Austria, where sufficient data on PM2.5 and PM10 concentrations from the past two decades were available. For this study, an industrial cluster is defined as a significant industrial region with more than 30 registered IPPC facilities and hosting major emitters, for example these from the PRTR reportings since 2007. This approach to the definition of industrial regions in Austria was confirmed as appropriate by an expert from the Environment Agency of Austria (Umweltbundesamt). The leading identified industrial clusters in Austria are the “Großraum Linz” with 111 registered IPPC facilities, followed by the ”Großraum Mur-Mürz Furche” in Styria with 48 IPPC, the ”Großraum Graz” in Styria with 39 IPPC facilities, and the “Großraum Wien” with 38 IPPC facilities. [86]

In the following short descriptions of the defined industrial regions, only some of the largest pollutant emitters are listed to give the reader an impression of the industries and companies represented in each region.

The industrial regions of Austria

The industrial region of “Großraum Wien” (greater Vienna)

IPPC facilities and PRTR reports

The industrial cluster “Großraum Wien" includes 38 IPPC facilities (including the OMV refinery in Schwechat in Lower Austria) and one facility that has exceeded the maximum PM10 emissions, according to PRTR reports, namely the OMV refinery in Schwechat at the boarder of Vienna. In addition to this, other major emitters are from the energy and waste management company Wien Energie GmbH and Wiener Fernwärme GmbH, with numerous IPPC facilities in Vienna, construction companies like Porr, Wienerberger AG, Swietelsky and Strabag, as well as the chemical company Borealis Polyolefins GmbH.

Historical development of the industrial region and important industrial companies

After the Second World War, the initial focus in Vienna was on reconstruction. The heavily damaged city was divided into four occupation sectors under Allied administration. The political and economic structure was gradually restored, with an economic upturn supported by the Marshall Plan beginning in 1950. Vienna benefited economically from industrialization and the expansion of infrastructure, including the construction of UNO City and the Danube Island project, which combined flood protection and relaxation areas. The fall of the Iron Curtain after 1989 strengthened Vienna's bonding with Eastern Europe and strengthened the local industry, which was further intensified. Vienna increasingly developed into an international hub for politics, business and culture, and industry. In the industrial region “Großraum Wien”, a variety of industries are well-established, including the construction industry, chemical industry, petroleum and polymer industry and the energy, heating and waste management sector. These various sectors together form a diverse industrial landscape that plays a critical role in Vienna’s economic development. [87]

The OMV refinery in Schwechat, which has played a key role in Austria's energy supply for over 60 years, is a central pillar of the industrial region “Großraum Wien”. With its high production capacity, it meets the demand for fuels, heating oil, and petrochemical products, contributing significantly to the region's economic strength. Through continuous modernization and investment in new technologies, the refinery remains competitive and meets modern sustainability and energy efficiency requirements. Next to the refinery is the Borealis Polyolefine GmbH, which is part of the Borealis Group, one of the global leaders in advanced and circular polyolefin solutions and the European market leader in basic chemicals and mechanical plastic recycling, as well as a major producer of plastics such as polyethylene and polypropylene. Borealis currently operates six of these large-scale industrial plants in Schwechat, the first industrial plant for the production of polypropylene was opened back in 1961. Together, the OMV refinery and Borealis form one of Austria's most important and largest industrial complexes, supporting the domestic economy and playing a key role on a European level. Both companies increasingly rely on advanced technologies to reduce emissions and air pollutants. The Schwechat site illustrates the balancing act between economic progress and the need to

meet ecological standards. In recent years, the need to further reduce air pollution in the region has been emphasized, as it significantly impacts air quality in Vienna, which is especially important for its two million residents and for tourists. This is why the third package of measures against particulate matter was adopted in Vienna back in 2011. [88] [89] [90] [91]

Meteorological phenomenon in the “Wiener Becken”

Similar to the previous example and the explanation of industrial snow in Linz, this phenomenon is also possible in the industrial area of Vienna. At the beginning of 2024, this phenomenon clearly came into effect. It only snowed in inner parts of Vienna's city center, caused by anthropogenic emissions from Viennese industry, which served as ice nuclei. Due to the cold air layer close to the ground and the high fog often found in the “Wiener Becken” during the winter months, this industrial snow event occurred also in Vienna.

The “Wiener Becken”, as well as the “Grazer Becken”, which will be discussed in the next section, is predestined for high fog weather conditions. In winter, the “Wiener Becken” is particularly sensitive to high fog, which often persists for days and has a strong impact on both the local climate and air quality due to the lack of mixing of the air. Under this fog, air pollution levels can rise considerably. An improvement usually only occurs with the change of the large-scale weather situation, which dissolves the high fog. At the beginning of November 2024, particulate matter levels were measured in Vienna that exceeded the permitted limits. [92] This was due to winter inversion weather conditions that blocked the exchange of air, in combination with the heating season and air pollutants imports from neighboring regions. These conditions led to an unusually high concentration of PM10 and PM2.5 particles in Vienna's air under the fog layer, to be seen in Figure 12. High fog in general is caused by long-lasting high-pressure layers in which moist air is trapped under a warmer inversion layer. The inversion acts like a cover and prevents vertical air exchange, allowing moist air and pollutants to accumulate below the layer.

Figure 12: High fog weather situation in Vienna in November 2024 [93]

In the Vienna area, the formation of high fog is also influenced by the topography and the flow conditions. Cold, moist air from the Pannonian Plain flows in from the east or south-east and is lifted on the hills of the “Wienerwald” in the west, where condensation sets in. This creates a stable layer of fog, which lasts for a long time, especially with south-easterly weather currents.

This weather situation often results in cloudy and cold weather at lower altitudes, while sunny conditions often prevail at higher altitudes in the “Wienerwald” region or in the foothills of the Alps. For comparison to the other regions, the average amount of precipitation in Vienna since 1955 has been around 641 mm, well below the Austrian average of 1190 mm. [92] [94] [95] [96]

The industrial region of “Großraum Linz” (greater Linz)

IPPC facilities and PRTR reports

The industrial cluster “Großraum Linz" (greater Linz) in Upper Austria is home to 111 IPPC industrial facilities and major air pollutant emitters. Consistent with PRTR reports, the following companies in the area of Linz have exceeded the maximum values for PM10 emissions since 2007: the chemical company Borealis Polyolefine GmbH Linz, the pharmaceutical company Fresenius Kabi Austria GmbH in Linz, the paper manufacturer Smurfit Kappa Packaging Austria GmbH, and the largest emitter, the steel manufacturer voestalpine AG, with several locations in and around Linz. In addition to these very large emitters, this region also hosts a large number from other industrial sectors with other registered IPPC facilities. Some major industrial companies in this region include the large chemical company Linde Gas GmbH, the world-leading construction equipment company Doka GmbH, the packaging and paper manufacturing company Merckens GmbH, the glass manufacturer Vetropack Austria GmbH, construction and raw materials companies Swietelsky AG and Bernegger GmbH, aluminum producer Nemak Linz GmbH, iron foundries Gienanth Steyr Guss GmbH, and energy companies like Linz AG, eww Gruppe and Energie AG Oberösterreich (including Energie AG Oberösterreich Umweltservice, i.e. waste incineration plants). [86]

Historical development of the industrial region and important industrial companies

Industrialization in Upper Austria began in the second half of the 19th century and was strongly influenced by the expansion of transportation infrastructure, particularly the introduction of steam navigation on the Danube and the construction of railway lines such as the Kaiserin-Elisabeth-Bahn. These developments made the greater Linz area a central industrial location, especially for shipyards, locomotive factories, and the textile industry. The industrial boom initially took place outside the city center, leading to rapid population growth, which was offset by the development of new neighborhoods. Significant figures like Josef Werndl played a key role in establishing industrial enterprises, particularly in the weapons factory in Steyr. The construction of modern transportation systems, such as the tram and the Pöstlingbergbahn, supported the region's urbanization and economic progress. In the post-war period, Linz continued to develop, not only as an industrial center but also as a cultural hub. The founding of the Johannes Kepler University and the Art University, as well as the establishment of cultural institutions such as the Brucknerhaus and the Ars Electronica Center, underscore the city's transformation, beside its importance for the industry, into an important educational and cultural location. Despite this cultural development, industry remained a central part of the economy in Upper Austria. Other industrial sectors, such as metal, paper, and food processing, contributed to economic growth throughout the region. Linz remained an industrial center point, gaining international importance especially with the metal company voestalpine. Overall, Upper Austria's industrialization and the associated urban and cultural developments made it a central hub for economy and industry in Austria. [97] [98]

The voestalpine AG with its main steel plant in Linz (Figure 13) has a long and significant history, spanning many decades and playing a crucial role in Austrian industry to this day. The company developed into a pioneer in steel production after the Second World War. With the invention of

the Linz-Donawitz process, a major technological breakthrough was achieved, revolutionizing the steel industry worldwide and making Linz a central hub for steel production with €16.7 billion in revenue in 2023. Over the past four decades, voestalpine has increasingly focused on more sustainable steel production. This is particularly relevant in the context of particulate matter pollution from steel production, because in addition to carbon monoxide and dioxide, particulate matter, nitrogen oxides, NMVOCs, inorganic chlorine compounds, zinc, benzene and lead are released into the air during pig iron and steel production in relevant quantities. The company has made significant investments in technologies to reduce emissions and particulate matter and develop more environmentally friendly production processes. Since the 1980s, the modernization of production facilities has been accelerated, including the introduction of the MEROS system for exhaust gas cleaning, specifically designed to minimize air pollutants. In recent years, ambitious projects to reduce CO_2 emissions have been a key focus. One of the flagship projects is the planned construction of electric arc furnaces by 2027, which will gradually replace blast furnace operations. This is expected to reduce CO_2 emissions in Austria by about 5%. This transformation of production processes is part of the comprehensive climate protection program "greentec steel," making voestalpine one of the pioneers of environmentally friendly steel production in Europe. Overall, voestalpine remains a key player not only due to its size and importance in Austrian industry but also because of its ongoing efforts to reduce its ecological footprint. [99] [100]

Figure 13: voestalpine large-scale industrial park in Linz [101]

Meteorological phenomenon in Linz

An interesting weather phenomenon that occurs in Linz due to the local industry is the so-called industry snow. This occurs because large quantities of water are needed to cool industrial processes. In this case the steel production of voestalpine in Linz uses water for their cooling processes, this water then evaporates into water vapor and is released into the surrounding air through chimneys. These exhaust gas plumes mostly consist of large amounts of water vapor with also a proportion of air pollutants. Due to an annual amount of about five million tons of water vapour, the phenomenon of industrial snow occurs in Linz during the colder winter months. The following Figure 14 shows the affected areas in Linz where industrial snow occurs. It should be noted that the voestalpine plant and the "Linz Neue Welt" measuring station, which will be discussed in more detail in chapter “Analysis and results of the particulate matter concentration (PM10 and PM2.5) in the industrial cluster “Großraum Linz””, are located at the blue part of the industrial snow plume in Figure 14. North of the blue area of the industrial snow plume is the "Linz Römerberg" measuring station, which will be also discussed in more detail later.

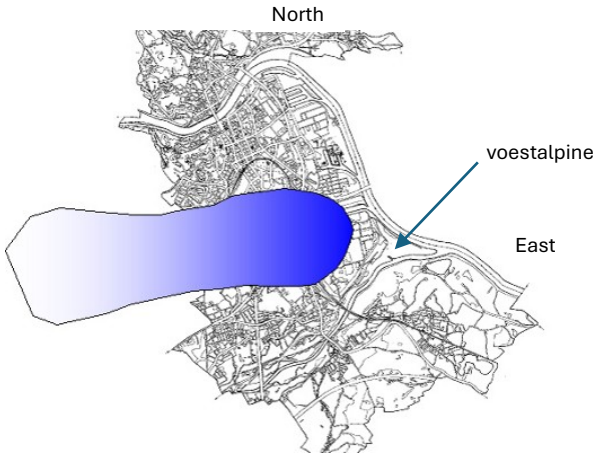

Figure 14: Spatial spread of industrial snow in Linz near the voestalpine location [102]

Industrial snow is formed when the molecules of the water vapor from the industrial processes nucleate and condense to droplet and ice particles, which is discussed in the chapter “Homogeneous and heterogeneous nucleation processes”. This water vapor in Linz mostly comes from combustion processes from the industry, energy production from thermal power plants, district heating plants and cooling towers of the coking plants in Linz. To name two specific examples, the steel company voestalpine and Agrolinz Melamin are two main contributors. [103]
Certain meteorological conditions must occur to enable the formation of industrial snow. Winter high-pressure weather conditions, high humidity, fog or high fog and low wind conditions with temperatures below freezing point are favorable. Due to the increased humidity from the industrial water vapor and the cold temperatures, snow crystals can now form and fall as industrial snow.

Due to this phenomenon in Linz, measurements of pollutants from industrial snow and natural snow were carried out in Linz in order to evaluate the health consequences for humans.

It turned out that, although the majority of the exhaust plumes consist of water vapor, the pollutant load of industrial snow was five times higher than that of natural snow. The pollutants produced during industrial processes are transferred directly into the ice nuclei and further snow crystal formation. The limit values were exceeded in the area of iron and manganese, mainly caused by the local steel industry in Linz. The limit values for ammonium and nitrite were also exceeded, mainly due to the local chemical industry in Linz. In addition to industry, the high level of traffic also plays a role, which is discussed in the chapter “Analysis and results of the particulate matter concentration (PM10 and PM2.5) in the industrial cluster “Großraum Linz””. Industrial snow most commonly occurs in Linz during the first half of January, primarily affecting the eastern parts of the city near the industrial area. In addition to cold temperatures and inversion weather conditions, an easterly wind is typically present. The average amount of precipitation in Linz since the beginning of the 1990s is around 840 mm, which is below the Austrian average of 1190 mm. [102] [104] [105]

The industrial region of “Großraum Graz” (greater Graz)

IPPC facilities and PRTR reports

The industrial cluster “Großraum Graz" in Styria is home to 39 registered IPPC facilities, as well as one industrial company that has exceeded the PM10 limit according to PRTR reports since 2007, namely the pulp and paper company Sappi Austria Produktions-GmbH & Co. KG. Additionally, other major air pollutant emitters include the Stahl- und Walzwerk Marienhütte GmbH, Andritz AG, raw material producer Intercal Austria GmbH, paper and cardboard manufacturer MM Frohnleiten GmbH, automotive manufacturer Magna Steyr AG, and energy company Energie Steiermark AG.

Historical development of the industrial region and important industrial companies

The industrial development in Graz began in the 19th century, strongly driven by the establishment of the railway in 1844. Companies such as Andritz (founded in 1852), Puch, and the Reininghaus Brewery were established, taking advantage of the region’s strategic location and its raw material resources. This period of industrialization brought technological innovations and significant population growth. However, in the early decades of the 20th century, the industrial sector in Graz was severely affected by the world wars and economic crises. Despite these setbacks, the region recovered after World War II, largely due to governmental support and the introduction of new technologies. From the 1950s onwards, Graz entered a period of growth characterized by international collaboration and technological innovations. The industry in Graz diversified into sectors such as mechanical engineering, automotive sector, paper production, energy sector and new technologies, forming the foundation of the region’s modern economic structure. [106] [107]

An important sector in Graz is the automotive industry, with Magna as one of its key players. The region, which has long been considered a significant hub for automotive production and supply, is now facing considerable pressure due to the current shift towards electric vehicles and the associated requirements. Many suppliers, who work closely with international manufacturers, must adapt their production, which involves substantial investments. The EU-wide transition to electromobility, which is particularly noticeable in Graz, coincides with a complex economic environment. Rising energy prices and uncertainties in global supply chains exacerbate these challenges. Companies like Magna, which are heavily export-oriented, are tasked with realigning their production capacities while also managing increasing costs. The industry's dependence on decisions at the European level, as well as slow political action regarding the infrastructure for electric vehicles, also impacts the entire automotive sector in the region. The automotive industry in Graz, which has been a major economic driver for decades, is now forced to develop new strategies to remain competitive on the international stage. [108]

Meteorological phenomenon of the “Grazer Becken”

The “Grazer Becken” is particularly noteworthy in a meteorological sense because it is very poorly aerated in the colder months of the year and can therefore hold particulate matter for a particularly long time and in high concentrations. This is why one of the highest levels of particulate matter pollution and nitrogen dioxide in the whole of Austria is measured in winter in Graz. In addition, there is the factor of heating and especially domestic fires, which, in addition to the local industry and traffic, further increases particulate matter pollution under these fog layers. Progress has already been made in reducing emissions, as less heating is provided by conventional ovens due to the expansion of district heating. [109]

In general, an inversion weather situation occurs when the change of temperature increases with altitude, so $\frac{\mathrm{dT}}{\mathrm{dz}} > 0$, with *T* as the temperature and *z* as the altitude, and the vertical exchange of air is blocked. In high-pressure areas, air masses sink over large areas. During the descent, the air heats up adiabatically and loses relative humidity in the process. At a certain height, the heated air spreads horizontally and forms a stable layer. Cooler and more humid air masses remain below this layer, which are insulated from exchange with the air above by the stable structure. As a result, air pollutants accumulate in the cooler air layer near the ground, which is particularly problematic in fall and winter. In the “Grazer Becken”, this effect is intensified by the topographical location, as cold air masses remain trapped in the valleys of Graz and can hardly escape. In order to reduce the concentration of air pollutants, traffic-related measures such as speed restrictions have been introduced (e.g. IG-L 100km/h). The average amount of precipitation in the “Grazer Becken” over the last 35 years was below the average Austrian value (1190 mm) at around 882 mm per year but is particularly affected by extreme weather events due to the Mediterranean influence. [110] [111]
The following Figure 15 shows well how a layer of clouds/fog hangs over the “Grazer Becken” and traps the air pollutants underneath, as there is only little air exchange with other air masses.

Figure 15: Inversion weather situation in the "Grazer Becken" during winter [112]

The industrial region of “Großraum Mur-Mürz-Furche” (greater Mur-Mürz-Furche)

IPPC facilities and PRTR reports

The industrial cluster “Großraum Mur-Mürz Furche" beginning in Mürzzuschlag, through Bruck an der Mur, Leoben to Knittelfeld/Judenburg as well as the Erzberg region in Styria, houses 48 IPPC facilities and five large industrial companies that, according to PRTR reports, have exceeded the maximum limits for PM10 emissions since 2007. These include the sites of the voestalpine steel company Donawitz Stahl GmbH and Böhler Edelstahl GmbH, the mining and metal company VA Erzberg GmbH, the energy and waste recovery company ENAGES GmbH, and the pulp producer Pöls AG. Additionally, this industrial cluster also hosts the plastic manufacturer SKF Austria AG, the magnesium (hydroxide) producers Styromag GmbH, Veitsch-Radex GmbH (RHI Magnesita), and Magnifin GmbH, the paper and packaging companies Brigl & Bergmeister GmbH and Norske Skog Bruck GmbH, as well as other iron and steel companies such as Breitenfeld Edelstahl AG, Stahl Judenburg GmbH, and additional voestalpine sites. The location of the “Großraum Mur-Mürz-Furche” in Styria is shown as the red area in the following Figure 16.

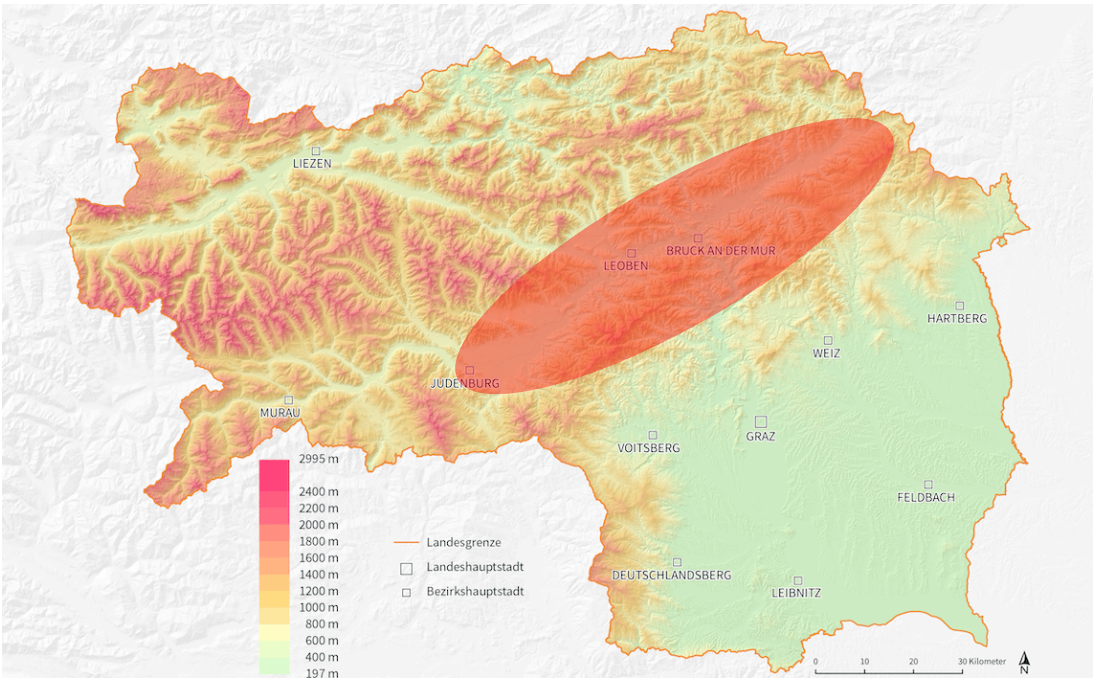

Figure 16: Geographical location (red area) of the “Großraum Mur-Mürz-Furche” in Styria [113]

Historical development of the industrial region and important industrial companies

In recent decades, the industrial landscape in the Mur-Mürz-Furche has undergone significant transformation and development. Historically, this region has been a major center of iron and steel production, largely due to the rich iron ore deposits at the Erzberg, which have been exploited since the Middle Ages. During the 19th century, the reliance on raw materials like iron ore and the availability of abundant forests for charcoal production laid the foundation for the region's industrial growth. Later, charcoal was replaced by lignite, leading to large-scale coal mining operations in Köflach-Voitsberg, Leoben, and Fohnsdorf to meet the demands of iron processing.

By the late 19th and early 20th centuries, heavy industry, particularly in Leoben-Donawitz, became the backbone of the regional economy, with steel plants and industries supplying materials for the machine-building, rail, and vehicle industries. The relatively poor quality of local iron ore, with an iron content of only about 30 %, limited its competitiveness compared to foreign ores with up to 80 % iron, which were imported to Austria more cost-effectively via the Danube. This reliance on local resources, combined with the region’s lack of rivers, created logistical challenges that increased transportation costs for both raw materials and finished products. The construction of the Semmering Railway in the 19th century helped mitigate some of these challenges, transforming the Mur-Mürz-Furche into one of Austria's most relevant industrial corridors. After World War II, much of the heavy industry in the Mur-Mürz-Furche was nationalized to support Austria’s economic recovery. While this state-controlled system initially boosted industrial output and employment, it ultimately delayed the region’s adaptation to global market conditions. The 1990s marked a turning point for the Mur-Mürz-Furche. Neoliberal reforms, including the privatization of industrial enterprises, allowed many companies to specialize in niche markets, leading to a gradual economic recovery. The region also benefited from Austria’s entry to the European Union and the subsequent opening of Eastern European markets, which repositioned the Mur-Mürz-Furche to a central hub in Europe. Cluster initiatives, such as those supporting the automotive and wood industries, further diversified the economy, fostering innovation and collaboration between businesses and research institutions. Today, while traditional heavy industries remain, the Mur-Mürz-Furche has seen significant advancements in technological innovation and the development of new industrial sectors. [113] [114]

The origins of one of the most important industrial plant in this area is the voestalpine Stahl Donawitz GmbH and trace back to 1436, when the first hammer mills for iron processing were documented. Since then, the Donawitz site has undergone continuous innovation and structural changes, evolving into a leading company in steel production. A major milestone was the introduction of puddling steel production between 1834 and 1837, followed by the construction of the first Martin furnace in 1878, marking the beginning of a new era in steel manufacturing. The establishment of the Donawitz-Vordernberg railway, and later the Vordernberg-Eisenerz line, enabled cost-efficient mass production of steel. In 1892, a new beam and rail rolling mill was built, positioning Donawitz as a central player in steel production within the Austrian monarchy. The installation of coke ovens in 1905 and the operation of the 14th Martin furnace in 1912 expanded the site to become the largest integrated steel plant in Europe. The challenges of World War I, including fuel shortages, were met by building a new furnace in 1928, which allowed for the production of specialty steels, such as electric manganese steel rails. After Austria’s annexation by Germany, the plant merged with other

facilities and was renamed "Reichswerke AG Alpine Montanbetriebe" in 1941. The focus shifted to wartime production, with full operation of all facilities and the construction of additional arc furnaces and a blooming mill. Post-World War II reconstruction efforts were supported by the Marshall Plan, which facilitated the construction of new production lines in the 1950s. In 1953, the second steel plant in the world was commissioned in Donawitz, equipped with two 30-ton converters. This process revolutionized steel production by enabling the cost-effective processing of iron and scrap into high-quality raw steel.
Key milestones in recent history include the merger of ÖAMG with voest in 1973, the public listing of voestalpine Stahl AG in 1995, and the construction of the world's most advanced compact steel plant in 2000. Further technological advancements followed, such as the commissioning of the second vacuum system in 2005 and the CC4 continuous casting plant in 2020, the most advanced of its kind globally, fully adhering to industry 4.0 standards. [115]

Meteorological phenomenon of the Mur-Mürz-Furche

The climate of the Mur-Mürz-Furche consists of several areas along the entire valley. Starting with the eastern part from Mürzzuschlag to the western part of the Mürz-valley, the region is characterized by a relatively sheltered position against airstreams from the west and north. Overall, the area experiences lower precipitation levels compared to the Styrian foreland, with approximately 1033 mm of annual precipitation in Mürzzuschlag. Precipitation tends to increase from west to east, especially in the winter period. The region also experiences around 80-90 days of fog per year. The general temperature conditions are moderately continental, and it is notable that in some parts of the Mürz-valley, due to its sheltered location, inversion weather patterns can occur, with limited vertical wind mixing. The area between Bruck an der Mur and Preg is one of the driest regions of the Mur-valley (annual precipitation of around 796 mm). This area is characterized by the dominance of the so-called Murtal winds, low snowfall in winter, and a higher likelihood of high- fog, which is then often cleared by the valley winds. The temperatures in this region are moderately cold in winter and warm in summer, with temperatures increasing towards the east. The western area stretches from Judenburg to Preg. This region is also continental in climate, with relatively dry winters and low snowfall, receiving annual precipitation levels of around 797 mm in Zeltweg. Due to its location in a basin, inversion weather conditions are more common, but in the western part of the area, these can be cleared by the Mur-valley winds. [116]

Methodology and results of the particulate matter concentration in the industry regions of Austria

The following chapters deal with the data acquisition and analysis methodology and the results of the various PM10 and PM2.5 concentrations of the different industrial regions of Austria as well as the background monitoring sites.

A key point that must be emphasized at this point is that the data sets for PM10 and PM2.5 concentrations, regardless of whether they originate from the European Environment Agency (EEA), Environmental Agency of Austria (Umweltbundesamt), the federal government or the federal states, do not publish any uncertainties in the data sets. This is due to the fact that the operators of the monitoring networks have to prove regularly that they meet the quality targets of the European Air Quality Directive and the Austrian Immission Control Act-Air (IG-L). As long as these quality objectives are met, additional uncertainty analysis is not required and are therefore not reported and published. This was additionally confirmed via mail by an air expert from the Environmental Agency of Austria.

Analysis and results of the particulate matter concentration (PM10 and PM2.5) in the industrial cluster “Großraum Wien”

The following analysis of particulate matter in the industrial cluster “Großraum Wien” and later for “Großraum Linz” is split into data sets in the periods before 2012 and after 2012, and later be combined, as only different data sets from different data bases were available for each of these periods due to regulatory changes at European level. This has the advantage that the period from 20002-2022 can be divided into two sections and the development of the periods can be examined more specifically.

PM10 data acquisition between 2002-2012 in Vienna inner-city

For the analysis of PM10 concentration in the classified industrial region “Großraum Wien” around Vienna between January 1, 2002, and December 31, 2012, data from the European Environment Agency (EEA) was utilized. The dataset was generated from the EEA's download service and further analyzed. Historical air quality data from the database, spanning the period from 2002 to 2012, was providing data before the implementation of the European Air Quality Directive 2008/50/EC. From 2013 to 2022, another database (category E1a) was available and used for data acquisition. The member states of the European Union regularly report to the EEA, submitting their collected national air data, which the EEA then compiles and publishes collectively.

In this case the data consisted of hourly values, amounting to 24 data points per day. The EEA provided one nearly continuous dataset from the sampling station “AT/SPO.09.SCHA” located in the northwestern part of Vienna near Schafberg, covering data up to 2012. This continuity at one sampling spot was the reason for the choice of this location. For the year 2009, data from a nearby sampling station “AT/SPO-AT90AKC,” situated slightly closer to the inner city and near

the Vienna General Hospital (AKH), was used, as the data from the station “AT/SPO.09.SCHA” was not available (N/A) for this year.

A total of 87,671 hourly data points on PM10 concentrations were available from the sampling point “AT/SPO.09.SCHA” during this period. Each concentration value also had a verification indicator of either -1 or +1. If the verification value was +1, the measurement was valid, whereas a value of -1 indicated an incorrect or faulty reading, often due to equipment malfunctions (usually showing zero values in the concentration column). Notably, from the start of the dataset, January 1, until April 11, 2002, the verification value was -1 for 2,412 data points, leading to the exclusion of these values. Overall, 84,831 data points were correctly validated, with approximately 3.2 % of the whole data set being excluded because of the verification value -1.

At the sampling point “AT/SPO-AT90AKC” 8,759 hourly data samples were taken in 2009, of which 209 were labelled as unverified, so 2.4 % of the data was excluded. This means that 8,550 PM10 concentration values were taken to close the gap from 1 January 2009 to 31 December 2009 and complete the first series of data concentrations in Vienna inner-city. [117]

PM10 data acquisition between 2013-2022 in Vienna inner-city

To ensure the best possible consistency and gather PM10 concentration data at one location for the full period between 2002 and 2022, measurements were again generated from the monitoring station "AT/SPO.09.SCHA" in Vienna inner-city near Schafberg again. This station provided complete PM10 concentration data across the selected time frame. Over this period, a total of 87,647 hourly values were recorded. Of these, 1,144 measurements were flagged as invalid and subsequently excluded from the analysis, representing approximately 1.3 % of the overall dataset. The data analysis and evaluation followed the same methodology as previously applied to the 2002-2012 data series.

PM10 data acquisition between 2013-2022 at the industrial location Schwechat near Vienna

To allow for a comparison within Vienna inner-city with a large industry location, PM10 concentration data from the area near the Schwechat refinery was also included during the second recording period (2013-2022). The objective was to analyze how these values varied from the consistently measured inner-city data, as Schwechat is one of the main industry spots in Austria. It is important to highlight that the data from the station “AT/SPO.09.KE” near Schwechat were only available in the European Environment Agency's database for this specific period, not for the years 2002-2012.

During this time, a total of 81,072 measurements were recorded at this station on an hourly basis. Of these, 554 readings were marked as invalid and thus excluded from the analysis, accounting for approximately 0.7 % of the total measurements. Additionally, to note is, that for the year 2021, only data from the last three months (October, November, and December) were available.

Combined PM10 concentration results from Vienna inner-city and Schwechat

Even though the PM10 values have generally decreased in the second period (average concentration was 17.4 $\frac{\mu g}{m^3}$) from 2012-2022 compared to the first period from 2002-2012 in Vienna inner-city (average concentration was 23.2 $\frac{\mu g}{m^3}$), it will be shown that the PM10 concentrations near Schwechat's industrial cluster were significantly higher with an average of 20.5 $\frac{\mu g}{m^3}$ in the second period between 2013-2022.

The following Figure 17 presents all previously discussed PM10 concentrations for Vienna inner-city (blue line) from 2002 to 2022 and PM10 concentrations near Schwechat (orange line) from 2013-2022. The hourly measurement data was carefully analyzed and aggregated first into daily and then into monthly averages to provide a clear graphical representation, which is shown in the following Figure 17. The dotted lines represent a trend line, visualizing the average decrease in particle levels over the past 20 years in Vienna inner-city and in Schwechat. A clear decrease in the PM10 concentration in Vienna inner-city is seen in the blue dotted line, representing the decrease in the concentration. Same applies for the orange dotted line representing the decrease in PM10 concentration in Schwechat but showing clearly higher values than the ones from Vienna inner-city. This could be due to the fact that the industry located in Schwechat has a greater impact on particulate matter concentration than in Vienna's city. It should be added that there is also a freeway (A4 Ost-Autobahn) with lots of traffic in direction to the Vienna Airport close to the Schwechat refinery, which can also have a significant impact on particulate matter pollution.

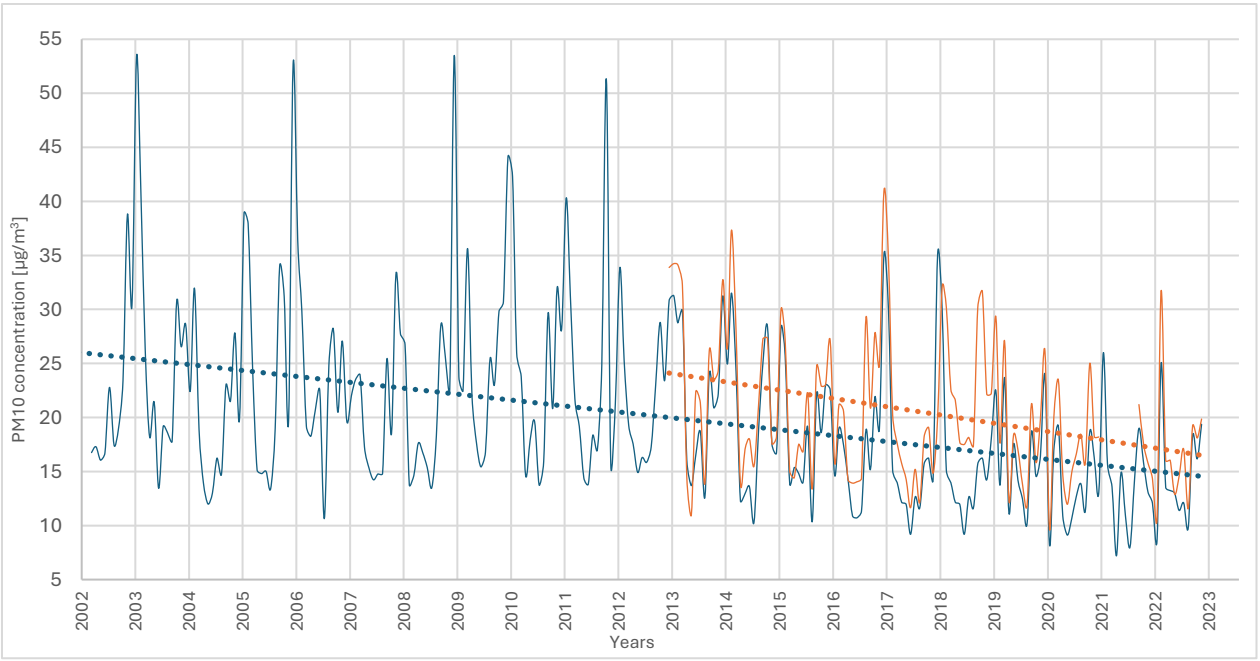

Figure 17: PM10 concentration [µg/m³] in Vienna inner-city (blue line) 2002-2022 and in Schwechat (orange line) 2013-2022

Table 2, which is showing all annual average values, the average PM10 concentration during the second period (2013-2022) at the sampling station in Vienna inner-city is approximately 25 % lower than the average PM10 concentration during the first period (2002-2012) at the same

location. The average PM10 concentration near Schwechat in the second period (2013-2022) shows a reduction of about 10 % compared to the average PM10 concentration at the Vienna-inner city stations during the first period. This decline in PM10 levels highlights the overall improvement in air quality, though the Schwechat region still maintains higher PM10 levels.

Table 2 shows the values and the annual change of the PM10 concentration to the previous year. The limit value of 40 $\frac{\mu g}{m^3}$ permitted by the EU was not exceeded in any year in the period 2002-2022. The annual limit of 15 $\frac{\mu g}{m^3}$ recommended by the WHO was successfully undercut in the years 2020-2022 in Vienna inner-city.

Year	Average concentration of PM10 in Vienna inner-city [µg/m³]	Yearly change in PM10 concentration in Vienna inner-city [µg/m³]	Average concentration of PM10 in Schwechat [µg/m³]	Yearly change in PM10 concentration in Schwechat [µg/m³]
2002	21.2	N/A	N/A	N/A
2003	26.3	5.2	N/A	N/A
2004	20.4	-6.0	N/A	N/A
2005	23.5	3.1	N/A	N/A
2006	25.9	2.4	N/A	N/A
2007	20.2	-5.6	N/A	N/A
2008	20.1	-0.2	N/A	N/A
2009	26.4	6.3	N/A	N/A
2010	25.0	-1.4	N/A	N/A
2011	24.5	-0.5	N/A	N/A
2012	21.3	-3.2	N/A	N/A
2013	22.1	0.8	24.3	N/A
2014	20.9	-1.1	23.5	-0.8
2015	18.6	-2.3	20.4	-3.1
2016	16.3	-2.3	20.3	-0.1
2017	16.4	0.1	19.5	-0.8
2018	20.4	4.0	23.4	3.9
2019	16.2	-4.2	18.7	-4.7
2020	14.3	-1.8	18.1	-0.7
2021	14.2	-0.1	18.2	0.1
2022	14.5	0.3	16.9	-1.3

Table 2: Yearly average PM10 concentration [µg/m³] in Vienna inner-city and Schwechat (2002-2022) and its yearly change

PM2.5 data acquisition between 2005-2012 in Vienna inner-city

This section deals with the PM2.5 concentration in the greater Vienna area in the period 2002-2012. The data was again generated through the European Environment Agency databank, so two time periods 2002-2012 and 2013-2022 is also considered separately here. No data is available for the years 2002, 2003 and 2004, so the data analysis starts with the data from January 2005 and ends with December 2012. In contrast to the PM10 concentration data for Vienna inner-city and Schwechat, which was available on an hourly basis, the PM2.5 data here was available on a daily basis.

The only measuring station for which PM2.5 data was available in and near Vienna was the sampling point „AT/SPO.09.AKC " near the General Vienna Hospital (no data was available for the Schwechat location), which was already used for the PM10 concentration data in 2009. A total of 2,975 daily data records of PM2.5 concentration was available. It is worth noting that 86 measurements were not correctly validated and therefore 2.9 % incorrectly validated values of the 2,975 data points were excluded from the analysis.

PM2.5 data acquisition between 2013-2022 in Vienna inner-city

In order to show a consistent measurement series here as well, data from the "AT/SPO.09.AKC" measuring point was generated again. During this period (2013-2022), it was again possible to obtain hourly PM2.5 concentration data from the European Environment Agency, not daily data sets as for the first period. This was also done in order to have more granular data sets. A total of 78,864 measurement data were generated at this measuring point in the period 2013-2022, although no data were generated at this measuring point in 2016. A total of 1,355 of these were not correctly validated, which corresponds to around 1.7 % of all measurement data, of which 86.8 % were incorrectly validated in July and August 2015. Nevertheless, 84.4 % of the data measured in 2015 was validated as correct and was included in the overall data analysis. In order to supplement the missing PM2.5 concentration data sets from the year 2016, data for 2016 was taken from a nearby measuring station, namely from the measuring point "AT/SPO.09.KEND ", which is located in Vienna Ottakring.

Combined PM2.5 concentration results from Vienna inner-city

A clear decrease in the concentration of PM2.5 was observed between 2005-2022. The following Figure 18 shows the development of PM2.5 concentration in Vienna inner-city between the years 2005-2022. The hourly and daily measurement data was again carefully analyzed and aggregated into monthly averages to provide a clear graphical representation.

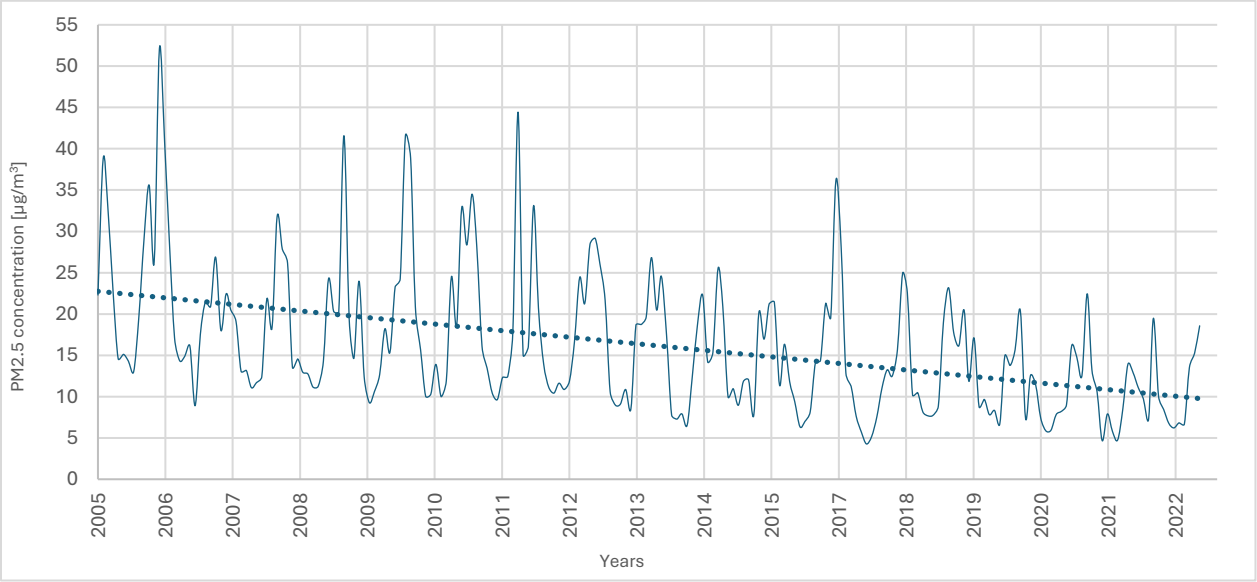

Figure 18: PM2.5 concentration [µg/m³] in Vienna inner-city (blue line) 2005-2022

The figure above clearly shows that the concentration of PM2.5 in Vienna has decreased significantly over the 17 years of recorded measurements. It is clear to see that there was an above-average peak at the end of the year 2005 and the beginning of 2006, also seen at the PM10 analysis of the Vienna region. In that time period, the main pollution hotspots for particulate matter were the cities of Vienna and Graz, followed by Linz. The permitted limit value for particulate matter (in case of PM10) was exceeded at 63 % of all measuring stations in Austria. The reasons for this were very high emissions of primary particles and a high number of precursor substances of secondary particles such as sulphur dioxide from industry, nitrogen oxides from traffic and ammonia from agriculture. There was also increased long-distance transportation of particulate matter from Eastern Europe and unfavorable distribution conditions. [118] This peak will also be seen in further analysis of the other industrial regions.

The blue dotted trend line shows the average decrease in PM2.5 concentration. The following

Table 3 shows the yearly average PM2.5 concentration in Vienna inner-city. If one now compares the yearly mean PM2.5 concentration in the first period (2005-2012) with the second period (2012-2022), the difference is clear: in the first period it was 19.8 $\frac{\mu g}{m^3}$ and in the second period only 13.4 $\frac{\mu g}{m^3}$, with a particular decline in the end of the second period. It is also clear to see at that point, that the concentration of PM2.5 in both periods is lower than the one of PM10 in both periods in Vienna inner-city and Schwechat.

Table 3 shows again the values and the annual change of the PM2.5 concentration to the previous year. The limit value of 25 $\frac{\mu g}{m^3}$ permitted by the EU was not exceeded in any year in the period 2005-2022. The annual limit of 5 $\frac{\mu g}{m^3}$ recommended by the WHO was never successfully undercut in the years 2005-2022.

Year	Average concentration of PM2.5 in Vienna inner-city [µg/m³]	Yearly change in PM2.5 concentration in Vienna inner-city [µg/m³]
2005	23.9	N/A
2006	23.2	-0.7
2007	17.8	-5.4
2008	17.4	-0.4
2009	18.9	1.5
2010	20.7	1.8
2011	20.1	-0.6
2012	16.8	-3.3
2013	17.5	0.7
2014	15.5	-2
2015	15.6	0.1
2016	13.5	-2.1
2017	12.9	-0.6
2018	14.6	1.7
2019	12.5	-2.1
2020	10.6	-1.9
2021	10.6	0
2022	10.8	0.2

Table 3: Yearly average PM2.5 concentration [µg/m³] in Vienna inner-city (2005-2022) and its yearly change

Analysis and results of the particulate matter concentration (PM10 and PM2.5) in the industrial cluster “Großraum Linz”

In this chapter, the data will be separated again in the two mentioned periods (before and after 2012) and later combined in the results as before, as the data is again generated by the European Environmental Agency databank.

PM10 data acquisition between 2005-2012 in Linz

In the greater Linz area, a total of 2231 daily measurements of PM10 concentrations were taken at the "AT/SPO.04.S431" monitoring station at “Linz Römerberg”, which is located north of the city center and about 4 km from heavy industry and close to a very busy road, in the period 2005-2012. This is the only measuring station in which a nearly continuous data set is available for this period from the EEA. Data for the years 2002-2005 was not available from the European Environment Agency. Likewise, no data is available at the monitoring station for the years 2007-2008.
For this reason, the only available PM10 concentration data for the period 2007-2008 was selected from another measuring station in "Linz Neue Welt"/ "AT/SPO.04.S416", which is located 600 m west of the main plant of the steel producer voestalpine. At this location, only data records from 2007 were available, which were included in the analysis. PM10 data for the year 2008 were not available for Linz from the EEA.

The PM10 concentration at the sampling station “Linz Römerberg” is stored as daily average data by the European Environment Agency. 44 of the 2,231 measurement data sets were classified as not correctly validated and were therefore excluded from the analysis, which corresponds to around 1.9 % of the total data volume. The concentration data for PM10 pollution at the "Linz Neue Welt" site, on the other hand, are available on an hourly basis. A total of 8,760 measurements were taken at this location, 70 of which were not validated as correct, which corresponds to around 0.8 % of the total data.

PM10 data acquisition between 2013-2022 in Linz

The station “Linz Römerberg” was again selected for the 2013-2022 period in order to achieve the greatest possible consistency in the measuring stations. A total of 87,647 hourly data records on PM10 concentration in Linz are available from the European Environment Agency. At this measurement point, a total of 1,815 measurement data sets were validated as incorrect and therefore excluded from the analysis, which corresponds to around 2.1 % of all data sets. 80.6 % of these incorrectly validated values were from the months of May, June and July 2017. Nevertheless, 83.3 % of all values measured in 2017 were correctly validated and were included in the analysis.

PM10 data acquisition between 2013-2022 at the industrial location of the voestalpine in Linz

In order to take again, as in the example of Vienna and the industry location near the Schwechat refinery, the measurement data of the PM10 concentration near a significant and large industrial region, the measurement data from the location of the measuring station "AT/SPO.04.S416"/"Neue Welt Linz" was also taken, as these were also available for the second period (2013-2022) at the European Environment Agency. As mentioned, this measuring point is only 600 m to the west from the main industrial plants of the voestalpine.

The data was again available on an hourly basis. A total of 87,467 data records on PM10 concentration were available over this time horizon, of which 5,887, around 6.7 % of the data set, were not correctly validated. 85.1 % of this incorrectly validated data originates from the years 2018 (mainly February, March and April) and 2019 (mainly April, May and June).

Additional PM10 data acquisition between 2005-2022 in Linz

In addition to the European Environment Agency, which has PM10 concentration data available on an hourly or daily basis, the City of Linz has also published data from 2005 onwards, in which the monthly average PM10 concentration values of measuring points in the greater Linz area (Linz/Traun/Enns) were published. The measuring points in greater Linz from this new data source are as follows: "24er Turm", "BH Urfahr", "Linz Römerberg", "ORF-Zentrum", "Linz Neue Welt", "Kleinmünchen", "Steyregg-Weih", "Steyregg-Au", "Asten", "Traun", "Enns Kristein" and "Stadtpark". In order to provide a more general overview and comparison of the PM10 concentration development in this greater Linz area to the concentration exclusively in Linz city, all PM10 concentration values of these stations are combined and summarized in an average general PM10 value for the greater area of Linz. This is then compared with the specific PM10 values close to the industrial plant on the location „Linz Neue Welt“ and with the busy road at the location „Linz Römerberg“. It should be emphasized that not all of these measuring stations were actively in operation in all years between 2005-2022. [119]

Combined PM10 concentration results from Linz

The following Figure 19 shows the complete PM10 concentration development of the region of Linz from 2005-2022 with granular data from the European Environmental Agency and monthly data of the state Upper Austria. The hourly and daily measurement data was again carefully analyzed and aggregated into monthly averages to provide a clear graphical representation. The blue and solid line shows the development of PM10 concentration at the "Linz Römerberg" monitoring station, the orange line at the "Linz Neue Welt" monitoring station and the green line the averaged combined concentration of the before mentioned additional measuring stations in the greater area of Linz. The blue dotted trend line represents the average change in concentration from the "Linz Römerberg" location from 2005-2022, the orange dotted line from the "Linz Neue Welt" location from 2013-2022 and the green dotted trend line the change of all stations in greater Linz from 2005-2022.

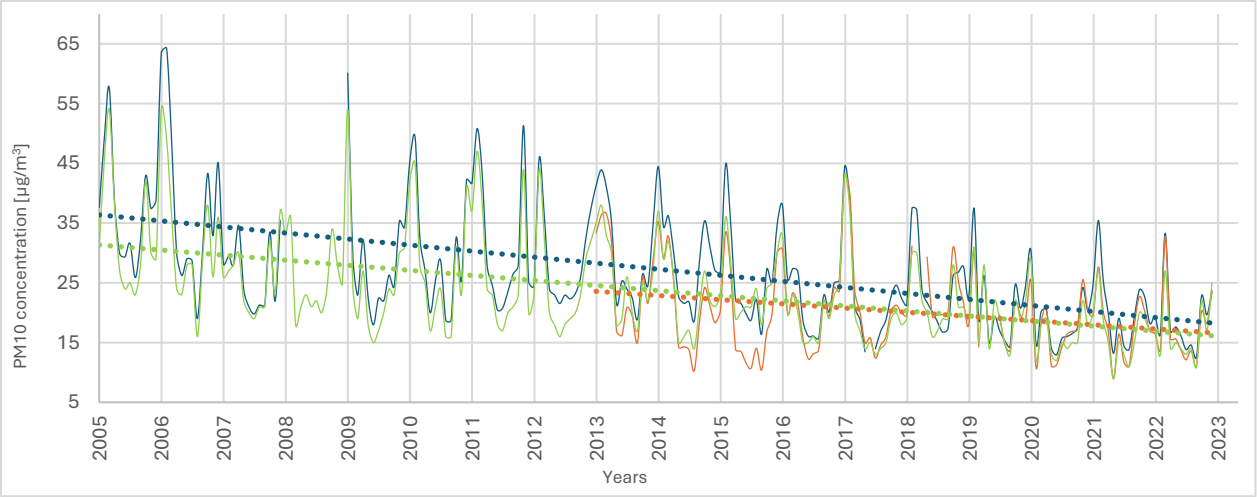

Figure 19: PM10 concentration [µg/m^3] in “Linz Römerberg” (blue line) from 2005-2022 and in “Linz Neue Welt” (orange line) from 2013-2022 as well as the averaged concentration in greater Linz (green line) from 2005-2022

This Figure 19 above shows that the concentration of PM10 in Linz has decreased significantly at both measuring stations in Linz and in greater Linz in general. We again find the peak in the concentration in the year 2006 as mentioned before. However, it is striking that the concentration at the "Linz Neue Welt" measuring point is lower than that at the “Linz Römerberg" measuring station. This could indicate that the heavy traffic in the city center of Linz, near Römerberg, has a greater influence on the PM10 concentration than the voestalpine industrial plant, as the data from “Linz Neue Welt” fits in well with the results of the greater Linz area. As mentioned before, voestalpine is a pioneer in the steel industry in terms of environmental and climate protection despite its high energy consumption, which is reflected in the latest technologies for energy usage and filter technology. This could be the reason, why the concentration is not that high as expected.

The data from the state of Upper Austria also showed, that from 2005 to 2022, the measuring stations "Linz Römerberg" and "Linz Neue Welt" were the measuring stations in the whole of Upper Austria that had the most daily PM10 limit value exceedances (> 50 $\frac{\mu g}{m^3}$). This shows that the analysis of especially these two measuring stations represents a relevant field of research and that the local heavy industry, in addition to dense traffic, plays a decisive role regarding PM10 concentration in Upper Austria. A trend towards a clear reduction in these limit value exceedances is also given by the analysis, in line with the results shown in the Figure 19 above. The comparison of the green and blue dotted line clearly shows that the concentration at the "Linz Römerberg" site is also significantly higher than the average exposure in greater Linz area, but this difference in concentration values has decreased in recent years. If one compares this average PM10 pollution in greater Linz, again the green dotted line, with the trend line from the industrial site "Linz Neue Welt", the values are very similar with regard to the decrease in the concentration of PM10. [120]

A comprehensive dust deposition program was also carried out in Linz in 2017, measuring the settled larger core dust particles on the ground in Linz over time, in contrast to particulate matter, which represents the mentioned airborne particles suspended in the atmosphere. Measuring points were set up at a total of 100 different measuring points in the greater Linz area, which measured dust deposition. The results showed that more than 90 % of the measuring points had a dust deposition below the specified limit values, but in the vicinity of the industrial

area, dust quantities above the limit value were detected, which indicates the increased dust pollution caused by industrial processes. In general, dust particle quantities have decreased in relation to the measurement results from older decades (1990s and 1950s), especially in the area of heavy metals. The results showed that concentrations of sodium, potassium and phosphorus from industry processes were detected above the limit values. [121]

The following Table 4 shows the yearly average PM10 concentration in the area of Linz at the different sampling stations. If one now compares the yearly mean PM10 concentration in the first period (2005-2012) with the second period (2012-2022), the difference is clear: in the first period it was at "Linz Römerberg" 31.8 $\frac{\mu g}{m^3}$ and in the second period only 23.7 $\frac{\mu g}{m^3}$, an average period decrease of around 8 $\frac{\mu g}{m^3}$. In comparison, the average value for the period 2013-2022 in "Linz Neue Welt" was 20.1 $\frac{\mu g}{m^3}$, around 15 % smaller than the concentration at "Linz Römerberg". The general value for the greater Linz area for the first period (2005-2012) was 27.7 $\frac{\mu g}{m^3}$ and for the second period (2013-2022) 20.5 $\frac{\mu g}{m^3}$.

Table 4 shows again the values and the annual change of the PM10 concentration to the previous year. The limit value of 40 $\frac{\mu g}{m^3}$ permitted by the EU was not exceeded in any year in the period 2005-2022 at the sampling stations "Linz Römerberg", "Linz Neue Welt" or for the general greater Linz area value. The annual limit of 15 $\frac{\mu g}{m^3}$ recommended by the WHO was never successfully undercut in the years 2005-2022 for all of these. To note is, that in the year 2006, the average yearly concentration at "Linz Römerberg" was very close to the permitted limit by being only 1.6 $\frac{\mu g}{m^3}$ away from this limit value.

Year	Average concentration of PM10 in Linz Römerberg [µg/m³]	Yearly change in PM10 concentration in Linz Römerberg [µg/m³]	Average concentration of PM10 in Linz Neue Welt [µg/m³]	Yearly change in PM10 concentration in Linz Neue Welt [µg/m³]	Average concentration of PM10 in greater Linz area (all stations) [µg/m³]	Yearly change in PM10 concentration in greater Linz area (all stations) [µg/m³]
2005	37.6	N/A	N/A	N/A	33.1	N/A
2006	38.4	0.8	N/A	N/A	32.3	-0.8
2007	26.5	-11.9	N/A	N/A	25.5	-6.8
2008	N/A	N/A	N/A	N/A	25.4	-0.1
2009	29.2	N/A	N/A	N/A	25.2	-0.3
2010	30.4	1.2	N/A	N/A	27.4	2.3
2011	31.9	1.5	N/A	N/A	27.8	0.3
2012	28.2	-3.7	N/A	N/A	24.6	-3.2
2013	29.9	1.7	25.2	N/A	25.8	1.3
2014	29.4	-0.5	21.4	-3.8	23.1	-2.8
2015	26.2	-3.2	18.5	-2.9	24.2	1.1
2016	23.2	-3	20	1.5	20.5	-3.7
2017	24.1	0.9	21.7	1.7	20.4	-0.1
2018	24.5	0.4	22.9	1.2	21.8	1.4
2019	21.2	-3.3	18.9	-4	19.9	-1.9
2020	18.6	-2.6	17.4	-1.5	16.8	-3.1
2021	20.7	2.1	17.5	0.1	16.7	-0.2
2022	19	-1.7	17.3	-0.2	15.4	-1.3

Table 4: Yearly average PM10 concentration [µg/m³] in Linz (2005-2022) and its yearly change

PM2.5 data acquisition between 2009-2022 in Linz

For the period 2002-2012, continuous values of the PM2.5 concentrations from the European Environment Agency are not available at a measuring station. The only available data set at the EEA in this period was between 2009-2012 from the measuring station "Linz Stadtpark", which is located in the center of Linz in a residential area with trees and smaller green lands. For these years 2009 to 2012, a total of 1,487 daily data sets of PM2.5 concentrations were available from the "Linz Stadtpark" monitoring station at the databank of the EEA, of which 31 (2.1 % of the data) were not correctly validated and were therefore excluded from the analysis. For the second period and years 2013-2022, PM2.5 concentration data in “Linz Stadtpark” was available from the European Environment Agency on an hourly basis. For this period, 78,864 data sets with PM2.5 concentrations were available, of which 961 (1.2 %) were not correctly validated and were therefore excluded from the analysis. Data from the year 2016 was not available for this monitoring station.

For the period 2013-2022, a total of 87,647 hourly PM2.5 concentration measurement data were available for the "Linz Neue Welt" measurement station, which was already used for PM10 concentration. Of these, 3,224 (3.7 % of the data) were validated as incorrect and were

excluded from the analysis. As already described, this measuring point is only 0.6 km away from the heavy steel industry in Linz. It should be noted that no data was available from the EEA at this location for the months of March and April in 2018. PM2.5 data from earlier years, before 2013, are not available from the EEA.

The "Linz Römerberg" monitoring station was also used again for the PM2.5 concentration analysis, as with PM10. Here too, only data from the period 2013-2022 was available and not from years before. Here, 87,647 PM2.5 concentration data points were available on an hourly basis. 1,812 measurement records (2.1 % of the total data set) were incorrectly validated and excluded from the analysis, of which over 80 % were incorrectly validated in 2017. No data is available from the EEA for June 2017 at this station.

It should be mentioned that, in contrast to the PM10 analysis in Linz, there was no monthly PM2.5 data for the greater Linz area from the State Upper Austria.

Combined PM2.5 concentration results from Linz

The following Figure 20 shows the evaluation of the data of the three PM2.5 concentration measuring points described above. The hourly and daily measurement data was again carefully analyzed and aggregated into monthly averages to provide a clear graphical representation.
A reduction in concentration can be seen for all in the period from 2009 to 2022. The highest average concentration can be observed at the “Linz Römerberg” monitoring station again represented by the solid blue and blue dotted trend line, followed by “Linz Neue Welt” with the solid orange and orange dotted trend line and “Linz Stadtpark” with the solid green and green dotted trend line. This can be again explained by the geographical location of the three stations, as the “Linz Römerberg” station is as known close to a very busy road and only a few kilometers away from heavy industry, while the “Linz Neue Welt” station is located right next to heavy industry. Interestingly, the difference in the average concentration of “Linz Römerberg” becomes larger over time compared to the other two measurement points, which is shown by the increasing distance between the dotted blue line to the other two dotted lines. The measuring station at “Linz Stadtpark” has the average lowest of the three concentrations, which is in greener area of the city of Linz. All three concentration curves show here a peak in the winter of 2016/2017, which can also be seen especially good in Figure 17 and Figure 18 in the analysis from the region of Vienna. During the winter of 2016/2017, unusually high levels of particulate matter were recorded, which can be attributed to several factors. On the one hand, the low temperatures present at the time played a role, while on the other hand, certain weather conditions contributed to the accumulation of pollutants in the region. In addition, there was an increased influx of pollutants from eastern areas, particularly from Hungary and Serbia, through long-distance transportation. Under these special meteorological conditions, concentrations of particulate matter were measured that significantly exceeded the average level of previous years. [122]

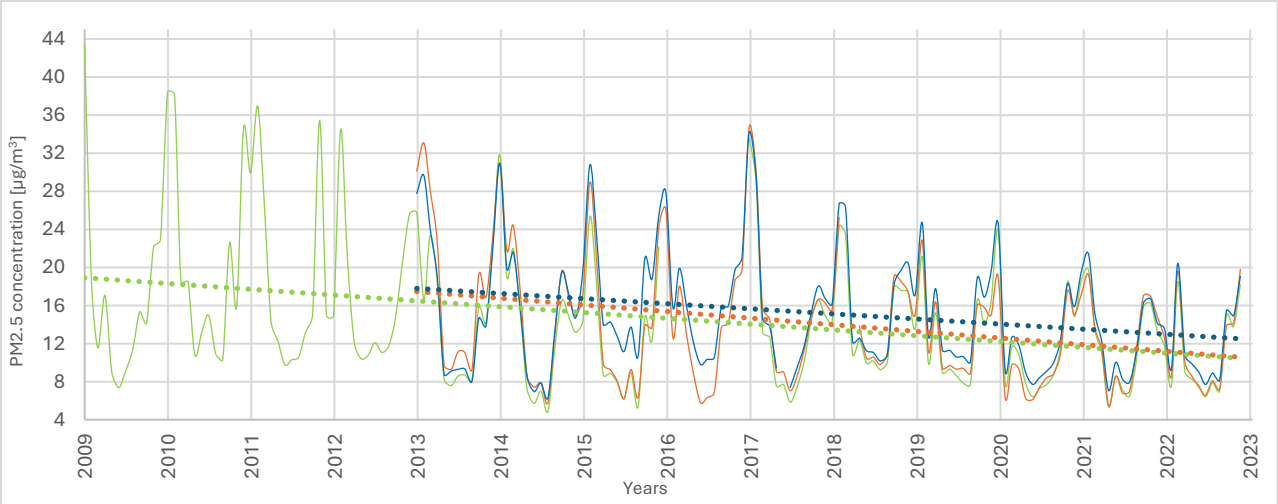

Figure 20: PM2.5 concentration [µg/m³] in Linz Stadtpark (green line) from 2009-2022, Linz Neue Welt (orange line) from 2013-2022 and Linz Römerberg (blue line) from 2013-2022

This Figure 20 above clearly shows that the concentration of PM2.5 in Linz has decreased significantly over the 13 years of recorded measurements. In comparison to the concentration of PM10 in Linz, to be seen in Figure 19 and Table 4, the concentration of PM2.5 is much lower than the one of PM10 as expected and in line with the different limit values for PM10 and PM2.5.

The following Table 5 shows the yearly average PM2.5 concentration in Linz. If one now looks at the yearly mean PM2.5 concentration between the periods 2009-2012 and 2013-2022, the difference of the locations and the difference to the PM10 concentration is clear. At the measuring station "Linz Stadtpark", the average concentration in the first period between 2009-2012 was 18.2 $\frac{\mu g}{m^3}$ and in the second period only 13.1 $\frac{\mu g}{m^3}$, showing a strong decline of more than 25 % in the second period to the first period and being the lowest value for the second period. As mentioned, for the other two stations data only for the second period was available. At the measurement station "Linz Römerberg" the average concentration of the second period was 15.2 $\frac{\mu g}{m^3}$, while at "Linz Neue Welt" it was lower with 14.0 $\frac{\mu g}{m^3}$. For each of them in the period 2013-2022 the concentration of PM10 was much higher, for "Linz Römerberg" with 23.7 $\frac{\mu g}{m^3}$ and 20.1 $\frac{\mu g}{m^3}$ for "Linz Neue Welt".

The following Table 5 shows again the values and the annual change of the PM2.5 concentration to the previous year. The limit value of 25 $\frac{\mu g}{m^3}$ permitted by the EU was not exceeded in any year in the period 2009-2022. The annual limit of 5 $\frac{\mu g}{m^3}$ recommended by the WHO was never successfully undercut in the years 2009-2022.

Year	Average concentration of PM2.5 in Linz Römerberg [µg/m³]	Yearly change in PM2.5 concentration in Linz Römerberg [µg/m³]	Average concentration of PM2.5 in Linz Neue Welt [µg/m³]	Yearly change in PM2.5 concentration in Linz Neue Welt [µg/m³]	Average concentration of PM2.5 in Linz Stadtpark [µg/m³]	Yearly change in PM2.5 concentration in Linz Stadtpark [µg/m³]
2009	N/A	N/A	N/A	N/A	16.8	N/A
2010	N/A	N/A	N/A	N/A	20.5	3.7
2011	N/A	N/A	N/A	N/A	18.9	-1.6
2012	N/A	N/A	N/A	N/A	16.6	-2.3
2013	16.2	N/A	18.6	N/A	14.8	-1.8
2014	15.2	-1.0	15.7	-2.9	14.1	-0.7
2015	17.9	2.7	14.0	-1.7	12.7	-1.3
2016	16.3	-1.7	13.7	-0.3	N/A	N/A
2017	17.0	0.8	15.6	1.9	14.4	N/A
2018	16.3	-0.8	15.0	-0.6	14.8	0.4
2019	15.0	-1.2	13.2	-1.9	12.4	-2.4
2020	12.5	-2.6	10.5	-2.7	11.4	-0.9
2021	13.3	0.8	12.4	2.0	12.1	0.7
2022	12.3	-0.9	11.4	-1.0	11.0	-1.1

Table 5: Yearly average PM2.5 concentration [µg/m³] in Linz (2009-2022) and its yearly change

Analysis and results of the particulate matter concentration (PM10 and PM2.5) in the industrial cluster “Großraum Graz” and “Mur-Mürz-Furche”

PM10 data acquisition between 2005-2022 in Graz and the Mur-Mürz-Furche

In order to generate, analysis and compare the values of PM10 and PM2.5 concentrations between Graz, the Mur-Mürz-Furche and the other regions, the particulate matter concentration data sets from the "LUIS - Online Luftgütedaten" database of the State of Styria were selected for these two industrial regions, as the EEA did not have any data of PM10 and PM2.5 for the Mur-Mürz-Furche region.
The LUIS database, on the other hand, had monthly data from several different geographical locations in the Mur-Mürz-Furche. The concentration data for the city Graz of PM10 and PM2.5 was also available for a continuous long period and on a monthly basis. Another advantage of the LUIS database was that, unlike the EEA database, the data for PM10 and PM2.5 concentrations could be accessed without period differences. Therefore, for the industrial region Graz, the “Graz-Süd Tiergartenweg” air quality monitoring station was chosen to ensure the longest possible and most consistent measurement period for PM10 (and later PM2.5). The PM10 concentration data was available from February 2005 to December 2022. [123]

As mentioned, the Mur-Mürz-Furche was classified as another industrial region in Austria, where there exists a strong steel and iron ore industry. The chosen PM10 measuring stations there were Mürzzuschlag (start of measurement in 2005), Kapfenberg (start of measurement in 2006), Bruck an der Mur (start of measurement in 2007), Leoben Donawitz (start of measurement in 2006), Knittelfeld (start of measurement in 2003), Zeltweg (start of measurement in 2005) and Judenburg (start of measurement in 2003). It should be added that the Leoben Donawitz measuring station is located directly next to a large steel production site of voestalpine and that in general a large number of industrial companies from the steel, iron, wood, paper and cardboard industries are located in the entire Mur-Mürz-Furche. In the evaluation, the concentrations of all these different measuring stations will be integrated into one average value for the Mur-Mürz-Furche to represent the entire industry region. This will then be compared with the values from Graz, Linz, Vienna and the background measurements.

Due to the fact that the data for these two regions does not come from the EEA but from the LUIS database of the State of Styria, consistent data sets are generally available from LUIS without period separation as before for Vienna and Linz. In the case of data from the EEA, different periods and no continuous data set were available, as seen and explained before. Nevertheless, a distinction is also made here between the periods before and after 2012 in order to compare the concentrations with Linz and Vienna for these two time periods.

PM10 concentration results from Graz and the Mur-Mürz-Furche

The following Figure 21 shows the PM10 concentration values in Graz (blue solid line) and the average Mur-Mürz Furche (orange solid line) values. The two dotted trend lines (blue for Graz and orange for the Mur-Mürz-Furche) show the average concentration development over the measurement period in Graz and all measuring stations from the entire Mur-Mürz Furche combined in order to provide a clear comparison of the two industrial regions of Styria.

Here, too, it is immediately apparent that the peaks for the years 2006 and 2017 can be clearly identified for the Graz values.

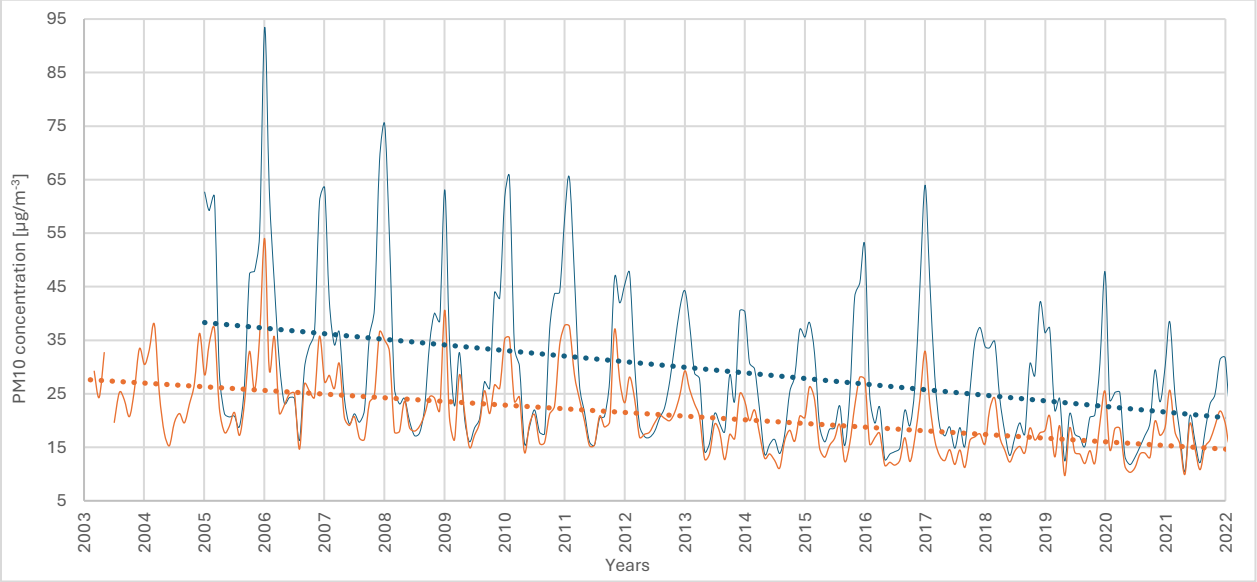

Figure 21: PM10 concentration [µg/m^3] in Graz (blue line) from 2005-2022 and in the Mur-Mürz-Furche (orange line) from 2003-2022

The average PM10 concentration in Graz has fallen significantly from 2005 to 2023, shown in the figure above. Until 2008, the average concentration was over 35 $\frac{\mu g}{m^3}$, then the average concentration constantly remained over 25 $\frac{\mu g}{m^3}$ until 2013, till it went down around 22 $\frac{\mu g}{m^3}$ at the end of 2022, which can be seen in more detail in the following Table 6.
The PM10 concentration in the Mur-Mürz-Furche is significantly lower in average than the concentration in Graz, as one can see from the dotted lines in the Figure 21 above. With the year 2013, the average concentration fell for the first time under 20 $\frac{\mu g}{m^3}$ and remained under this value till 2022, which was never achieved in Graz from 2005-2022. The more precise values can be seen in the following Table 6. It can also be seen that the basic behavior of the concentrations in both industrial regions is very similar, but the peaks of the values from Graz are significantly higher than those in the Mur-Mürz-Furche. This could be also strongly related to the weather and topological conditions in the two regions, which were discussed before. To mention it again shortly, the problem with Graz is the inversion weather situation especially in the cold months and the trapping of pollutants under a stable high fog layer in the “Grazer Becken”, while at the Mur-Mürz-Furche there exists partially mixing of the air by the Mur-winds.

Additionally, there is also a clear population difference in these two regions: The population in Graz is around 340,000 inhabitants (as of 2023), while the population in whole eastern Upper Styria, where the Mur-Mürz-Furche is a part of and located, is only around 160,000 inhabitants (as of 2020). This difference could be reflected in increased heating behavior and traffic in Graz and thus higher particulate matter concentration, besides the industrial activity. As a federal capital and cultural center, tourism could also be an additional factor for increased traffic and heating and thus increased particulate matter levels. However, the average PM10 concentration in Graz has fallen relatively more than in the Mur-Mürz-Furche, but has always remained well above the average annual values of the Mur-Mürz-Furche. [124] [125]

The following Table 6 shows the mean annual PM10 concentration values for both regions in more detail. The average concentration of PM10 for Graz up to 2012 was 34.3 $\frac{\mu g}{m^3}$, which was clearly the highest value in this period compared to these of Vienna and Linz. From 2012-2022, this decreased to 24.7 $\frac{\mu g}{m^3}$. It is interesting to note that in the Mur-Mürz-Furche, the average value of the first period was below the value of the second period in Graz, namely 24.3 $\frac{\mu g}{m^3}$. In the second period from 2012, the average PM10 concentration in the Mur-Mürz-Furche was only 17.1 $\frac{\mu g}{m^3}$, which fits in very well with the results from Linz and Vienna. Graz therefore had the highest average PM10 pollution of the selected industrial regions in Austria.

The following Table 6 shows again the values and the annual change of the PM10 concentration to the previous year. The limit value of 40 $\frac{\mu g}{m^3}$ permitted by the EU was not exceeded in any year in the period 2003-2022 at the sampling station in Graz or the Mur-Mürz-Furche but was quite close in the year 2006 in Graz with 39.7 $\frac{\mu g}{m^3}$. The annual limit of 15 $\frac{\mu g}{m^3}$ recommended by the WHO was never successfully undercut in the years 2003-2022 for Graz and the Mur-Mürz-Furche.

Year	Average concentration of PM10 in Graz [µg/m³]	Yearly change in PM10 concentration in Graz [µg/m³]	Average concentration of PM10 in Mur-Mürz-Furche [µg/m³]	Yearly change in PM10 concentration in Mur-Mürz-Furche [µg/m³]
2003	N/A	N/A	25.5	N/A
2004	N/A	N/A	24.8	-0.7
2005	37.8	N/A	25.2	0.4
2006	39.7	1.8	26.8	1.6
2007	35.1	-4.6	23.7	-3.1
2008	35.3	0.2	24.1	0.4
2009	30.4	-4.8	22.9	-1.2
2010	33.9	3.4	23.0	0.1
2011	34.1	0.3	25.7	2.7
2012	28.4	-5.7	21.5	-4.2
2013	26.7	-1.7	19.6	-1.9
2014	24.5	-2.2	17.4	-2.2
2015	26.8	2.3	18.5	1.1
2016	24.0	-2.8	16.6	-1.8
2017	29.0	5.0	17.3	0.7
2018	25.7	-3.3	16.8	-0.6
2019	23.9	-1.8	15.3	-1.5
2020	22.7	-1.2	15.8	0.6
2021	21.7	-1.0	16.7	0.9
2022	22.0	0.3	16.8	0.1

Table 6: Yearly average PM10 concentration [µg/m³] in Graz (2005-2022) and the Mur-Mürz-Furche (2003-2022) and its yearly changes

PM2.5 data acquisition between 2007-2022 in Graz

The data acquisition and analysis for the PM2.5 concentration in Graz and the Mur-Mürz-Furche is based on similar arguments as for the PM10 concentration, but unfortunately no values for the PM2.5 concentration were available for the Mur-Mürz-Furche at the LUIS data base. For the analysis of PM2.5 concentration in Graz, data from the "Graz-Süd Tiergartenweg" and "Graz Nord" monitoring stations were available from the LUIS data bank. The measurement data was available for the "Graz-Süd Tiergartenweg" measuring station from 2007 to 2022, for the "Graz Nord" measuring station from 2009 to 2022.

PM2.5 concentration results from Graz

At the "Graz-Süd Tiergartenweg" monitoring station, the average PM2.5 concentration has fallen significantly, as shown by the blue lines in the following Figure 22. As with the previous analysis of particulate matter concentration trends, concentrations are significantly higher in the cooler months of the year than in the warmer months of the year, because of increased heating activity. While the yearly average concentration was still higher than 20 $\frac{\mu g}{m^3}$ on average until 2013, it continued to fall steadily under this mark in the following years and almost reached an average PM2.5 concentration of around 15 $\frac{\mu g}{m^3}$ in 2022, with the exception and the explained peak again in 2017 of reaching over 20 $\frac{\mu g}{m^3}$. The PM2.5 concentration at the "Graz Nord" monitoring station, represented from the orange lines in the following Figure 22, whose measurement data is available from 2009, also shows a clear reduction in pollution here. While the annual average pollution was always under 20 $\frac{\mu g}{m^3}$, except the year 2011 with the maximum value at over 20 $\frac{\mu g}{m^3}$, it was steadily above 13 $\frac{\mu g}{m^3}$ until 2019. This shows the significant difference in concentration in Graz between these two stations. From 2019 onwards, it was steadily under 13 $\frac{\mu g}{m^3}$ with the minimum record value of below 12 $\frac{\mu g}{m^3}$ in 2022.

The trends of the concentration of the two measuring stations are very similar in terms of the PM2.5 concentrations directions and corresponding peaks, as seen by the behavior of the solid blue and orange line. The visible difference is that the average annual concentration at the measuring station at the "Graz Nord" site was lower in every year than at the "Graz-Süd Tiergartenweg" measuring station from 2009 onwards. This counts also for the monthly values, except for four months (May 2017, August 2021, September 2002, April 2023) showed by the analysis. This could be due to the fact that the "Graz-Süd Tiergartenweg" measuring station is located in the commercially and industrially dominated area of Graz, whereas "Graz Nord" is located in the more dispersed residential area. [126]

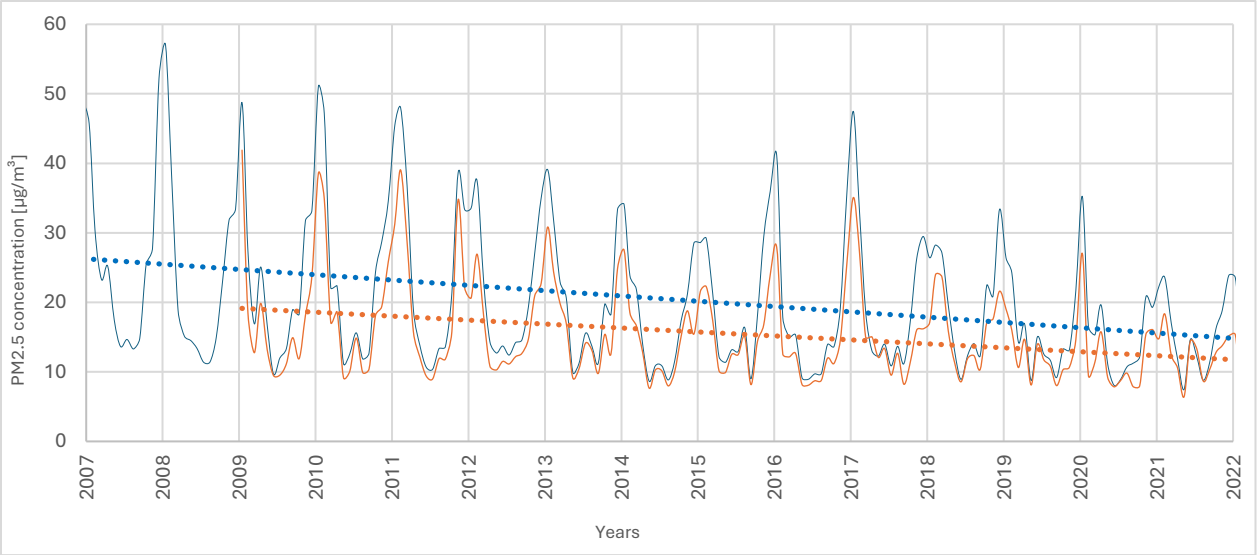

Figure 22: PM2.5 concentration [µg/m³] in Graz-Süd Tiergartenweg (blue line) from 2007-2022 and Graz Nord (orange line) from 2009-2022

The following Table 7 shows the mean annual PM2.5 concentration values for both measuring stations in Graz in detail. The average concentration of PM2.5 for "Graz-Süd Tiergartenweg" up to 2012 was 24.0 $\frac{\mu g}{m^3}$, which was clearly the highest value during this period compared to the PM2.5 concentrations in Vienna and Linz, although the shorter duration of the available data in comparison to Vienna may exclude even higher concentration values. From 2012-2022, this decreased to 18.0 $\frac{\mu g}{m^3}$, again being the highest value in comparison to Vienna and Linz for this period. The station "Graz-Süd Tiergartenweg", therefore had the highest average PM2.5 and PM10 pollution of the industrial regions in Austria. For "Graz Nord" we find that the average value of the first period was below the value of the second period in "Graz-Süd Tiergartenweg", namely 17.9 $\frac{\mu g}{m^3}$. In the second period from 2012, the average PM2.5 concentration in the "Graz Nord" was only 14.2 $\frac{\mu g}{m^3}$, which fits in very well with the results from Vienna and Linz.

The following Table 7 shows again the values and the annual change of the PM10 concentration to the previous year. The limit value of 25 $\frac{\mu g}{m^3}$ permitted by the EU was exceeded in the years 2007, 2008 and 2011 in the period 2007-2022, which is particularly noticeable compared to the other results of Vienna and Linz. The annual limit of 5 $\frac{\mu g}{m^3}$ recommended by the WHO was never undercut in the years 2007-2022.

Year	Average concentration of PM10 in Graz-Süd Tiergartenweg [µg/m^3]	Yearly change in PM10 concentration in Graz-Süd Tiergartenweg [µg/m^3]	Average concentration of PM10 in Graz Nord [µg/m^3]	Yearly change in PM10 concentration in Mur-Mürz-Furche [µg/m^3]
2007	25.1	N/A	N/A	N/A
2008	25.2	0.1	N/A	N/A
2009	22.7	-2.5	16.5	N/A
2010	24.4	1.7	18.7	2.3
2011	25.5	1.0	20.5	1.7
2012	21.3	-4.2	16.0	-4.5
2013	20.8	-0.5	16.6	0.6
2014	18.0	-2.7	15.0	-1.6
2015	19.2	1.1	14.7	-0.3
2016	17.5	-1.7	13.4	-1.3
2017	21.2	3.7	16.8	3.4
2018	19.6	-1.6	15.5	-1.3
2019	16.6	-3.0	13.0	-2.5
2020	16.0	-0.6	12.1	-0.9
2021	15.3	-0.7	12.7	0.6
2022	15.6	0.3	11.9	-0.7

Table 7: Yearly average PM2.5 concentration [µg/m^3] in Graz-Süd Tiergartenweg (2007-2022) and the Graz Nord (2009-2022) and its yearly changes

Analysis and results of the particulate matter concentration (PM10 and PM2.5) from the background measuring stations in Austria

PM10 data acquisition between 2002-2022 at the background measuring stations in Austria

The data for the concentration of PM10 at the background measuring points in Austria are not deposited at the database of the EEA but are available in the database of the Environmental Agency of Austria. These concentration data of PM10 in the rural background, for comparison to the industrial regions of Vienna, Linz, Graz and Mur-Mürz-Furche are available for nine measuring stations in Austria from 2002 to 2022. Background measurements of PM10 concentration were not carried out at each of these monitoring stations every year. With the exception of the years 2002 (five monitoring stations), 2003 (seven monitoring stations), 2006 (eight monitoring stations) and 2012 (eight monitoring stations) PM10 concentration measurements were carried out at all nine background monitoring stations in all other years.

The nine measuring stations are located, from east to west, in Illmitz at Neusiedlersee in Burgenland, in Pillersdorf near Retz in Lower Austria, in Masenberg in Styria, in Heidenreichstein in Lower Austria, in Grünbach near Freistadt in Upper Austria, in Zöbelboden in Upper Austria, in Enzenkirchen im Sauwald in Upper Austria, in Vorhegg near Kötschach-Mauthen in Carinthia and in Heiterwang in Tyrol. From these stations the available data were taken, and one average background values was created, representing the background PM10 concentration in Austria's rural areas, excluding monitoring stations located on mountain peaks. For the comparability, again the average values for the first period 2002-2012 and the second period 2013-2022 are also shown in Figure 23. [127]

PM2.5 data acquisition between 2002-2022 at the background measuring stations in Austria

Particulate matter data for rural background concentrations of PM2.5 are only available from the Environmental Agency of Austria from 2013 to 2022 from eight different rural background measurement stations, again none from the EEA database.

These eight stations are, from east to west, as follows: Illmitz am Neusiedlersee in Burgenland, Groß-Enzersdorf - Glinzendorf in Lower Austria, Neusiedl im Tullnerfeld in Lower Austria, Trasdorf im Tullnerfeld in Lower Austria, Zwentendorf im Tullnerfeld in Lower Austria, Pillersdorf bei Retz in Lower Austria, Grünbach bei Freistadt in Upper Austria and Enzenkirchen im Sauwald in Upper Austria. Here too, an annual representative value for rural background levels of PM2.5 in Austria is created from the available data from rural monitoring stations, excluding monitoring stations located on mountain peaks. No data is available for the period before 2012. [127]

PM10 and PM2.5 concentration results from the background measuring stations in Austria

The following Figure 23 shows the mean concentrations of PM10 and PM2.5 from the rural background monitoring stations in Austria mentioned above. Each of the red dotted lines represents the limit values according to the EU Ambient Air Quality Directive at 25 $\frac{\mu g}{m^3}$ for PM2.5

and 40 $\frac{\mu g}{m^3}$ for PM10. The blue lines represent the rural background PM10 concentration development, the orange line the one of the rural background PM2.5 concentration, the dotted trend lines show the change in average concentration. Clearly notable is, that both lines are clearly below the permitted annual concentration limits and also decreased over time. It is noteworthy that the concentration of PM10 and PM2.5 has behaved very similarly since the year 2013. The average deviation of the two values between 2013-2023 was 7.9 %, corresponding to an average difference in concentration between PM10 and PM2.5 of 0.75 $\frac{\mu g}{m^3}$, with the greatest differences in the year 2020. This goes hand in hand with the expectation, that in the rural background area are clearly less primary particle emissions sources for bigger particles than in the industrial areas.

It is also noticeable to see, that both concentrations show a peak in 2018. Among other things, this could be due to the desert dust episodes, especially from the Sahara, which occurred in 2018 and transported Saharan dust to Austria. These natural events and their influence on the particulate matter concentration even had to be considered for example in the 2018 environmental report of the State of Styria. This natural contribution had to be subtracted from the amount of particulate matter recorded at the Styrian measuring points to meet the limit values set by the EU. This was possible according to Articles 20 and 21 of the European Air Quality Directive, because under specific circumstances, particulate matter contributions from natural sources are allowed to be deducted from the measured concentration. [128] [129]

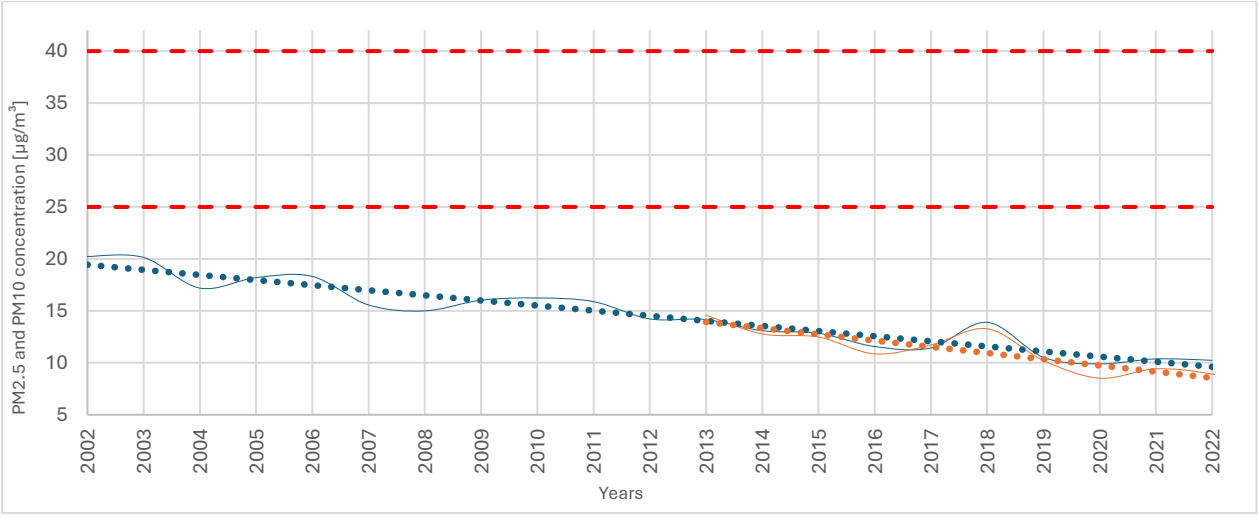

Figure 23: PM10 concentration [µg/m³] (blue lines) from 2002-2022 and PM2.5 concentration [µg/m³] (orange lines) from 2013-2022 at background measuring stations in Austria

The following Table 8 once again shows the values of the average annual concentration levels of PM10 and PM2.5 and the yearly changes of the values to their previous years in the rural area of Austria. It is immediately apparent that the concentration levels are significantly lower than those from the industrial regions of Vienna, Linz, Graz and the Mur-Mürz-Furche, as shown in the results of the industrial region Vienna, the industrial region Linz as well as for the industrial region Graz and Mur-Mürz-Furche. A more detailed graphical representation of all these values is provided in the next section.

Year	Average concentration of PM10 at background measuring stations [µg/m³]	Yearly change in PM10 concentration at background measuring stations [µg/m³]	Average concentration of PM2.5 at background measuring stations [µg/m³]	Yearly change in PM2.5 concentration at background measuring stations [µg/m³]
2002	20.2	N/A	N/A	N/A
2003	20.1	-0.1	N/A	N/A
2004	17.2	-3.0	N/A	N/A
2005	18.2	1.0	N/A	N/A
2006	18.3	0.1	N/A	N/A
2007	15.6	-2.7	N/A	N/A
2008	15.0	-0.6	N/A	N/A
2009	16.0	1.0	N/A	N/A
2010	16.2	0.2	N/A	N/A
2011	15.9	-0.4	N/A	N/A
2012	14.2	-1.7	N/A	N/A
2013	14.2	-0.1	14.6	N/A
2014	13.1	-1.1	12.8	-1.8
2015	12.8	-0.2	12.5	-0.3
2016	11.6	-1.3	10.9	-1.6
2017	11.4	-0.1	11.7	0.9
2018	13.9	2.5	13.3	1.6
2019	10.5	-3.4	10.2	-3.1
2020	9.9	-0.6	8.5	-1.7
2021	10.4	0.5	9.4	0.9
2022	10.2	-0.1	8.9	-0.5

Table 8: Yearly average PM10 concentration [µg/m³] from 2002-2022 and PM2.5 concentration [µg/m³] from 2013-2022 at the background measuring stations and its yearly changes

In no year during the period 2002-2022, the PM10 annual mean limit value of 40 $\frac{\mu g}{m^3}$ from the EU Air Quality Directive for PM10 was exceeded at any of the background measuring stations. The PM10 daily average limit value of 50 $\frac{\mu g}{m^3}$, whereby 35 exceedances are permitted under the EU Directive and 25 under the national Immission Control Act-Air, was also not exceeded at any of the rural background measuring stations. The limit value for PM10 recommended by the WHO for the annual mean value with 15 $\frac{\mu g}{m^3}$ was successfully undercut in the years from 2012 onwards till 2022. These shows the better air quality in rural areas clearly in comparison to the analyzed industrial areas in Austria. Also, for PM2.5, in no year during the period 2013-2022 was the PM2.5 annual mean limit value of 25 $\frac{\mu g}{m^3}$ from EU Air Quality Directive exceeded at any of the background measuring stations. The annual limit value recommended by the WHO of 5 $\frac{\mu g}{m^3}$ was not reached at any background station. The only annual average value below 10 $\frac{\mu g}{m^3}$ before 2022 was reached in 2020, possibly due to the corona pandemic and the lockdowns, where, in addition to the shutdown of industry, the social life was significantly reduced. In general, not reaching the WHO limit value shows the clear need for a further reduction in PM2.5 concentrations in Austrian air, as even at rural background measuring points, pollution is too high according to the WHO and having a negative effect on human health.

Conclusion and comparison of the results of the particulate matter concentration (PM10 and PM2.5) of the industrial regions and the background measuring stations in Austria between 2002-2022

This section now combines and compares all the results of the PM10 and PM2.5 concentrations in the four defined industrial regions in Austria as well as the background measurements and being visualized.
The previous data analysis showed that the concentration of particulate matter pollution decreased in every industrial region at every measuring station between 2002-2022 for PM10 and between 2005-2022 for PM2.5. It should be briefly noted that the analysis of weather effects and different times of the day was not the focus of this study. The classification of the particulate matter emitters to sectors, which play a decisive role in terms of understanding the development of particulate matter concentration in Austria, is analyzed in more detail in the sub-chapter “Sectoral influence on particulate matter concentrations in Austria”.

Comparison of the PM10 concentrations in Austria

The following Figure 24 shows all annual mean concentrations of PM10 in all industrial regions as well at the background stations in Austria.

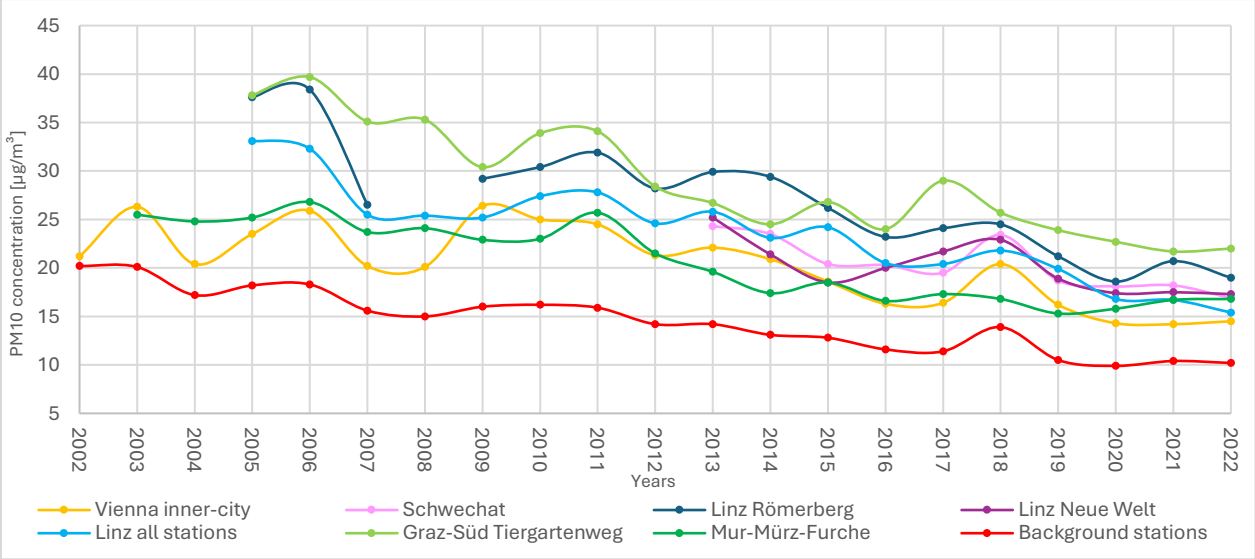

Figure 24: PM10 concentration [µg/m³] from 2002-2022 in the industrial regions and at the background measuring stations in Austria

It is clear to see that the background measurements, marked as the red line in the Figure 24, show by far the lowest concentration of PM10 and were in the mean considerably below the values of the industrial regions. This clearly shows that densely populated and industrially active regions have a much higher PM10 pollution than rural, non-industrially populated regions.

It is also clear to see in the Figure 24 that the values in Graz (light green line) and greater Linz area (light blue line), especially “Linz Römerberg” (dark blue line), were the ones where the highest levels of PM10 were measured over the years. As mentioned before, the station “Linz

Römerberg" is one of the stations with the highest value overall in all Austria. This can be explained by the particularly high volume of traffic there, apart from the large-scale industry in overall Linz. In the case of Graz, in addition to the industry, the heavy inner-city traffic and the nearby freeway A2 probably play a decisive role at the location "Graz-Süd Tiergartenweg". The basin location of the city of Graz (the "Grazer Becken") and the resulting weather conditions can also be attributed, which significantly prolongs the concentration of PM10 over time.

Interestingly, the PM10 measurement locations near large industrial plants at "Linz Neue Welt" (purple line) and Schwechat (pink line) are found in the middle of the concentration's values. In the case of "Linz Neue Welt", the measurement location next to the main voestalpine site, could be explained by the special measures taken by voestalpine to reduce emissions of pollutants and also traffic is rather low compared to the city center. In the case of the Schwechat and the nearby OMV refinery, similar arguments as for the industrial location "Linz Neue Welt" can be used as an explanation. The OMV Group as well tries to keep the emissions of air pollutants it produces as low as possible. In addition, the area around Schwechat is very flat and extensive and the air is very well mixed by winds. In general, the filter systems in large industrial plants have improved significantly in Austria due to the increasing legal requirements (e.g. usage of best available technique) and strong attempts are being made to use renewable energy on a large scale instead of conventional energy in order to reduce the particles produced by the combustion processes.

The Mur-Mürz-Furche (green line) and Vienna inner-city (orange line) form the lower end of the concentration levels of PM10 in the industrial regions. This is particularly interesting in the case of Vienna inner-city, as it is the federal capital of Austria with a population of almost two million. Besides the reduction improvements in the industry, for example in the case of traffic, the enormous expansion of public and climate-neutral transport and legal measures in Vienna has reduced the use of private combustion cars in recent years, also by subsidies for private electric cars. Similarly, in the area of urban heating, the expansion of Vienna's district heating system (Wiener Fernwärme) could help reduce particulate matter pollution from conventional heating systems like wood-burning ovens. The system already supplies over 400,000 residential units, while newer buildings in the city feature better thermal insulation and are increasingly adopting heat pumps. In the case of the Mur-Mürz-Furche, the extensive and wide area, even if in a valley location, and the relatively good air mixing through winds can explain the low concentration of PM10. Another factor could be the lower population density and thus reduced traffic and heating activities in this region. [130] [131] [132]

In conclusion, the combined average PM10 concentration reduction of all analyzed industrial regions from the first available year of data to the year 2022 fell about -38.4 %, when including the reduction of the background measuring stations value it fell about – 40.2 % in Austria. Among the industrial regions, the Graz region recorded the highest average PM10 concentration at the "Graz-Süd Tiergartenweg" monitoring station, with 28.9 $\frac{\mu g}{m^3}$ (2005–2022). This was followed by the Linz region at the "Linz Römerberg" station with 27.0 $\frac{\mu g}{m^3}$ (2005–2022), the greater Linz region with 23.7 $\frac{\mu g}{m^3}$ (2005–2022), the Mur-Mürz-Furche with 20.7 $\frac{\mu g}{m^3}$ (2003–2022), the Vienna region at inner-city stations with 20.4 $\frac{\mu g}{m^3}$ (2002–2022), the Vienna region near Schwechat with 20.3 $\frac{\mu g}{m^3}$ (2013–2022), and the Linz region at "Linz Neue Welt" with 20.1 $\frac{\mu g}{m^3}$ (2013–2022). In comparison, the average PM10 concentration at the rural background stations was significantly lower with 14.5 $\frac{\mu g}{m^3}$ (2002–2022).

The largest individual reductions in PM10 concentrations were observed in the greater Linz area with a decrease of -53.5 % (2005–2022). This was followed by the rural background stations with -49.5 % (2002–2022), the Linz region at the "Linz Römerberg" station with -49.4 % (2005–2022), the Graz region at the "Graz-Süd Tiergartenweg" station with -41.8 % (2005–2022), the Mur-Mürz-Furche with -34.1 % (2003–2022), the Vienna region at inner-city stations with -31.6 % (2002–2022), the Linz region at "Linz Neue Welt" with -31.3 % (2013–2022), and the Vienna region near Schwechat with -30.5% (2013–2022).

It can also be clearly stated that apart from the long-term reduction at all stations, the differences in the concentrations of particulate matter have come closer over the last years. For example, the values in 2005 (first year with data of more than one industrial region) were significantly further apart than the ones of 2022, namely the biggest difference of two measurements stations in industry regions in 2005 was 14.3 $\frac{\mu g}{m^3}$ between Vienna inner-city and Graz. On the other hand, the biggest difference in 2022 of two industrial measurement stations was again Vienna inner-city and Graz with only 7.5 $\frac{\mu g}{m^3}$. This is a decrease in difference of -47.6 %. When taking into the account the values of the background stations, the biggest difference in 2005 between the background and an industry region was Graz with 19.6 $\frac{\mu g}{m^3}$, and in 2022 again with Graz with 11.8 $\frac{\mu g}{m^3}$, which is a decrease of -39.8 %.

This confirms effectiveness of the laws and measures across all sectors that have been taken into action to this date, as the overall concentration fell in the industrial regions of around -38.4 %, while additionally the concentration differences in the industrial regions fell around -47.6 %, meaning that the values of the concentration converge towards each other and that very high values have gradually decreased over the years.

Comparison of the PM2.5 concentrations

The following Figure 25 shows all annual mean concentrations of PM2.5 in all industrial regions as well at the background stations in Austria.

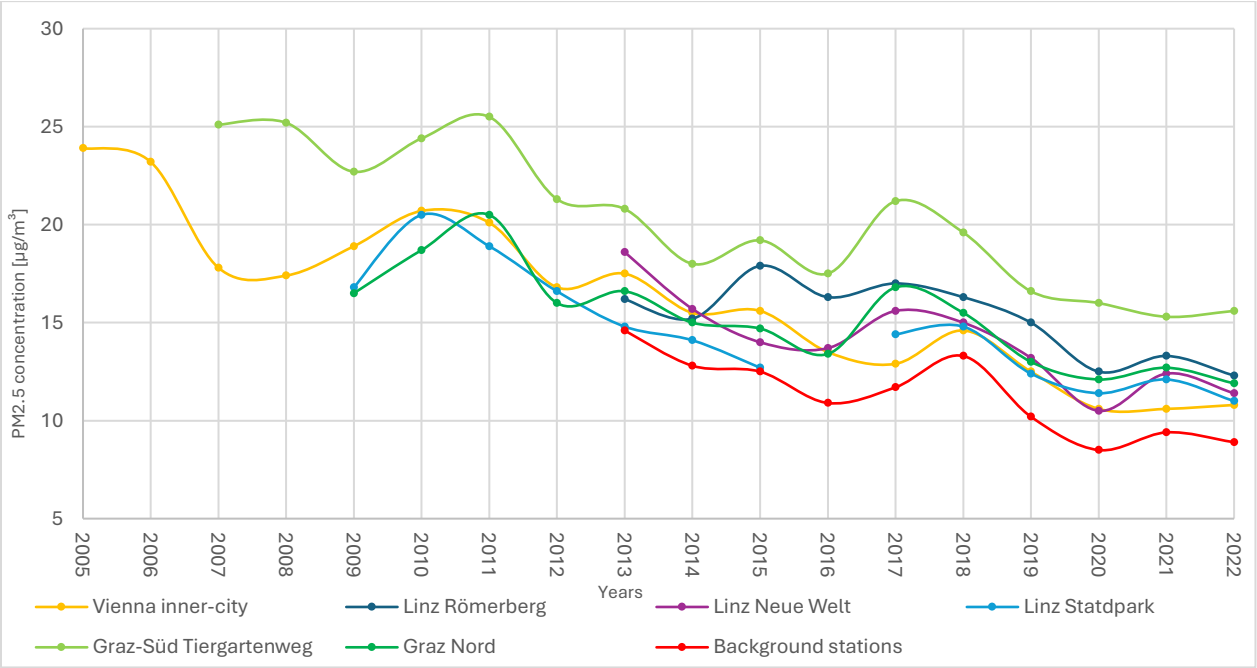

Figure 25: PM2.5 concentration [µg/m^3] from 2005-2022 in the industrial regions and at the background measuring stations in Austria

The concentration of PM2.5 in the years 2005-2022 also shows that in Austria the background monitoring stations (red line) have on average the lowest PM2.5 pollution compared to the industrial regions. Interestingly, the values of “Linz Stadtpark” (light blue line) in 2013 and 2015 were very close to the values of the background monitoring sites.

Once again, the highest pollution is found in Graz, more precisely again at the „Graz-Süd Tiergartenweg” (light green line) measuring station, which, as already mentioned, is in a very commercially and industrially dominated region. The “Linz Römerberg” (dark blue line), which, as already described, is located in a very densely trafficked area and is the one stations in Upper Austria with the highest average concentration, also has the second highest average concentration again.

The second locations in Linz and Graz also have an average relatively high concentration of PM2.5. The average concentration at the “Graz Nord” (green line) location is slightly higher than that in “Linz Neue Welt” (purple line). Both locations do not have as high a traffic volume as the previous locations. The voestalpine industrial plant at the “Linz Neue Welt” site appears to play only a subordinate role in this case. Interestingly, the Vienna inner-city station near the general hospital with lot of traffic is only the next most affected, followed by the least polluted site at “Linz Stadtpark”, which is surrounded by residential buildings in a greener area.

In conclusion, the combined average PM2.5 concentration reduction of all analyzed industrial regions from the first available year of data to the year 2022 fell about -36.3 %, when including the reduction of the background measuring stations value it fell about – 36.7 %.

For PM2.5, the Graz region again recorded the highest average concentration at the "Graz-Süd Tiergartenweg" monitoring station, with 20.3 $\frac{\mu g}{m^3}$ (2007–2022). This was followed by the Vienna region at inner-city stations with 16.3 $\frac{\mu g}{m^3}$ (2005–2022), the Graz region at "Graz Nord" with 15.2 $\frac{\mu g}{m^3}$ (2009–2022), the Linz region at "Linz Römerberg" with 15.2 $\frac{\mu g}{m^3}$ (2013–2022), the Linz region at "Linz Stadtpark" with 14.7 $\frac{\mu g}{m^3}$ (2009–2022), the Linz region at "Linz Neue Welt" with 14.0 $\frac{\mu g}{m^3}$ (2013–2022), and finally, the rural background stations with 11.3 $\frac{\mu g}{m^3}$ (2013–2022).

The largest individual reductions in PM2.5 concentrations were achieved in the Vienna region at inner-city stations, with a decrease of -54.8 % (2005–2022), followed by the rural background stations with -39.0 % (2013–2022). The Linz region recorded a decrease of -38.7 % at the "Linz Neue Welt" station (2013–2022), followed by the Graz region at the "Graz-Süd Tiergartenweg" station with -37.8 % (2007–2022). Further reductions were observed in the Linz region at "Linz Stadtpark" with -34.5 % (2009–2022), the Graz region at "Graz Nord" with -27.9 % (2009–2022), and finally, the Linz region at "Linz Römerberg" with -24.1 % (2013–2022).

Also, in addition to the overall long-term decrease at all stations, the variations in particulate matter concentrations between different locations have minimized in recent years too. Again here an example: The values in 2007 (first year with data of more than one industrial region) had a bigger difference than the ones of 2022, namely 7.3 $\frac{\mu g}{m^3}$ again between Vienna inner-city and “Graz-Süd Tiergartenweg”. The largest difference in 2022 of two industrial measurement stations was again Vienna inner-city and Graz with 4.8 $\frac{\mu g}{m^3}$, which corresponds to a decrease of -34.2 %.

This also confirms existing reduction measures for PM2.5, because concentrations in the industrial regions fell on average between the first available measurement year and 2022, by -36.3 % on average. Again, the maximum differences in concentrations in the industrialized regions have come closer, namely by -34.2 %, which is lower than in the case of PM10. The background monitoring sites also have the lowest average PM2.5 levels and show that PM2.5 emissions are lowest in rural, non-densely populated and industry-free regions in Austria.

Sectoral influence on particulate matter concentrations in Austria

It should be emphasized quickly at that point too, that also at European Level, the concentrations of PM10 have also fallen by 30 % and PM2.5 by 32 % between 2005 and 2020, but air pollution remains one of the most significant threats to human health in Europe, particularly affecting those living in urban areas. As we saw in the analysis before, the concentrations of particulate matter in industrial and urban regions are much higher than in rural regions and according to a report by the EEA, 96 % of the urban population in the European Union is exposed to fine particulate matter levels exceeding the limits set by the WHO. According to the Environmental Agency of Austria, significant contributions to this reduction in particulate matter concentration have come from positive developments in the industrial sector, especially for PM10 in the energy-intensive heavy industry (e.g., steel and iron production), the chemical industry, industrial food processing and production, the paper and cardboard industry, the mineral processing industry, and mining industry sectors, particularly the reduction in coal usage in production, increased efficiency, and improved combustion and filtering technologies. Due to the continuous monitoring of air pollutants in the last years in

Austria, many measures have been implemented in all federal states of Austria to reduce this pollution through the beforementioned Immission Control Act-Air, such as particulate filter requirements for machinery in the mining sector and maximum emission limits for industrial plants. Additionally, more efficient propulsion and exhaust treatment technologies have played a significant role. [51]

In the following figures, Figure 26 and Figure 27, it can be observed that the industrial sector was the main contributor to PM10 emissions in Austria and third largest for PM2.5 emissions in the year 2021. According to the Austrian Air Pollutant Inventory (Luftschadstoff-Inventur), the industrial production sector consist of four main sources: pyrogenic emissions from industry (emissions generated from combustion processes used in industrial activities which typically include the burning of fossil fuels in industrial processes), process emissions from industry (emissions released during the production processes, not related to fuel combustion, but due to chemical reactions and material transformations), off-road industrial equipment (e.g., construction work and machinery), and particulate matter emissions from mining, bulk material handling mineral processing activities. It should be noted that the overall emissions of all relevant air pollutants (PM10, PM2.5, NOx, SO2, CO, Cd, Hg, Pb, PAK, Dioxin, HCB, PCB) in Austria have decreased since 1990, according to the Environmental Agency of Austria, but the relative share of PM10 emissions from the industrial sector in Austria's total PM10 emissions has increased since 1990, while the contribution of PM2.5 from the industrial sector has slightly decreased.

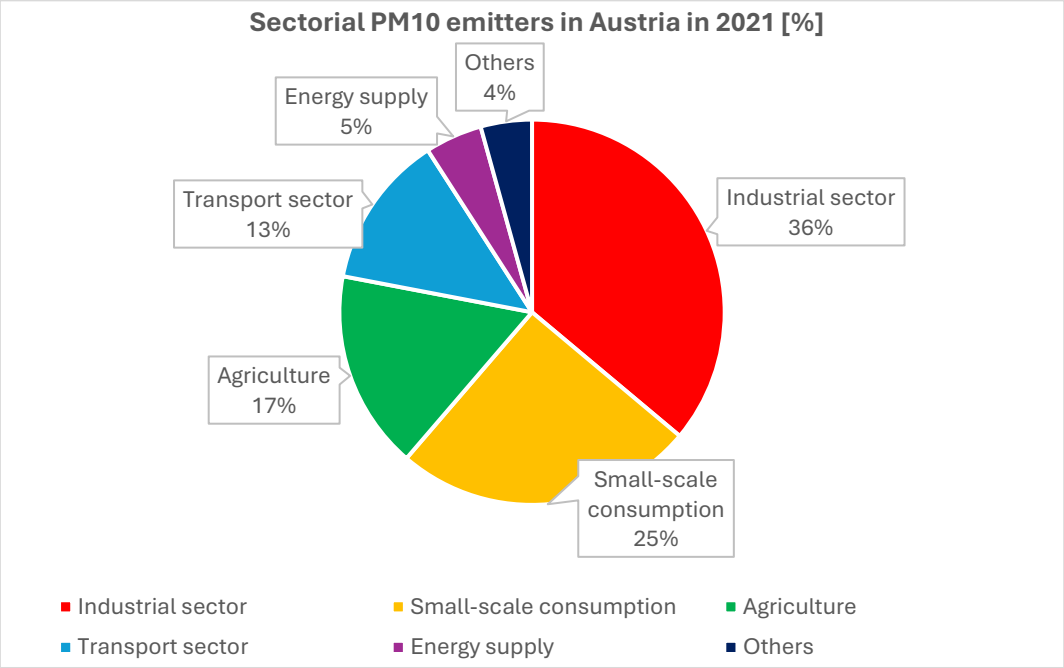

Figure 26: PM10 emitters [%] separated by sectors in Austria in 2021 [51]

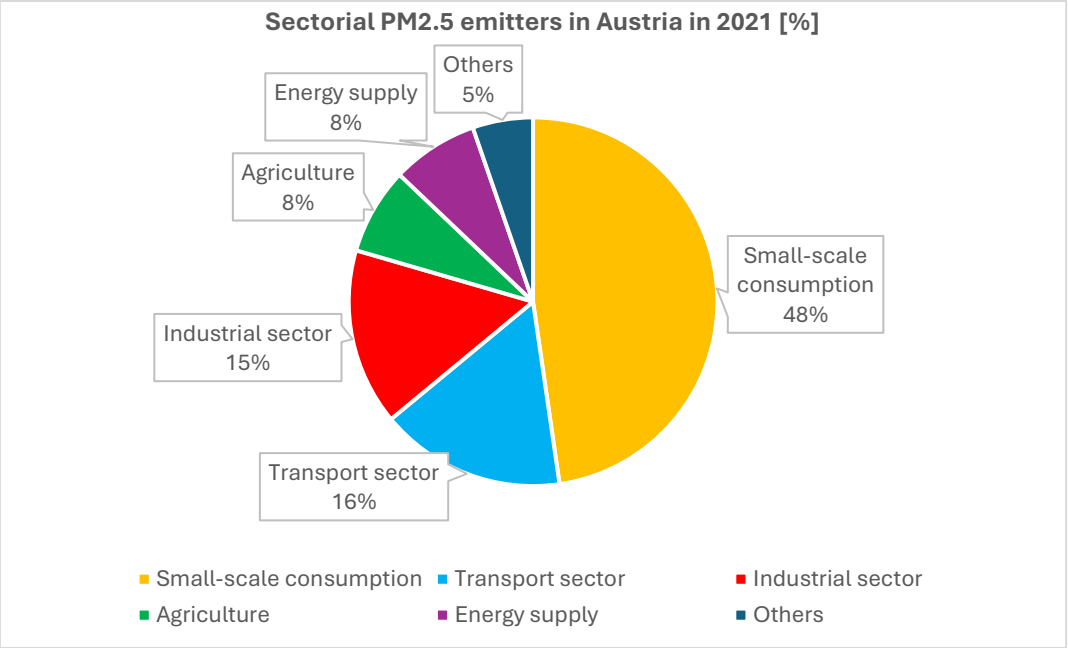

Figure 27: PM2.5 emitters [%] separated by sectors in Austria in 2021 [51]

On a smaller scale important is the energy supply sector (5 % for PM10 and 8% for PM2.5 in 2021), including emissions from pipeline compressors, the extraction and distribution of coal, natural gas, and oil with volatile emissions, thermal power plants (including waste-to-energy facilities), energy use in oil and gas extraction, and refineries.

In the same magnitude as energy supply (4 % for PM10 and 5 % for PM2.5), the “Other” sector includes waste masnagement, landfills, waste incineration, the application of paints and coatings, and waste fermentation.

The small-scale consumer sector, which is mainly responsible for the conventional production of hot water and heat for rooms in private and public buildings, as well as the transport sector and the agricultural sector are of relevance in Austria. In the year 2021, the small-scale consumption sector made 25 % of the PM10 and 48 % of the PM2.5 emissions. The agricultural sector plays as mentioned also a relevant role with regard to the formation of particulate matter, as a lot of ammonia is used in agriculture, and this contributes to the formation of secondary particles and by mechanical dispersion of dust particles. In the case of the transport sector, in addition to the burning of fuel in engines, tire abrasion and the dispersion of dust particles are also relevant, and nitrogen oxides are also a factor that should not be underestimated with regard to gaseous precursor substances for secondary particles. [51] [133]

Outlook

The results of this study illustrate the success of regulatory measures and technological advances in reducing particulate matter concentrations (PM10 and PM2.5) in the industrial regions of Austria. Nevertheless, long-term monitoring of these levels remains crucial as industrial sources continue to have a significant impact on regional air quality. Future research could focus on the further development of modern measurement techniques that provide more precise data on particulate matter pollution and identify specific emission sources more accurately. In addition, the investigation of the interactions between climatic changes and also meteorological phenomena and the development of particulate matter concentrations is a promising field of research that can contribute to the development of effective adaptation strategies.

A comparison of the efficiency of measures in different regions or countries in the European Union and worldwide could provide valuable insights for optimizing air pollution control strategies. A further in-depth analysis of long-term health effects, particularly in vulnerable population groups, would also be of great importance in order to establish more precise guideline values and more effective protective measures. Politically and socially, a central focus is on the promotion of sustainable technologies and the further reduction of industrial emissions. The implementation of the European Green Deal and the achievement of climate neutrality by 2050 offer a promising perspective here but require decisive action and increased interdisciplinary cooperation.

In conclusion, this work underlines the need to further strengthen technical and political measures for air pollution control in order to continue the positive trends of recent decades. Only by continuously adapting and optimizing strategies will it be possible to sustainably improve air quality and at the same time protect the health of the population.

References

[1] W. Hinds, Aerosol technology : properties, behavior, and measurement of airborne particles, New York : John Wiley & Sons, Ins., 1999.

[2] P. Winkler, "Aerosolphysics Lecture Script," Paul Winkler, University of Vienna, Faculty of Physics, Vienna, 2021.

[3] E. David S., "Aerosol Science and Technology: History and Reviews," Research Triangle Institute. RTI International, North Carolina, 2011.

[4] "Verzeichnis der künstlerischen, wissenschaftlichen und kulturpolitischen Nachlässe in Österreich," Österreichsiche Nationalbibliothek im Auftrag des Bundesministeriums, June 2010. [Online]. Available: https://data.onb.ac.at/nlv_lex/perslex/PQ/Preining_Othmar.htm. [Accessed October 2024].

[5] K. Wyer, D. Kelleghan, V. Vidal-Blanes, G. Schauberger and T. Curran, "Ammonia emissions from agriculture and their contribution to fine particulate matter: A review of implications for human health," *Journal of Environmental Management,* no. Volume 323 (ISSN 0301-4797), pp. 116285-116285, 2022-12.

[6] W. Roedel and T. Wagner, Physik unserer Umwelt: Die Atmosphäre, Berlin, Heidelberg: Springer-Verlag Berlin Heidelberg, 2017.

[7] J. H. Seinfeld and S. N. Pandis, Atmospheric Chemistry and Physics: From Air Pollution to Climate Change, 3rd Edition, New Jersey: John Wiley & Sons, 2016.

[8] W. Roedel, "Measurement of sulfuric acid saturation vapor pressure. Implications for aerosol formation by heteromolecular nucleation," *Journal of Aerosol Science,* vol. 10, pp. 375-386, 1979.

[9] H. Georgii and U. Lenhard, "Contribution to the atmospheric NH3 budget," *Pure and Applied Geophysics,* Vols. 116 (2-3), pp. 385-392, 1978.

[10] P. Middelton, "A re-examination of atmospheric sulfuric acid aerosol formation and growth," *Journal of aerosol science,* vol. 11 (4), pp. 411-414, 1980.

[11] P. Middelton and C. Kiang, "A kinetic aerosol model for the formation and growth of secondary sulfuric acid particles," *Journal of aerosol science,* vol. 9 (4), pp. 359-385, 1978.

[12] P. Winkler and P. Wagner, "Characterization techniques for heterogeneous nucleation from the gas phase," *Journal of Aerosol Science,* vol. 159, p. 105875, 2022.

[13] D. Gillette, "A wind tunnel simulation of the erosion of soil: Effect of soil texture, sandblasting, wind speed, and soil consolidation on dust production," *Atmospheric Environment,* vol. 12, no. 8, pp. 1735-1743, 1978.

[14] W. Elbert, P. Taylor, M. Andreade and U. Pöschl, "Contribution of fungi to primary biogenic aerosols in the atmosphere: wet and dry discharged spores, carbohydrates, and inorganic ions," *Atmospheric Chemistry and Physics,* vol. 7 (17), p. 4569–4588, 2007-09.

[15] H. W. Li, K. S. Chen, C. H. Lai, T. Y. Chen, Y. C. Lin, Y. C. Lin, C. H. Chen, Y. P. Peng and M. H. Lin, "Characterization of ambient particulate matters in an industry-intensive area in central Taiwan," *Atmosphere,* vol. 12 (7), p. 926, 2021-07.

[16] "Umweltbundesamt," 17 May 2024. [Online]. Available: https://www.umweltbundesamt.de/daten/klima/atmosphaerische-treibhausgas-konzentrationen#kohlendioxid. [Accessed 23 September 2024].

[17] H. Yu, Y. J. Kaufman, M. Chin, G. Feingold, L. A. Remer, T. L. Anderson, Y. Balkanski, N. Bellouin, O. Boucher, S. Christopher, P. DeCola, R. Kahn, D. Koch, N. Loeb, M. S. Reddy, M. Schulz, T. Takemura and M. Zhou, "A review of measurement-based assessments of the aerosol direct radiative effect and forcing," *Atmospheric chemistry and physics,* vol. 6 (3), pp. 613-666, 2006-02.

[18] M. Wild, D. Folini, C. Schär, N. Loeb, E. Dutton and G. König-Landlo, "The global energy balance from a surface perspective," *Climate Dynamics,* vol. 40, pp. 3107-3134, 2012.

[19] S. Twomey, "The Influence of Pollution on the Shortwave Albedo of Clouds," *Journal of the atmospheric sciences,* vol. 34 (7), pp. 1149-1152, 1977-07.

[20] U. Dusek, G. Frank, L. Hildebrandt, J. Curtius, J. Schneider, S. Walter, D. Chand, F. Drewnick, S. Hings, D. Jung, S. Borrmann and M. Andreae, "Size Matters More Than Chemistry for Cloud-Nucleating Ability of Aerosol Particles," *Science,* vol. 312 (5778), pp. 1375-1378, 2006.

[21] "India's Deadly Air Pollution Keeps Getting Worse Not Better," Bloomberg, 2022. [Online]. Available: https://www.bloomberg.com/news/articles/2022-01-11/india-s-deadly-air-pollution-keeps-getting-worse-not-better. [Accessed November 2024].

[22] R. J. Charlson, J. Langner, H. Rodhe, C. B. Leovy and S. Warren, "Perturbation of the northern hemisphere radiative balance by backscattering from anthropogenic sulfate aerosols," *Dynamic Meteorology and Oceanograph,* vol. 43 (4), pp. 152-163, 1991.

[23] P. Goldsmith, H. Delafield and L. Cox, "Measurement of the deposition of submicron particles in gradients of vapour pressure and of the efficiency of this mechanism in the capture of particulate matter by cloud droplets in nature," *Pure and Applied Geophysics,* vol. 50, pp. 278-280, 1961.

[24] P. Wang, S. Grover and H. Pruppacher, "On the Effect of Electric Charges on the Scavenging of Aerosol Particles by Clouds and Small Raindrops," *Journal of the Atmospheric Sciences,* vol. 35, no. 9, pp. 1735-1743, 1978-01.

[25] K. Bower and T. Choularton, "Cloud processing of the cloud condensation nucleus spectrum and its climatological consequences," *Quarterly Journal of the Royal Meteorological Society,* vol. 119, no. 512, pp. 655-679, 1993.

[26] M. Krämer, N. Beltz, D. Schell, L. Schütz, C. Sprengard-Eichel and S. Wurzler, "Cloud processing of continental aerosol particles : experimental investigations for different drop sizes," *Journal of Geophysical Research,* vol. 105, no. D9, pp. 11739-11752, 2000.

[27] S. Wurzler, R. R. Reisin and Z. Levin, "Modification of mineral dust particles by cloud processing and subsequent effects on drop size distributions," *Journal of Geophysical Research,* vol. 105, no. D4, pp. 4501-4512, 2000.

[28] R. Jaenicke, "Über die Dynamik atmosphärischer Aitkenteilchen," *Berichte der Bunsengesellschaft für Physikalische Chemie,* vol. 82 (11), pp. 1198-1202, 1978-11.

[29] R. Jaenicke, "Atmospheric aerosols and global climate," *Journal of Aerosol Science,* no. 11 (5), pp. 577-588, 1980.

[30] "Saharastaub in Österreich am Osterwochenende," Der Standard, 3 March 2024. [Online]. Available: https://www.derstandard.at/story/3000000213932/saharastaub-in-oesterreich-am-osterwochenende. [Accessed October 2024].

[31] U. E. M. I. u. T. Bundesministerin für Klimaschutz, "Verordnung der Bundesministerin für Klimaschutz, Umwelt, Energie, Mobilität, Innovation und Technologie über das Messkonzept zum Immissionsschutzgesetz – Luft (IG-L-Messkonzeptverordnung 2012 – IG-L-MKV 2012)," Wien, 2012.

[32] W. Spangl and C. Nagl, "Jahresbericht der Luftgütemessungen 2010," Österreichisches Umweltbundesamt, Wien, 2011.

[33] W. Spangl, "Luftgütemessungen und meterologische Messungen - Jahresbericht Hintergrundmessnetz 2023," Umweltbundesamt . [Online]. Available: https://www.umweltbundesamt.at/fileadmin/site/publikationen/rep0891.pdf. [Accessed November 2024].

[34] H. Gressenberger, "Luftgütemessungen der Steiermark - Jahresbericht 2022," Dezember 2023. [Online]. Available: https://www.umwelt.steiermark.at/cms/beitrag/12936319/19221910/. [Accessed November 2024].

[35] W. Spangl and J. Schneider, "Jahresbericht der Luftgütemessungen in Österreich 2001," Österreichisches Umweltbundesamt, Vienna, 2002.

[36] W. N. C. Spangl, "Luftgütemessungen in Österreich 2020," Österreichisches Umweltbundesamt, Vienna, 2021.

[37] "Digitel DHA-80 High Volume Aerosol Sampler (HVS) Product Information," [Online]. Available: https://digitel.aflip.in/product_information_DHA-80.html#page/8. [Accessed October 2024].

[38] "DIN EN 12341:2014-08," DIN Media, August 2014. [Online]. Available: https://www.dinmedia.de/de/norm/din-en-12341/195550191#:~:text=werden%2C%20zu%20harmonisieren.-,Die%20DIN%20EN%2012341%20umfasst%20%2D%20eine%20Beschreibung%20eines%20manuellen%20gravimetrischen,Anforderungen%20an%20die%20Eignungspr%C3%BCfung%20von. [Accessed October 2024].

[39] S. B. Jerez, Y. Zhang, J. W. McClure, L. Jacobson, A. Heber, S. Hoff, J. Koziel and D. Beasley, "Comparison of Measured Total Suspended Particulate Matter Concentrations Using Tapered Element Oscillating Microbalance and a Total Suspended Particulate Sampler," *Journal of the Air & Waste Management Association,* vol. 56 (3), pp. 261-270, 2006-03.

[40] "TEOM 1405-F Ambient Particulate Monitor with FDMS Option," 2007. [Online]. Available: https://assets.thermofisher.com/TFS-Assets/LSG/manuals/EPM-manual-1405F.pdf. [Accessed 2024].

[41] H. Patashnick and E. G. Rupprecht, "Continuous PM-10 Measurements Using the Tapered Element Oscillating Microbalance," *Journal of the Air & Waste Management Association,* vol. 41, no. 8, pp. 1079-1083, 1991.

[42] P. A. Baron, P. Kulkarni and K. & Willeke, Aerosol measurement : principles, techniques, and applications, Hoboken Wiley,, 2011.

[43] "BAM 1020 Continuous Particulate Monitor," August 2019. [Online]. Available: https://metone.com/wp-content/uploads/2019/10/BAM-1020-1.pdf. [Accessed October 2024].

[44] "Operational Manual BAM 1020 Particulate Monitor BAM 1020-9805 Rev G," 2024. [Online]. Available: https://metone.com/wp-content/uploads/2024/02/BAM-1020-9805-Manual-Rev-G-Reduced.pdf. [Accessed October 2024].

[45] K. Shukla and S. G. Aggarwal, "A Technical Overview on Beta-Attenuation Method for the Monitoring of Particulate Matter in Ambient Air," *Aerosol and Air Quality Research,* vol. 22 (12), pp. 1-21, 2022-12.

[46] J. M. Jaklevic, R. C. Gatti, F. S. Goulding and B. W. & Loo, "A .beta.-gage method applied to aerosol samples," *Environmental Science & Technology,,* vol. 15, no. 6, pp. 680-686, 1981.

[47] R. Evans, The atomic nucleus, New York: McGraw-Hill., 1955.

[48] F. Klein, C. Ranty and L. Sowa, "A new examination of the validity of the principle of beta radiation absorption for determination of ambient air dust concentrations," *Journal of Aerosol Science,* vol. 15, no. 3, pp. 391-395, 1984.

[49] "Grimm Environmental Dust Monitor (EDM) #180 User Manual," December 2003. [Online]. Available: http://www.lisa.u-pec.fr/~formenti/Tools/Manuals/GRIMM_model1.180_Manual_2004.pdf. [Accessed October 2024].

[50] J. Spielvogel, S. Hartstock and H. Grimm, "New methods and standards for fine dust," *Journal of Physics Conference Series,* vol. 170 (1), p. 012024, 2009.

[51] M. Anderl, M. Gangl, L. Makoschitz, K. Pazdernik, D. Perl and S. Poupa, "Emissionstrends 1990-2021 - Ein Überblick über die Verursacher von Luftschadstoffen in Österreich," Österreichisches Umweltbundesamt, Wien, 2023.

[52] J. Lelieveld, J. S. Evans, M. Fnais, D. Giannadaki and A. Pozzer, "The contribution of outdoor air pollution sources to premature mortality on a global scale," *Nature (London),* vol. 525 (7569), pp. 367-371, 2015.

[53] T. Münzel, H. Omar, D. Andreas, J. Lelieveld and e. al., "Luftverschmutzung und Herz-Kreislauf-Erkrankungen," *Springer Medizin,* vol. 46 (2), pp. 120-128, 2021.

[54] A. J. Coehn, M. Brauer, R. Burnett, H. R. Anderson, J. Frostad and e. al., "Estimates and 25-year trends of the global burden of disease attributable to ambient air pollution: an analysis of data from the Global Burden of Diseases Study 2015," *The Lancet (British Edition),* vol. 389 (10082), pp. 1907-1918, 2017-05.

[55] R. Burnett, H. Chen, M. Szyszkowic, N. Fann, B. Hubbell and e. al., "Global estimates of mortality associated with long-term exposure to outdoor fine particulate matter," *Proceedings of the National Academy of Sciences,* vol. 115 (38), pp. 9592-9597, 2018.

[56] M. Sanjoy, S. Ahmed, K.-S. Maninder and M. Suman, "Health Risks of Major Air Pollutants, their Drivers and Mitigation Strategies: A Review," *Air, Soil and Water Research,* vol. 16, 2023-01.

[57] T. Münzel, T. Gori, S. Al-Kindi, D. John, J. Lelieveld and e. al, "Effects of gaseous and solid constituents of air pollution on endothelial function," *European heart journal,* vol. 39 (38), pp. 3543-3550, 2018-10.

[58] M. R. Miller, J. B. Raftis, J. P. Langrish, S. G. McLean, P. Smutrtai and e. al., "Correction to "Inhaled Nanoparticles Accumulate at Sites of Vascular Disease"," *ACS nano,* vol. 11 (10), pp. 10623-10624, 2017-10.

[59] R. Atkinson, S. Kang, H. Anderson, I. Mills and H. Walton, "Epidemiological time series studies of PM2.5 and daily mortality and hospital admissions: a systematic review and meta-analysis," *Thorax,* vol. 69 (7), pp. 660-665, 2014-07.

[60] E. Samoli, R. Peng, T. Ramsay, M. Pipikou, G. Touloumi and e. al., "Acute Effects of Ambient Particulate Matter on Mortality in Europe and North America: Results from the APHENA Study," *Environmental Health Perspectives,* vol. 116 (11), pp. 1480-1486, 2008.

[61] G. Cesaroni, F. Forastiere, M. Stafoggia and e. al., "Long term exposure to ambient air pollution and incidence of acute coronary events: prospective cohort study and meta-analysis in 11 European cohorts from the ESCAPE Project," *BMJ (Online),* vol. 348, pp. f7412-f7412, 2014-01.

[62] H. Mustafic, P. Jabre, C. Caussin, M. H. Murad and S. Escolano, "Main air pollutants and myocardial infarction: a systematic review and meta-analysis," *JAMA,* vol. 307 (7), pp. 713-721, 2012.

[63] K. E. Cosselman, A. Navis-Acien, J. D. Kaufman and e. al., "Environmental factors in cardiovascular disease," *Nature Reviews Cardiology,* vol. 12 (11), pp. 627-642, 2015-11.

[64] T. Münzel, M. Sorensen, T. Gori, F. P. Schmidt and X. Rao, "Environmental stressors and cardio-metabolic disease: part II-mechanistic insights," *European heart journal,* vol. 38 (8), pp. 557-564, 2017-02.

[65] D. L. Crouse, P. A. Peters, A. Van Donkelaar, M. S. Goldberg and P. J. Villeneuve, "Risk of nonaccidental and cardiovascular mortality in relation to long-term exposure to low concentrations of fine particulate matter: a Canadian national-level cohort study," *Environmental Health Perspectives,* vol. 120 (5), pp. 708-714, 2012-05.

[66] S. Weichenthal, P. J. Villeneuve, R. T. Burnett, A. Van Donkelaar and R. M. Martin, "Long-term exposure to fine particulate matter: association with nonaccidental and cardiovascular mortality in the agricultural health study cohort," *Enviromental Health Perspective,* vol. 122 (6), pp. 609-615, 2014-06.

[67] P. Yin, M. Brauer, A. Cohen, R. T. Burnett and H. Liu, "Long-term Fine Particulate Matter Exposure and Nonaccidental and Cause-specific Mortality in a Large National Cohort of Chinese Men," *Enviromental Health Perspectives,* vol. 125 (11), pp. 117002-117002, 2017-11.

[68] H. Chen, R. T. Burnett, R. Copes, J. C. Kwong, Villeneuve and P. J., "Ambient Fine Particulate Matter and Mortality among Survivors of Myocardial Infarction: Population-Based Cohort Study," *Enviromental Health Perspectives,* vol. 124 (9), pp. 1421-1428, 2016-09.

[69] J. Wing, B. Sanchez, S. Adar, Meurer, William and L. Morgenstern, "Synergism of Short-Term Air Pollution Exposures and Neighborhood Disadvantage on Initial Stroke Severity," *Stroke,* vol. 48 (11), pp. 3126-3129, 2017-11.

[70] A. Shah, J. Langrish, H. Nair, D. McAllister and A. Hunter, "Global association of air pollution and heart failure: a systematic review and meta-analysis," *The Lancet (British edition),* vol. 382 (9887), pp. 1039-1048, 2013-09.

[71] H. Liu, Y. Tian, J. Song, Y. Cao, X. Xiang and C. Huang, "Effect of Ambient Air Pollution on Hospitalization for Heart Failure in 26 of China's Largest Cities," *The American Journal of Cardiology,* vol. 121 (5), pp. 628-633, 2018.

[72] R. Liang, B. zhang, X. Zhao, Y. Ruan and H. Lian, "Effect of exposure to PM2.5 on blood pressure: a systematic review and meta-analysis," *Journal of Hyptertension,* vol. 32, pp. 2130-2141, 2014.

[73] P. Giorgini, P. Di Giosia, D. Grassi, M. Rubenfire and R. Brook, "Air Pollution Exposure and Blood Pressure: An Updated Review of the Literature," *Current Pharmaceutical Design,* vol. 22, pp. 28-51, 2016.

[74] B. Wang, D. Xu, Z. Jing, D. Liu and S. Yan, "Effect of long-term exposure to air pollution on type 2 diabetes mellitus risk: a systemic review and meta-analysis of cohort studies," *Current pharmaceutical design,* vol. 22 (1), pp. 28-51, 2014.

[75] I. Eze, L. Hemkens, H. Bucher, B. Hoffmann and C. Schindler, "Association between ambient air pollution and diabetes mellitus in Europe and North America: systematic review and meta-analysis," *Enviromental Health Perspective,* vol. 123 (5), pp. 381-389, 2015.

[76] "Stadt Wien IG-L," 16 September 2024. [Online]. Available: https://www.wien.gv.at/umwelt/luft/messwerte/grenzwerte.html#:~:text=*%20Bei%20Feinstaub%20PM%2010%20ist,%C3%BCber%20dieser%20Schwelle%20gez%C3%A4hlt%20werden..

[77] "Nationale Ruftreinhalteprogramme," Rechtsinformationssystem des Bundes, 23 November 2018. [Online]. Available: https://www.ris.bka.gv.at/eli/bgbl/i/2018/75/P6/NOR40209488. [Accessed June 2024].

[78] "Umweltbundesamt NIR," 2023. [Online]. Available: https://www.umweltbundesamt.at/studien-reports/publikationsdetail?pub_id=2474&cHash=682457cf175c26a3d9639b6ef68c1c3b.

[79] "Umweltbundesamt IIR," 2023. [Online]. Available: https://www.umweltbundesamt.at/studien-reports/publikationsdetail?pub_id=2473&cHash=9847baeb3164c2e5ea8e5d7c260e1629.

[80] "Grenz-, Ziel- und Schwellenwerte," Umweltbundesamt, 2024. [Online]. Available: https://www.umweltbundesamt.at/umweltthemen/luft/daten-luft/luft-grenzwerte. [Accessed November 2024].

[81] "PRTR - Pollutant Release and Transfer Register," Österreichisches Umweltbundesamt , [Online]. Available: https://www.umweltbundesamt.at/umweltthemen/industrie/daten-industrie/prtr. [Accessed August 2024].

[82] "PRTR Nationales Register," Österreichisches Umweltbundesamt , [Online]. Available: https://secure.umweltbundesamt.at/PRTR-web/auswahlNachSchadstoffen.do?txid=515ddaa425da2db3c7df42cfbf2f8efb3f70e938. [Accessed August 2024].

[83] "Richtlinie 2010/75/EU des Europäischen Paralments und des Rates über Industrieemissionen (integrierte Vermeidung und Verminderung der Umweltverschmutzung)," European Union, 2010.

[84] "Amendment Industrial Emissions 2010/75/EU," European Union, 5 April 2022. [Online]. Available: https://eur-lex.europa.eu/legal-content/EN/TXT/?uri=CELEX%3A52022PC0156. [Accessed August 2024].

[85] "Industrieemissionsrichtlinie," Bundesministerium für Klimaschutz, Umwelt, Energie, Mobilität, Innovation und Technologie - Industrieemissionsrichtlinie, [Online]. Available: https://www.bmk.gv.at/themen/klima_umwelt/betrieblich_umweltschutz/anlagenbezogen_uws/industrieemissions_rl.html. [Accessed August 2024].

[86] "IPPC Austria," Bundesministerium für Klima und Umweltschutz, 2024. [Online]. Available: https://edm.gv.at/natippc/#/installations. [Accessed September 2024].

[87] "Industrie - Wien," Wirtschaftskammer Österreich, 17 September 2024. [Online]. Available: https://www.wko.at/wien/industrie/start.

[88] "Raffinerie Schwechat: 60 Jahre und noch lange nicht pensionsreif," OMV, 17 September 2024. [Online]. Available: https://www.omv.com/de/blog/raffinerie-schwechat-60-jahre-und-noch-lange-nicht-pensionsreif.

[89] "Borealis in Schwechat," Borealis Österreich, 17 September 2024. [Online]. Available: https://www.borealisgroup.com/%C3%B6sterreich/standorte/schwechat.

[90] T. Puchinger, "Raffinerie Schwechat: 60 Jahre ohne Stillstand," ORF, 30 April 2018. [Online]. Available: https://noe.orf.at/v2/news/stories/2909529/. [Accessed 30 April 2018].

[91] "Maßnahmen zur Senkung der Luftverschmutzung, 3. Maßnahmenpaket," April 2011. [Online]. Available: https://www.wien.gv.at/umwelt/luft/massnahmen/index.html#massnahmen. [Accessed October 2024].

[92] "Schlechte Luftgüte „drückt“ auf Wien," Wien ORF, 10 November 2024. [Online]. Available: https://wien.orf.at/stories/3280654/. [Accessed November 2024].

[93] "Feinstaubbelastung kann Entzündungen und Krankheiten auslösen," Der Standard, 12 November 2024. [Online]. Available: https://www.derstandard.at/story/3000000244604/feinstaubbelastung-kann-entz252ndungen-und-andere-krankheiten-ausl246sen. [Accessed November 2024].

[94] E. Schrittwieser, "Industrieschnee brachte weiße Bezirke in Wien," Die Presse, 17 January 2024. [Online]. Available: https://www.diepresse.com/18001449/industrieschnee-brachte-weisse-bezirke-in-wien. [Accessed November 2024].

[95] A. Dobek, "Auswertung von Nebel und Hochnebel, sowie Prognose mittels logistischer Regression für den Flughafen Wien - Schwechat," Universität Wien, Wien, 2009.

[96] "Wind, Niederschlag und Schnee in Wien 1955 bis 2023," Stadt Wien, [Online]. Available: https://www.wien.gv.at/statistik/lebensraum/tabellen/wind-schnee-regen-zr.html. [Accessed February 2025].

[97] "Geschichte und Geographie - Industrialisierung," Land Oberösterreich, September 2024. [Online]. Available: https://www.land-oberoesterreich.gv.at/24430.htm.

[98] "Geschichte der Stadt Linz," Stadtgeschichte Linz, September 2024. [Online]. Available: https://stadtgeschichte.linz.at/8187.php.

[99] "Unsere Geschichte," voestalpine, 16 September 2024. [Online]. Available: https://www.voestalpine.com/group/de/konzern/ueberblick/historie/.

[100] "Umweltbundesamt," Emissionen aus Betrieben der Metallindustrie, 4 March 2024. [Online]. Available: https://www.umweltbundesamt.de/daten/umwelt-wirtschaft/industrie/emissionen-aus-betrieben-der-metallindustrie#emissionen-aus-prtr-betrieben-der-roheisen-und-stahlerzeugung. [Accessed October 2024].

[101] "Voestalpine - Über uns," voestalpine Steel & Service Center GmbH, 2024. [Online]. Available: https://www.voestalpine.com/ssc/Unternehmen/Ueber-uns. [Accessed November 2024].

[102] "Wasserdampf und "Industrieschnee"," Magistrat Linz, [Online]. Available: https://www.linz.at/umwelt/4222.php. [Accessed November 2024].

[103] W. Hager, "„Industrieschnee“ in Linz," Magistrat der Landeshauptstadt Linz, Linz.

[104] D.-M. S. Trippler, "Industrieschnee," Deutscher Wetterdienst, 6 December 2016. [Online]. Available: https://www.dwd.de/DE/wetter/thema_des_tages/2016/12/6.html. [Accessed November 2024].

[105] "Klima," Stadt Linz, [Online]. Available: https://www.linz.at/zahlen/095_Umwelt/020_Klima/010_Normalwerte/. [Accessed February 2025].

[106] "From a small iron foundry to a globally leading technology group," Andritz Group, 2024. [Online]. Available: https://www.andritz.com/group-en/about-us/gr-history. [Accessed September 2024].

[107] "Graz," Graz Museum, 2024. [Online]. Available: https://360.grazmuseum.at/en/epochen/1809-1914/. [Accessed 2024].

[108] T. Arnold, "Magna in der Krise: Wie die steirische Autoindustrie an europäischen Fehlentscheidungen leidet," Industriemagazin, 8 August 2024. [Online]. Available: https://industriemagazin.at/news/magna-in-der-krise-wie-die-steirische-autoindustrie-an-europ%C3%A4ischen-fehlentscheidungen-leidet/. [Accessed September 2024].

[109] "Grazer Luft," Umwelt Graz, 2024. [Online]. Available: https://www.umwelt.graz.at/cms/ziel/6669434/DE/#:~:text=Das%20Grazer%20Becken%20z%C3%A4hlt%20aufgrund,Belastung%20im%20Grazer%20Becken%20bei.. [Accessed November 2024].

[110] T. Wagnest, "Klima- und Wetterphänomene der Steiermark," July 2021. [Online]. Available: https://unipub.uni-graz.at/obvugrhs/content/titleinfo/6473395/full.pdf. [Accessed November 2024].

[111] "Klima Informations System," Stadt Graz - Stadtvermessungsamt, [Online]. Available: https://geodaten.graz.at/portal/apps/experiencebuilder/experience/?draft=true&id=59f2927dc3134c03af2a09d9c25aa19a&page=IMPRESSUM. [Accessed February 2025].

[112] "Inversionswetterlage im Grazer Becken," Wetterzeugen, 18 December 2020. [Online]. Available: https://www.wetterzeugen.at/inversionswetterlage-im-grazer-becken/. [Accessed November 2024].

[113] J. Breitfelder and E. Pirker, "Regionalgeographisches Kurzportrait der Steiermark," Schulatlas Steiermark, 2024. [Online]. Available: https://www.schulatlas.at/1-basisinformationen-und-grundlagen/1-2-kurzportrait/. [Accessed November 2024].

[114] O. Bender and P. Pindur, "Erzberg, Eisenwurzen und „Mur-Mürz-Furche“ - Entwicklung einer historischen Eisen- und Stahlindustrieregion in den österreichischen Alpen," *Geographische Rundschau,* pp. 56(5): 16-23, 2004.

[115] "Die historische Entwicklung der voestalpine Stahl Donawitz - Know-how seit mehr als 140 Jahren," voestalpine, 2024. [Online]. Available: https://www.voestalpine.com/stahldonawitz/de/unternehmen/geschichte/. [Accessed October 2024].

[116] "Klimaregionen der Steiermark," Umwelt Steiermark - Land Steiermark, 2024. [Online]. Available: https://www.umwelt.steiermark.at/cms/ziel/25206/DE/. [Accessed November 2024].

[117] "European Enviromental Agency - Air Quality Download Service," 2024. [Online]. Available: https://eeadmz1-downloads-webapp.azurewebsites.net/. [Accessed September 2024].

[118] W. Spangl, C. Nagl and L. Moosmann, "Jahresbericht der Luftgütemessungen in Österreich 2006," Umweltbundesamt, Wien, 2007.

[119] "Immissionen – Feinstaub (PM 10)," Magistrat der Landeshauptstadt Linz, [Online]. Available: https://www.linz.at/zahlen/095_Umwelt/015_Luft/020_Immissionen/IFSTA.PDF. [Accessed August 2024].

[120] "PM10-Überschreitungstage," 11 November 2024. [Online]. Available: https://www2.land-oberoesterreich.gv.at/imm/pdfberichte?file=Ueberschreitungen_heuer. [Accessed 11 November November].

[121] "Staubniederschlag in Linz 2017," Magistrat Linz, 2017. [Online]. Available: https://www.linz.at/umwelt/Staubniederschlagsmessung_in_Linz_2017.php. [Accessed November 2024].

[122] I. Buxbaum, C. Nagl and W. Spangl, "Analyse der Feinstaub-Belastung 2009-2017," Umweltbundesamt, Wien, 2018.

[123] "LUIS - Online Luftgütedaten," Land Steiermark, 2024. [Online]. Available: https://app.luis.steiermark.at/luft2/suche.php. [Accessed October 2024].

[124] B. Friedl, D. Janisch, C. Kaltenegger, N. KAtz, E. Kirschner, A. Niederl and S. Sarcletti, "Östliche Obersteiermark - WIBIS Steiermark," April 2021. [Online]. Available: https://wibis-steiermark.at/fileadmin/user_upload/wibis_steiermark/regionsprofile/2021-11/AT223_PROFIL_1_FactText_28.04.2021.pdf. [Accessed October 2024].

[125] "Zahlen + Fakten: Bevölkerung, Bezirke, Wirtschaft, Geografie," Stadt Graz, 2024 January 01. [Online]. Available: https://www.graz.at/cms/beitrag/10034466/7772565/zahlen_fakten_bevoelkerung_bezirke_wirtschaft.html. [Accessed October 2024].

[126] "Kontinuierliches Immissionsmessnetz," Umwelt Steiermark - Land Steiermark, 2024. [Online]. Available: https://www.umwelt.steiermark.at/cms/beitrag/10021933/2061730/. [Accessed November 2024].

[127] "Dashboard Luftschadstoff-Emissionen und Luftqualität in Österreich," Österreichisches Umweltbundesamt, 2024. [Online]. Available: https://www.umweltbundesamt.at/umweltthemen/luft/luftschadstoffe/dashboard. [Accessed September 2024].

[128] "Saharastaub ist wieder im Anflug," ORF Niederösterreich, 24 April 2018. [Online]. Available: https://noe.orf.at/v2/news/stories/2908830/. [Accessed November 2024].

[129] T. Pongratz, "27. Umweltbericht Steiermark," 2020. [Online]. Available: https://www.umwelt.steiermark.at/cms/dokumente/12567945_135844225/6b3b3611/7%20Luft.pdf. [Accessed November 2024].

[130] G. Strobl, "Heizungsumstellung stellt Wien auf bisher schwerste Probe," Der Standard, 24 June 2024. [Online]. Available: https://www.derstandard.at/story/3000000225553/heizungsumstellung-stellt-wien-auf-bisher-schwerste-probe. [Accessed November 2024].

[131] A. Wallisch, "Wien Energie," Wiener Klimagesetz in Begutachtung, 11 September 2024. [Online]. Available: https://positionen.wienenergie.at/blog/wiener-klimagesetz/#:~:text=Klares%20Ziel%20ist%20die%20Klimaneutralit%C3%A4t,den%20Auswirkungen%20des%20Klimawandels%20befassen.. [Accessed November 2024].

[132] "Erfindungsmeldung: Hybrider Hochleistungsabscheider „MiniMax“," Universität Stuttgart Institut für Mechanische Verfahrenstechnik, 24 September 2024. [Online]. Available: https://www.imvt.uni-stuttgart.de/institut/aktuelles/news/Erfindungsmeldung-Hybrider-Hochleistungsabscheider-MiniMax/. [Accessed November 2024].

[133] "Vorläufige Feinstaubbilanz 2018," Umweltbundesamt, 2 January 2019. [Online]. Available: https://www.umweltbundesamt.at/aktuelles/presse/news2019/news20190102. [Accessed November 2024].

Appendix

List of Figures:

List of Formulas:

List of Tables: